

**Chondrogenic Differentiation
of Human Mesenchymal Stem Cells
and Articular Cartilage Reconstruction**

Dissertation zur Erlangung des naturwissenschaftlichen
Doktorgrades der Julius-Maximilians-Universität Würzburg

vorgelegt von

Andrea Heymer

aus Königs Wusterhausen

Würzburg, 2008

Eingereicht am:

Mitglieder der Promotionskommission:

Vorsitzender:

Gutachter: PD Dr. med. Ulrich Nöth

Gutachter: Prof. Dr. rer. nat. Roland Benz

Tag des Promotionskolloquiums:

Doktorurkunde ausgehändigt am:

Hiermit erkläre ich ehrenwörtlich, dass ich die vorliegende Dissertation selbstständig angefertigt und keine anderen als die von mir angegebenen Hilfsmittel und Quellen verwendet habe. Des Weiteren erkläre ich, dass diese Arbeit weder in gleicher noch in ähnlicher Form in einem Prüfungsverfahren vorgelegen hat und ich noch keinen Promotionsversuch unternommen habe.

Oberstenfeld, 17. Juli 2008

Andrea Heymer

Table of contents

1 Summary	1
1.1 Summary.....	1
1.2 Zusammenfassung.....	2
2 Introduction	5
2.1 Structure and composition of articular cartilage.....	5
2.2 Articular cartilage damage and repair.....	7
2.3 Mesenchymal stem cells.....	8
2.3.1 Definition of mesenchymal stem cells.....	8
2.3.2 Chondrogenesis.....	9
2.4 Scaffolds for cartilage tissue engineering.....	10
2.5 Bioreactor cultivation for cartilaginous tissue growth.....	12
2.6 Cellular imaging.....	14
2.6.1 Use of superparamagnetic iron oxide particles for MR imaging.....	14
2.6.2 Labeling of cells with very small superparamagnetic iron oxide particles (VSOPs) for cellular MR imaging.....	15
2.7 Objective of the study.....	16
3 Materials and methods	18
3.1 Materials.....	18
3.1.1 Consumables.....	18
3.1.2 Chemicals and reagents.....	18
3.1.3 Cell culture media and additives.....	20
3.1.4 Components for the fabrication of collagen hydrogels.....	21
3.1.5 Antibodies.....	21
3.1.6 Enzymes.....	22
3.1.7 Primers.....	22
3.1.8 Buffers and other solutions.....	23
3.1.9 Kits.....	25
3.1.10 Equipment.....	25
3.1.11 Software and online sources.....	26
3.2 Methods.....	27
3.2.1 Isolation and culture of human mesenchymal stem cells (hMSCs).....	27
3.2.2 Phenotypic characterization of hMSCs.....	27
3.2.3 Labeling of hMSCs with very small superparamagnetic iron oxide particles (VSOPs).....	28
3.2.3.1 Labeling protocol.....	28

3.2.3.2	Detection of iron oxide particles within VSOP-labeled hMSCs	28
3.2.3.3	Cellular viability and apoptosis	29
3.2.3.4	Proliferation assays	30
3.2.3.5	Differentiation of hMSCs	30
3.2.4	Fabrication and culture of hMSC collagen hydrogels	31
3.2.4.1	Fabrication of hMSC collagen hydrogels	31
3.2.4.2	Cell proliferation in hMSC collagen hydrogels	32
3.2.4.3	Chondrogenic differentiation of hMSCs in collagen hydrogels	32
3.2.5	Bioreactor cultivation of hMSC collagen hydrogels	32
3.2.6	High-field MR imaging	34
3.2.7	Histology and immunohistochemistry	34
3.2.7.1	Oil red O staining	34
3.2.7.2	Alizarin red S staining	35
3.2.7.3	Hemalaun&Eosin (H&E) staining	35
3.2.7.4	Alcian blue staining	35
3.2.7.5	Immunohistochemical staining for collagen type II	35
3.2.8	Gene expression analyses	35
3.2.8.1	Total RNA isolation	35
3.2.8.2	cDNA synthesis	36
3.2.8.3	Reverse transcriptase polymerase chain reaction (RT-PCR)	36
3.2.8.4	Agarose gel electrophoresis	37
4	Results	38
4.1	Characterization of hMSCs	38
4.2	Fabrication and culture of hMSC collagen hydrogels	40
4.2.1	Contraction of hMSC collagen hydrogels	40
4.2.2	Cell proliferation in hMSC collagen hydrogels	42
4.2.3	Chondrogenic differentiation of hMSCs in collagen hydrogels	47
4.3	Mechanical stimulation of hMSC collagen hydrogels	56
4.3.1	Cellular behavior of hMSCs in collagen hydrogels during bioreactor cultivation	56
4.3.2	Influence of mechanical stimulation on the gene expression of hMSCs in collagen hydrogels	59
4.4	Labeling of hMSCs with VSOPs for cellular MR imaging	61
4.4.1	Detection of iron oxide particles within VSOP-labeled hMSCs	61
4.4.2	Influence of VSOP labeling on the cellular viability and apoptosis of hMSCs	62
4.4.3	Influence of VSOP labeling on the proliferation capacity of hMSCs	63
4.4.4	Differentiation of VSOP-labeled hMSCs	65
4.5	MR imaging of VSOP-labeled cells in collagen hydrogels	68

4.5.1	Detection limit of MRI	68
4.5.2	Long-term MRI of VSOP-labeled hMSC collagen hydrogels	70
4.5.3	Discrimination of living and dead VSOP-labeled hMSCs in collagen hydrogels	71
5	Discussion	73
5.1	Cellular behavior of hMSCs in collagen hydrogels.....	73
5.1.1	Contraction of hMSC collagen hydrogels.....	74
5.1.2	Cellular survival in hMSC collagen hydrogels	75
5.2	Chondrogenic differentiation of hMSCs in collagen hydrogels	77
5.2.1	Detection of cartilage- and bone-specific gene expression	77
5.2.2	Different patterns of matrix accumulation within chondrogenic differentiated hMSC collagen hydrogels.....	79
5.2.3	Variations in the chondrogenic differentiation capacity of hMSC collagen hydrogels	81
5.2.4	Enhancement of chondrogenesis	82
5.3	Mechanical stimulation of hMSC collagen hydrogels	83
5.3.1	Establishment of culture conditions	83
5.3.2	Alterations in the gene expression of hMSCs in collagen hydrogels after mechanical stimulation	84
5.4	Labeling of hMSCs with VSOPs for cellular MR imaging	87
5.4.1	Intracellular iron content and its effect on cellular viability and proliferation	87
5.4.2	No adverse effect of VSOP labeling on the differentiation ability of hMSCs	89
5.5	MRI of hMSC collagen hydrogels	90
5.6	Perspective	93
6	References	95
7	Appendix	111
7.1	Abbreviations	111
7.2	Curriculum Vitae.....	113
7.3	Publications.....	114
7.4	Acknowledgement.....	116

1 Summary

1.1 Summary

Articular cartilage defects are still one of the major challenges in orthopedic and trauma surgery. Today, autologous chondrocyte transplantation (ACT), as a cell-based therapy, is an established procedure to treat focal articular cartilage defects. However, one major limitation of this technique is the dedifferentiation of chondrocytes during expansion accompanied by a loss of the chondrogenic phenotype. Human mesenchymal stem cells (hMSCs) have an extensive proliferation potential and the capacity to differentiate into chondrocytes when maintained in a three-dimensional culture and treated with members of the transforming growth factor- β (TGF- β) family. They are therefore considered as candidate cells for tissue engineering approaches of functional cartilage tissue substitutes.

First in this study, hMSCs were embedded in a collagen type I hydrogel, which is already in clinical use for matrix-based ACT, to evaluate the cartilaginous construct *in vitro*. HMSC collagen hydrogels cultivated in different culture media showed a marked contraction, most pronounced in chondrogenic differentiation medium supplemented with TGF- β 1. After 14 days, the diameter of the constructs decreased to approximately 30%, independently from the initial cell seeding density. However, thereafter almost no contraction was observed. Regarding chondrogenic differentiation, the results demonstrate that hMSCs were able to undergo chondrogenesis when embedded in the collagen type I hydrogel and stimulated with chondrogenic factors (dexamethasone and TGF- β 1), as evaluated by the temporal induction of cartilage-specific gene expression, such as aggrecan and collagen types II and IX. Furthermore, the cells showed a chondrocyte-like appearance and were homogeneously distributed within a proteoglycan- and collagen type II-rich extracellular matrix, except a small area in the center of the constructs. A high level of collagen type X gene expression indicated a tendency to hypertrophy. Additionally, various osteogenic marker genes were expressed. The results suggest that further studies have to focus on the establishment of differentiation conditions which promote the development of a stable cartilage phenotype. In this study, chondrogenic differentiation could not be realized with every hMSC preparation. With the improvement of the culture conditions, e.g. the use of a different FBS lot in the gel fabrication process, a higher amount of cartilage-specific matrix deposition could be achieved. Nevertheless, the large variations in the differentiation capacity display the high donor-to-donor variability influencing the development of a cartilaginous construct. Taken together, the results demonstrate that the collagen type I hydrogel is a suitable carrier matrix for hMSC-based cartilage regeneration therapies which present a promising future alternative to ACT. Second, to further improve the quality of tissue-engineered cartilaginous constructs, mechanical stimulation in specific bioreactor systems are often employed. In this study, the effects of

mechanical loading on hMSC differentiation have been examined. HMSC collagen hydrogels were cultured in a defined chondrogenic differentiation medium without TGF- β 1 and subjected to a combined mechanical stimulation protocol, consisting of perfusion and cyclic uniaxial compression. In the loading experiments, constructs were exposed to sinusoidal loading with a maximum stimulation force of 4.2 kPa at a frequency of 0.002 Hz for 8 hours per day. Experiments were conducted for 11 consecutive days. Bioreactor cultivation neither affected overall cell viability nor the cell number in collagen hydrogels. Compared with non-loaded controls, mechanical loading promoted the gene expression of COMP and biglycan and induced an up-regulation of matrix metalloproteinase 3, suggesting a high matrix turnover. These results circumstantiate that hMSCs are sensitive to mechanical forces, but their differentiation to chondrocytes could not be induced. Further studies are needed to identify the specific metabolic pathways which are altered by mechanical stimulation.

Third, for the development of new cell-based therapies for articular cartilage repair, a reliable cell monitoring technique is required to track the cells *in vivo* non-invasively and repeatedly. This study aimed at analyzing systematically the performance and biological impact of a simple and efficient labeling protocol for hMSCs. Commercially available very small superparamagnetic iron oxide particles (VSOPs) were used as magnetic resonance (MR) contrast agent. Iron uptake via endocytosis was confirmed histologically with prussian blue staining and quantified by mass spectrometry. Compared with unlabeled cells, VSOP-labeling did neither influence significantly the viability nor the proliferation potential of hMSCs. Furthermore, iron incorporation did not affect hMSCs in undergoing adipogenic, osteogenic or chondrogenic differentiation, as demonstrated histologically and by gene expression analyses. The efficiency of the labeling protocol was assessed with high resolution MR imaging at 11.7 Tesla. VSOP-labeled hMSCs were visualized in a collagen type I hydrogel indicated by distinct hypointense spots in the MR images, resulting from an iron specific loss of signal intensity. Furthermore it was demonstrated, that magnetically labeled hMSCs can be detected over 10 weeks *in vitro*, confirmed by prussian blue staining. With the applied MR parameters cell numbers as low as 5×10^3 hMSCs/ml gel could be readily imaged. In summary, this labeling technique has great potential to visualize hMSCs and track their migration after transplantation for articular cartilage repair with MR imaging.

1.2 Zusammenfassung

Gelenkknorpeldefekte stellen immer noch eine der großen Herausforderungen in der Orthopädie und Unfallchirurgie dar. Als zellbasiertes Verfahren ist die Autologe Chondrozytentransplantation (ACT) heute in der klinischen Routine etabliert und wird zur Behandlung von fokalen Defekten unter anderem am Kniegelenkknorpel eingesetzt. Ein großer Nachteil dieser Methode ist jedoch die Dedifferenzierung der Knorpelzellen und der damit verbundene

Verlust des chondrozytären Phänotyps während der Expansion der Zellen. Humane mesenchymale Stammzellen (hMSZ) verfügen über ein ausgeprägtes Proliferationspotential und besitzen die Fähigkeit, in dreidimensionalen Kultursystemen und unter dem Einfluss von Wachstumsfaktoren der TGF β -Familie zu Knorpelzellen zu differenzieren. Sie werden daher als alternative Zellen für das Tissue Engineering von funktionellem Knorpelersatzgewebe in Betracht gezogen.

In der vorliegenden Arbeit wurden erstens hMSZ in ein Kollagen Typ I Hydrogel eingebracht, welches sich bereits im klinischen Einsatz für die matrixgekoppelte ACT befindet, und zunächst der Grad der chondrogenen Zelldifferenzierung im Konstrukt evaluiert. hMSZ-Kollagenhydrogele zeigten in allen Kultivierungsmedien eine deutliche Kontraktion, welche am stärksten im chondrogenen Differenzierungsmedium unter Zugabe von TGF- β 1 ausgeprägt war. Nach 14tägiger Kultivierung nahm der Durchmesser der Konstrukte, unabhängig von der eingebrachten Anfangszellzahl, auf ca. 30% des Ausgangsdurchmessers ab. Nach diesem Zeitraum war jedoch keine weitere Kontraktion zu beobachten. Im Hinblick auf die chondrogene Differenzierung zeigen die Ergebnisse, dass hMSZ nach Einbringen in Kollagen Typ I Hydrogele und Stimulation mit chondrogenen Faktoren (Dexamethason und TGF- β 1) zu Knorpelzellen differenzierten, nachgewiesen durch die Induktion von knorpelspezifischer Genexpression, wie z.B. Aggrekan und Kollagen Typ II und IX. Die Zellen wiesen eine Chondrozyten-ähnliche Morphologie auf und waren bis auf einen kleinen Bereich in der Mitte des Konstrukts homogen in einer Proteoglykan- und Kollagen Typ II-haltigen extrazellulären Matrix verteilt. Eine starke Kollagen Typ X Genexpression wies auf eine mögliche Hypertrophie der Zellen hin. Außerdem wurden zahlreiche osteogene Markergene exprimiert. Diese Ergebnisse machen deutlich, dass in zukünftigen Studien Differenzierungsbedingungen etabliert werden müssen, welche die Ausbildung eines stabilen chondrozytären Phänotyps ermöglichen. Eine chondrogene Differenzierung konnte in der vorliegenden Arbeit jedoch nicht mit jeder hMSZ-Präparation realisiert werden. Durch die Verbesserung der Kulturbedingungen, z.B. durch die Verwendung einer anderen Serumcharge im Gelherstellungsprozess, konnte eine Steigerung der knorpelspezifischen Matrixsynthese erzielt werden. Nichtsdestotrotz spiegeln die großen Schwankungen in der Differenzierungskapazität die hohe Variabilität zwischen verschiedenen Spendern wider, welche die Entwicklung eines knorpelartigen Gewebes beeinflussen. Zusammengefasst zeigen die Ergebnisse, dass das Kollagen Typ I Hydrogel eine geeignete Trägermatrix für hMSZ darstellt, um in Stammzell-basierten Knorpelregenerationstherapien zukünftig als vielversprechende Alternative zur ACT eingesetzt zu werden.

Um die Qualität eines *in vitro* generierten knorpelartigen Gewebes weiter zu verbessern, wird häufig eine mechanische Stimulation in spezifischen Bioreaktorsystemen durchgeführt. In der vorliegenden Arbeit wurden daher zweitens die Effekte von mechanischer Belastung auf

die Differenzierung von hMSZ untersucht. HMSZ-Kollagenhydrogele wurden im chondrogenen Differenzierungsmedium ohne TGF- β 1 kultiviert und einem kombinierten mechanischen Stimulationsprotokoll, bestehend aus Perfusion und zyklischer uniaxialer Kompression, ausgesetzt. In den Stimulationsversuchen wurde eine sinusförmige Beanspruchung mit einer maximalen Kraft von 4,2 kPa bei einer Frequenz von 0,002 Hz für 8 Stunden pro Tag appliziert. Dieses Protokoll wurde an 11 aufeinanderfolgenden Tagen ausgeführt. Die Kultivierung im Bioreaktor hatte weder einen Einfluss auf die Zellvitalität noch auf die Anzahl der Zellen im Kollagen Typ I Hydrogel. Die mechanische Beeinflussung steigerte im Vergleich mit den unbelasteten Kontrollgelen die Genexpression von COMP und Biglykan und führte zu einer Hochregulation von Matrix Metalloproteinase 3. Diese Ergebnisse belegen, dass hMSZ mechanosensitiv sind, jedoch konnte keine Differenzierung zu Knorpelzellen induziert werden. Hierfür sind weitere Studien notwendig, um spezifische Stoffwechselwege zu identifizieren, welche durch die mechanische Stimulation beeinflusst werden.

Drittens, für die Entwicklung von neuen zellbasierten Therapien für die Gelenkknorpelrekonstruktion ist eine zuverlässige Bildgebung auf zellulärer Ebene erforderlich, um die Zellen *in vivo* wiederholt nicht invasiv zu detektieren. Die vorliegende Arbeit hatte zum Ziel, systematisch die Effizienz und die biologischen Auswirkungen einer einfachen und dauerhaften Markierung für hMSZ zu untersuchen. Superparamagnetische Eisenoxidnanopartikel (VSOPs), ein kommerziell erhältliches Magnetresonanz (MR)-Kontrastmittel, wurden für die Markierung eingesetzt. Die Aufnahme der Eisenoxidnanopartikel durch Endozytose wurde histologisch mittels eisenspezifischer Berliner-Blau-Färbung nachgewiesen und durch Massenspektroskopie quantifiziert. Im Vergleich zu unmarkierten Zellen beeinträchtigte die VSOP-Markierung weder die Vitalität noch das Proliferationspotential der hMSZ. Weiterhin war durch die Aufnahme der Eisenoxidnanopartikel keine Beeinflussung der adipogenen, osteogenen oder chondrogenen Differenzierung der hMSZ zu verzeichnen, was durch histologische und Genexpressionsanalysen demonstriert werden konnte. Die Effizienz der Zellmarkierung wurde mittels hochauflösender MR-Bildgebung bei 11,7 Tesla beurteilt. VSOP-markierte hMSZ im Kollagen Typ I Hydrogel erschienen als hypointense Punkte in den MR-Bildern, hervorgerufen durch die typische, VSOP-bedingte Signalauslöschung. Außerdem wurden die markierten Zellen *in vitro* wiederholt über einen Zeitraum von 10 Wochen mittels MR-Bildgebung detektiert. Histologische Untersuchungen dieser Konstrukte bestätigten die MR-Ergebnisse. Weiterhin wurden auch geringe Zellkonzentrationen bis zu 5×10^3 hMSZ/ml Gel in den MR-Bildern visualisiert. Zusammenfassend lässt sich festhalten, dass diese Zellmarkierungsmethode in Verbindung mit der MR-Bildgebung über das Potential verfügt, nach einer Gelenkknorpelrekonstruktion Aufschluss über die Lokalisation und Migration der transplantierten hMSZ zu liefern.

2 Introduction

2.1 Structure and composition of articular cartilage

Articular cartilage is a hyaline cartilage covering the subchondral bone in diarthrodial joints. Its main function is providing a high load-bearing capacity and a high compressive stiffness to withstand the high stresses and strains developed during joint use. Its smooth surface together with the synovial fluid minimizes the friction between the gliding surfaces. Articular cartilage has a highly organized structure with a biphasic nature, consisting of fluid and a solid extracellular matrix (ECM) rich in collagens and proteoglycans [Cohen et al., 1998]. Tissue fluid is an essential part of hyaline cartilage, containing in addition to water metabolites and a large amount of electrolytes. The predominant collagen type found in the tissue, accounting for approximately 90%, is collagen type II, while the collagen types VI, IX, X, and XI represent a minor fraction. The other dominant components of the tissue are highly negatively charged proteoglycans, which include several proteins containing covalently bound glycosaminoglycan side chains. The major proteoglycan is aggrecan, which binds via link proteins to hyaluronan chains to form a large proteoglycan aggregate. Quantitatively minor components of articular cartilage are link protein, smaller proteoglycans, e.g. biglycan, decorin, and fibromodulin, and cartilage oligomeric matrix protein (COMP) [Kuettnner et al., 1992]. The high fixed charge density of the proteoglycan matrix maintains hydration and provides a high swelling pressure, which is counteracted by the stiff collagen network, giving the unique mechanical properties to the hyaline articular cartilage: tensile strength, provided by the collagen network, and compressive stiffness, provided by the proteoglycans. Articular cartilage has a very low cell volume density with an average value of 1.65% of the whole tissue volume [Hunziker et al., 2002]. The chondrocytes are surrounded by a narrow pericellular matrix with very little collagen but abundant proteoglycans. Mostly a few cells are together arranged in a territorial region, also called chondrons, surrounded by a web of thin collagen fibrils. The cells embedded in their ECM are isolated from the vasculature and thus their nutrient supply, provided by the synovial fluid, occurs by a combination of diffusion and hydraulic transport during joint compression [O'Hara et al., 1990]. Chondrocytes are metabolically active and responsible for the maintenance of the ECM, displaying a relatively slow state of matrix turnover. They are susceptible to mechanical stress and can respond with an altered rate of protein synthesis. Differentiated chondrocytes in adults are limited in their capability to divide and proliferate [Kuettnner et al., 1992].

The structure and composition of articular cartilage tissue vary throughout its depth. From the articular surface to the subchondral bone, four different zones can be distinguished (Fig. 1) [Poole et al., 2001]. In the superficial zone, a fibrillar collagen network dominates, with thin collagen fibrils and flattened chondrocytes aligned parallel to the surface. The content of pro-

teoglycan is lowest and the water content highest in this zone. Below the superficial zone is the middle or transitional zone with chondrocytes having a more rounded appearance. The ECM is rich in proteoglycans, and the orientation of the larger collagen fibrils is less organized. In the deep zone, the cell density, and the collagen and water content are lowest. The large collagen bundles are arranged perpendicular to the articular surface. Spherical chondrocytes are often arranged in a columnar fashion. The proteoglycan content is maximal in this zone. The uncalcified cartilage is delineated by the tidemark from the zone of calcified cartilage, which merges into the subchondral bone. The chondrocytes in this calcified zone usually express the hypertrophic phenotype with the secretion of collagen type X, but unlike in endochondral bone formation this calcified matrix is not fully resorbed and resists vascular invasion.

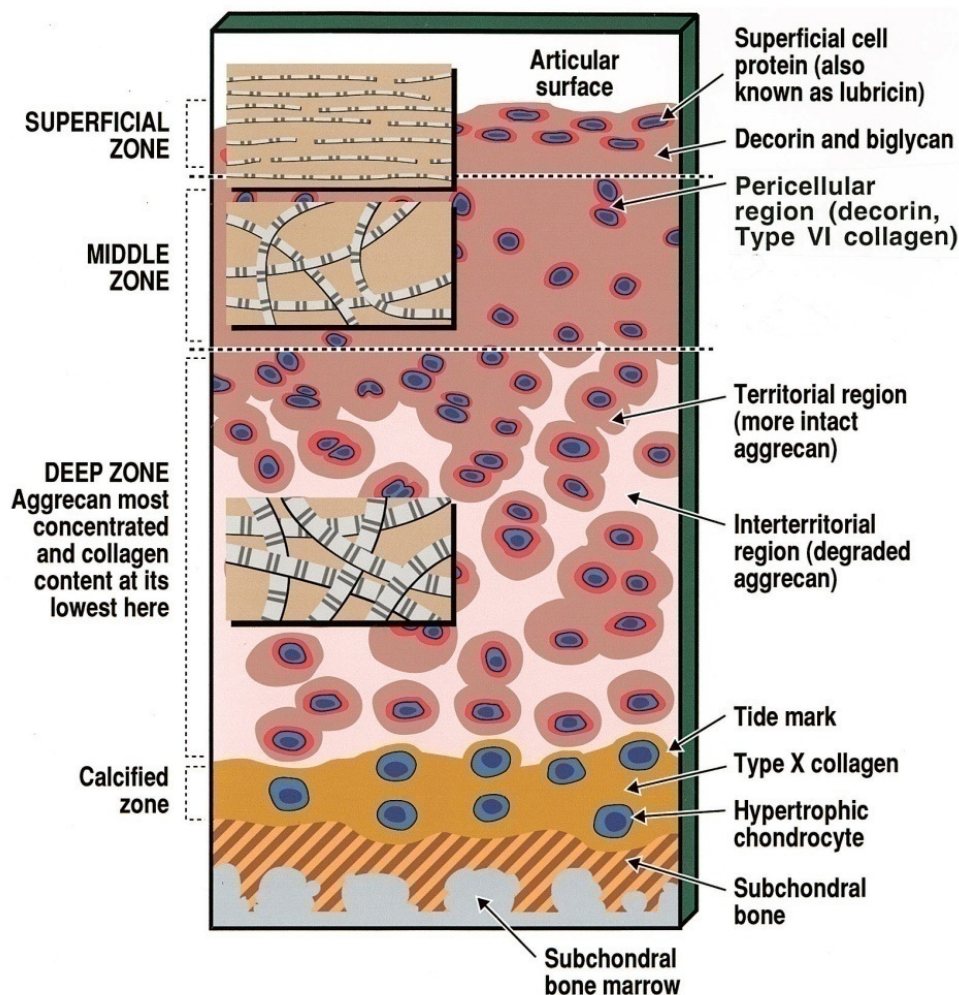


Fig. 1 Schematic representation of structure and composition of articular cartilage showing zonal and regional organization. *The insets show the relative diameters and arrangement of collagen fibrils in the different zones (from Poole et al., 2001).*

2.2 Articular cartilage damage and repair

The complex structure of articular cartilage can be damaged by even minor injuries, caused by trauma or degenerative joint diseases such as osteoarthritis (OA). It is well known that the intrinsic capacity for cartilage repair is limited [Buckwalter and Mankin, 1998]. Partial-thickness defects confined to the cartilage layer fail to heal spontaneously. This failure is possibly attributed to the avascularity and the low cellularity of the tissue, the immobility of chondrocytes, and the limited ability of mature chondrocytes to proliferate and alter their synthetic pattern [Newman, 1998]. However, full-thickness defects penetrating into subchondral bone show a limited spontaneous repair, involving blood clot formation and recruitment of cells and growth factors from the bone marrow. The less durable repair tissue typically has a composition and structure intermediate between hyaline cartilage and fibrocartilage [Hunziker, 2001]. For both kinds of defects, the natural repair does not lead to a fully functional hyaline cartilage and extensive degenerative changes of the fibrocartilaginous repair tissue occur within one year or less, indicated by depletion of matrix proteoglycans, fragmentation and fibrillation, increasing collagen content, and loss of cells [Shapiro et al., 1993; Buckwalter, 2002]. Moreover, a progression to severe forms of osteoarthritis is often observed [Buckwalter and Mankin, 1998].

With a progressively aging population, the repair of articular cartilage defects is therefore still one of the major challenges in orthopedic and trauma surgery. A number of treatment strategies are in clinical use, e.g. lavage and debridement, microfracture technique, transplantation of periosteal and perichondrial grafts, and transplantation of osteochondral autografts [Nehrer and Minas, 2000; Hunziker, 2001; Redman et al., 2005]. In recent years, a variety of tissue engineering approaches are thought to improve the repair by the generation of a functional cartilage tissue substitute [Temenoff and Mikos, 2000]. Tissue engineering is a multidisciplinary research area that incorporates both biological and engineering principles by the use of cells, biomaterial scaffolds and biochemical and physical regulatory factors for the purpose to generate new, living tissue as a replacement for the damaged tissue [Langer, 2000]. One of the first cell-based therapies employed in modern orthopedic surgery is the autologous chondrocyte transplantation (ACT), which is in clinical use for more than 10 years now [Brittberg et al., 1994; Peterson et al., 2000; Minas, 2001; Browne et al., 2005]. Further improvement of this technique resulted in the transplantation of autologous chondrocytes in the presence of biocompatible and biodegradable matrix scaffolds [Erggelet et al., 2003; Bartlett et al., 2005; Marcacci et al., 2005; Nehrer et al., 2006; Andereya et al., 2007]. However, a major limitation of this approach is the small number of chondrocytes available from the harvest site which makes an expansion in monolayer culture necessary, resulting in cell dedifferentiation and loss of the chondrogenic phenotype. To overcome this limitation, alternative cell sources have been extensively investigated.

2.3 Mesenchymal stem cells

2.3.1 Definition of mesenchymal stem cells

Mesenchymal stem cells (MSCs) are thought to be multipotent stem cells in an adult organism which can self-renew in an undifferentiated state as well as differentiate into specialized cell types (Fig. 2A) [Caplan, 1991]. They have received considerable attention in the field of tissue engineering because of their ability to differentiate into various tissues of mesenchymal origin (e.g. bone, cartilage, fat, muscle, marrow stroma, tendon, ligament, and other connective tissues) [Caplan, 1991; Pittenger et al., 1999]. MSCs can be easily isolated from bone marrow and various other tissues using different protocols and expanded *in vitro* to obtain sufficient numbers of cells for tissue engineering [De Ugarte et al., 2003; Tuli et al., 2003]. However, several studies indicated that the isolated cell populations represent a heterogeneous mixture of true multipotent stem cells and committed progenitor cells, each with restricted lineage-specific differentiation potential (Fig. 2B) [Muraglia et al., 2000; Bianco et al., 2001; Baksh et al., 2004].

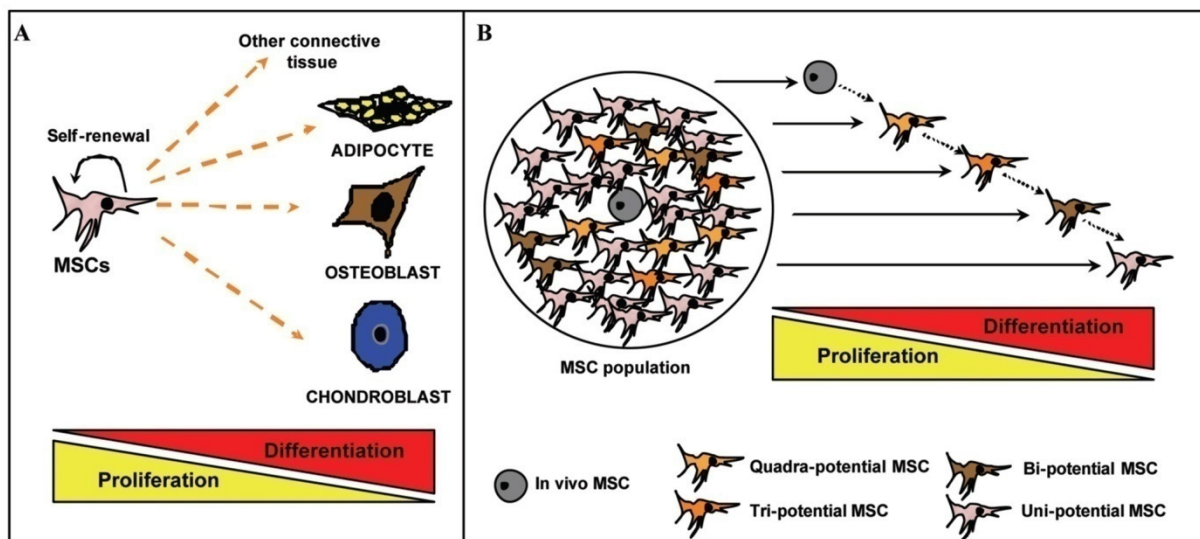


Fig. 2 Models of MSC differentiation. (A) In this theoretical model, MSCs in the bone marrow constitute a primitive stem cell population (multipotent MSCs), having the potential for self-renewal and proliferation as well as the capacity to differentiate into all connective tissue cell types, when exposed to a defined environment. (B) An alternative model illustrating MSCs in vivo as a population of cells with different differentiation potentials (i.e., quadra-, tri-, bi- and uni-potential). During *in vitro* culture, this heterogeneous mixture of stem and committed progenitor cells is limited in his multilineage differentiation potential, depending on the initial state of differentiation of the isolated cell population (from Baksh et al., 2004).

Numerous attempts have been undertaken to characterize the true multipotent stem cell, evaluating cell surface marker or gene expression profiles [Silva et al., 2003; Baksh et al., 2004; Song et al., 2006]. MSCs show a homogeneous expression of a broad set of cell-surface antigens, e.g. CD29, CD44, CD73, CD90, CD105, and Stro-1, while remaining negative for CD14, CD34, CD45, and other hematopoietic markers [Barry et al., 1999; Pittenger et

al., 1999; Barry and Murphy, 2004; Simmons and Torok-Storb, 1991]. However, all of these markers are also present on a variety of other cell types in the bone marrow, e.g. fibroblasts, endothelial cells, and therefore not sufficient to define MSCs. At present there exists no clear-cut definition of MSCs with e.g. an exclusively expressed surface marker, so that their characterization relies essentially on their functional properties [Tuan et al., 2003].

2.3.2 Chondrogenesis

Because of their ability to differentiate and form cartilage-like tissue under appropriate conditions MSCs are thought to replace chondrocytes in future clinical cell therapies [Johnstone and Yoo, 1999; Tuan et al., 2003]. Chondrogenesis of MSCs is usually induced upon culture conditions theoretically recapitulating articular cartilage formation during embryonic growth plate development [Caplan et al., 1997].

The process of cartilage development as a part of endochondral ossification begins with the condensation of mesenchymal progenitor cells, a requisite step in the chondrogenic pathway [DeLise et al., 2000; Kronenberg, 2003]. Prior to condensation, the undifferentiated MSCs produce an ECM rich in hyaluronan and collagen type I. As chondrogenesis proceeds, cells in the center of the condensations differentiate into chondroblasts and induce a change in the ECM composition by secreting cartilage-specific aggrecan, and collagen types II, IX, and XI [Sandell et al., 1994]. The chondrocytes encased in this ECM now acquire their characteristic round cell shape. The initial core cartilage enlarges through chondrocyte proliferation and matrix production and then proceeds through stages of maturation and hypertrophy accompanied by the expression of collagen type X. Hypertrophic chondrocytes direct the mineralization of their surrounding matrix, attract vascular and bone cell invasion, and then undergo apoptotic cell death [Kirsch et al., 1997]. In this so called primary center of ossification the termination of endochondral bone formation takes place by the replacement of the cartilage matrix by bone. At the top of the growth plate within the chondroepiphysis a secondary center forms, separating growth plate cartilage and articular cartilage. These two types of cartilage have to be distinguished, transient cartilage found in the growth plate and permanent, hyaline cartilage found on the articular joint surface. The exact mechanisms of articular cartilage development are still poorly understood; probably cells from an interzone, located between two skeletal anlagen, may be responsible for the formation of joint tissues and structures including articular cartilage [Archer et al., 2003; Pacifici et al., 2005]. As articular cartilage matures under the influence of functional loading, the morphological, biochemical, and mechanical characteristics of the tissue are established. The zonal variations of articular cartilage result from the developmental history and local mechanical environment [Carter et al., 2004]. Whereas articular chondrocytes derived from joint cartilage retain a stable and permanent phenotype with the main task of maintaining cartilage matrix and joint function, transient

chondrocytes from the growth plate display a very dynamic phenotype undergoing proliferation, maturation, hypertrophy and eventually apoptosis followed by the replacement by bone cells. It has to be pointed out that current differentiation protocols mimic cartilage formation in the growth plate leading to the described transient chondrocyte phenotype.

The process of chondrogenesis *in vivo* is directed by a highly regulated consortium of growth factors and signaling molecules in addition to cell–cell, cell–matrix, and biomechanical factors [DeLise et al., 2000]. While it is not possible to include all of the known regulators of MSC differentiation in an *in vitro* culture system, current tissue engineering approaches incorporate selected elements of normal development to promote chondrogenesis. Such key factors are a high cell density and a round cell shape [Daniels and Solursh, 1991; Tacchetti et al., 1992]. This can be achieved by the use of micromass or pellet cultures, providing three-dimensional, closely packed cellular aggregates allowing cell-cell interactions analogous to those occur in pre-cartilage condensation [Johnstone et al., 1998; Mackay et al., 1998]. Additionally, growth factors, cytokines, and certain supplements, e.g. members of the TGF- β superfamily and dexamethasone, and mechanical forces have a profound influence on MSC differentiation [Hickok et al., 1998; Yoo et al., 1998; Carter et al., 1998]. MSCs undergoing *in vitro* chondrogenic differentiation also mature to the hypertrophic phenotype, presented by the expression of collagen type X, similar to the events in endochondral bone formation. But in contrast to the *in vivo* findings, *in vitro* no matrix mineralization occurs.

Translating the micro-scale cartilage formation by MSCs *in vitro*, i.e. micromass or pellet culture, to larger-scale cartilage tissue engineering is a current challenge of musculoskeletal regenerative medicine. First clinical case reports of implanted human MSCs into osteochondral defects have shown cartilage-like tissue formation to a certain extent [Wakitani et al., 2002; Adachi et al., 2005].

2.4 Scaffolds for cartilage tissue engineering

Modern cell-based therapies for articular cartilage repair combine cells with a biomaterial to deliver and retain cells at the site of injury. Such biomaterials must be biocompatible and should promote cellular differentiation and maturation. They must moreover have adequate structural and mechanical integrity to withstand the mechanical forces typically experienced at the joint surface until replacement by the repair tissue occurs. Both natural and synthetic scaffolds are employed, fabricated in a variety of forms, including fibrous and nanofibrous structures, porous sponges, woven or non-woven meshes, and hydrogels [Kuo et al., 2006]. Solid biodegradable scaffolds are used to achieve a high initial mechanical stability. Major classes of biodegradable scaffolds include synthetic polymers like polylactic acid (PLA), polyglycolic acid (PGA), and their copolymer PLGA, and natural polymers like collagen, hyaluronan, and silk [Frenkel and Di Cesare, 2004]. Several of these materials have been investi-

gated concerning their potential to facilitate chondrogenic differentiation of MSCs [Angele et al., 1999; Martin et al., 2001; Meinel et al., 2004; Li et al., 2005]. Especially fibrous collagen type I scaffolds have been extensively employed as carrier matrices for chondrocytes and MSCs, often displaying a non-uniform distribution of cells throughout the matrix [Ben-Yishay et al., 1995; Nehrer et al., 1998; Ponticello et al., 2000; Pieper et al., 2002; Farrell et al., 2006].

Hydrogels are another class of biomaterials, which can be made from natural polymers like collagen, hyaluronan, fibrin, agarose, alginate, or synthetic polymers like poly(ethylene glycol) or polypeptides [Lee and Mooney, 2001]. They are attractive for articular cartilage engineering because of their ability to absorb and release large amounts of water which allows nutrient and waste transport [Wallace and Rosenblatt, 2003; Park et al., 2007]. Furthermore, cells encapsulated within these matrices are uniformly distributed and exposed to a three-dimensional surrounding, which keeps them in a spherical morphology and allows cell-cell and cell-matrix interactions, important factors to induce or maintain a chondrogenic phenotype [Daniels and Solursh, 1991]. In particular, collagen type I is the most abundant protein in skeletal tissues and therefore exhibits excellent cell and tissue compatibility [Lee et al., 2001]. It can be readily extracted from animal tissues such as rat tail tendon or bovine calf skin and be dissolved in dilute acid. The collagen type I solution forms a hydrogel upon raising temperature and pH to physiological conditions. Chondrocytes embedded in collagen hydrogels gradually proliferated and maintained their chondrogenic phenotype [Uchio et al., 2000; Iwasa et al., 2003]. Furthermore, compared to fibrous collagen matrices, collagen hydrogels permitted a homogenous cell distribution and a higher collagen type II gene expression of human chondrocytes [Gavenis et al., 2006]. Based on these reports, collagen hydrogels are used clinically as carriers for chondrocytes to repair cartilage defects [Ochi et al., 2002; Nöth et al., 2006; Andereya et al., 2007]. Using hMSCs as an alternative cell source for future cell-based therapies, several *in vitro* studies have already demonstrated the chondrogenic differentiation of hMSCs in collagen hydrogels [Yokoyama et al., 2005; Yoneno et al., 2005; Nöth et al., 2007]. However, the implantation of uncommitted MSCs embedded in hydrogels in different animal models improved the early healing response, but demonstrated significant long-term limitations, including thinning and fibrillation of the repair tissue by 6 to 8 months post-implantation [Wakitani et al., 1994; Wilke et al., 2007]. Unlike these reports, Yamazoe et al. [2007] observed no cartilage repair at all but a remarkable regeneration of the subchondral bone by the implanted MSCs. These studies indicate that the *in vivo* environment is not sufficient to promote chondrogenesis.

2.5 Bioreactor cultivation for cartilaginous tissue growth

To enhance the growth and quality of tissue-engineered cartilaginous constructs, bioreactor systems have been developed providing conditions to fabricate more functional tissue structures [Darling and Athanasiou, 2003]. Bioreactors are designed to optimize nutrient and gas supply to the cells in 3D matrices, especially if cells are to be maintained within larger constructs and at high density. External mass-transfer limitations can be reduced by the use of hydrodynamic bioreactors such as stirred spinner flasks or rotating wall vessels, where construct tumbling ensures efficient nutrient transport, or with direct perfusion bioreactors in which medium flows directly through the pores of the scaffold [Martin et al., 2004]. The flow conditions in bioreactors, both rotational and perfusion create mechanical and hydrodynamic forces that provide stimulation to the cells and influence cellular activity and phenotype with improvement of matrix composition and compressive properties of engineered cartilage tissues [Vunjak-Novakovic et al., 1999; Pazzano et al., 2000]. However, the effects of direct perfusion, rate of mass transfer and the level of shear stress to which the cells are exposed, are highly dependent on the medium flow-rate and the maturation stage of the constructs, as recently demonstrated for 3D cultures of chondrocytes [Davisson et al., 2002].

In vivo, articular cartilage is subject to several physical forces such as compression, fluid flow, and hydrostatic pressure, which modulate cellular proliferation, matrix metabolism, and matrix content in order to maintain the healthy status. Static compression, which causes constant tissue deformation at steady state, has been shown to inhibit matrix synthesis in articular cartilage explants [Sah et al., 1989; Guilak et al., 1994; Kim et al., 1996]. In contrast, the effects of dynamic compressive loading on metabolic activity show large variations [Sah et al., 1989; Steinmeyer and Knue, 1997; Wong et al., 1999]. Some studies have demonstrated an increase in biosynthetic activity, primarily proteoglycan synthesis [Parkkinen et al., 1992; Kim et al., 1994], while others have documented an inhibitory effect of dynamic loading with denaturation of collagen and cartilage degradation [Steinmeyer and Knue, 1997; Thibault et al., 2002]. These results reveal the complex response of the tissue to dynamic loading, dependent on many factors such as frequency and amplitude of compression [Sah et al., 1989]. It is generally assumed that the amount of intra-tissue fluid flow and matrix consolidation, which results from a specific loading protocol, is a key determinant of the biosynthetic response. The application of dynamic compressive loading in a moderate physiological range has been demonstrated to enhance cartilage-specific matrix synthesis in articular cartilage plugs *ex vivo*. Consistent with these findings there is evidence that mechanical stress as an important modulator of cell physiology may be used to improve or accelerate tissue regeneration and repair *in vitro* [Guilak et al., 2001]. Several tissue engineering studies have been well demonstrated that chondrocytes in a three-dimensional hydrogel respond to mechanical loading by increasing matrix synthesis and improving functional mechanical properties

[Buschmann et al., 1995; Lee and Bader, 1997; Chowdhury et al., 2003; Hung et al., 2004; Kisiday et al., 2004]. The applied loading regimes varied dramatically in strain amplitude (3-20%), frequency (0.01-3.0 Hz), and stimulation (1-10 hours per day) and overall cultivation time (2-39 days). The results of these studies suggest that the amplitude, frequency, seeding density, and duration of loading influence the outcome [Chowdhury et al., 2003; Hung et al., 2004; Kisiday et al., 2004]. In general, moderate magnitude loads applied at higher frequencies (0.3-1.0 Hz) showed a positive stimulus on chondrogenesis [Buschmann et al., 1995; Lee and Bader, 1997].

In addition to deformation, compressive loading results in fluid pressurization with increasing hydrostatic pressure arising from the small pore size and the high water content of the articular cartilage tissue [Kuo et al., 2006]. Chondrocytes respond to hydrostatic pressure with increasing production of ECM [Hall et al., 1991; Carver and Heath, 1999; Mizuno et al., 2002]. Based on important *in vivo* observations on the regeneration of full-thickness articular cartilage defects recent studies now investigated the influence of mechanical loading on mesenchymal stem cells. In highly loaded joint areas the cyclic hydrostatic compressive stress created during movement causes differentiation down the chondrogenic pathway, producing new cartilage [Carter et al., 1998; Tagil and Aspenberg, 1999]. *In vitro*, a few studies demonstrated an acceleration of chondrogenesis upon dynamic mechanical loading in MSC-seeded constructs in the presence of TGF- β [Angele et al., 2004; Huang et al., 2004a]. Furthermore, previous studies provided evidence that specific mechanical forces (hydrostatic pressure or compressive loading) applied to MSC-seeded constructs might not only enhance the development of an engineered tissue but also direct the differentiation of multipotent cells along the chondrogenic lineage [Miyamishi et al., 2006; Mauck et al., 2007; Terraciano et al., 2007]. Because of the complexity of physical forces applied by simple compression, the exact physical stimulus responsible for the stimulation is difficult to discriminate and has not been clearly identified. However, the stimulatory signals that modulate cellular response may include cell deformation, fluid shear, increased interstitial pressure and physicochemical changes including altered matrix water content, fixed charge density, mobile ion concentrations, and osmotic pressure. Any of these mechanical, chemical, or electrical signals may modulate matrix metabolism [Mow et al., 1999; Grodzinsky et al., 2000]. Additionally, dynamic loading conditions increase the mass transport of nutrients, signaling molecules and oxygen which can interact synergistically with the mechanical signals to facilitate cell proliferation and matrix synthesis. Current approaches focus on the development of devices that combine the advantages of several mechanical stimuli in a single bioreactor in order to elicit a yet better response from the cells. Combinations of hydrodynamic reactors and compressive loading have been proposed to couple the positive influence of enhanced nutrient transport with the

application of mechanical forces to direct cellular activity and phenotype [Démarteau et al., 2003; Seidel et al., 2004].

The use of bioreactors in applying mechanical forces to 3D constructs means an important step towards the development of functional grafts through enhancing cell differentiation and/or extracellular matrix deposition in engineered tissues for the treatment of lost or damaged body parts. Furthermore, engineered tissues could provide reliable *in vitro* model systems to facilitate a fundamental understanding of the effects of physical forces on developing tissues, and to predict the responses of an engineered tissue to physiological forces on surgical implantation [Martin et al., 2004].

2.6 Cellular imaging

An important issue to successfully develop stem cell-based therapies is to localize and monitor migration of the transplanted cells in the repair tissue. Today, cellular imaging is an established technique to monitor cell behavior *in vivo*. It can be defined as the 'non-invasive and repetitive imaging of targeted cells and cellular processes in living organisms' [Bulte and Kraitchman, 2004]. In the future, this technique should avoid invasive and irreversible tissue removal procedures, which are necessary for traditional histopathological methods of cell detection. Among different imaging modalities, magnetic resonance imaging (MRI) stands out in terms of resolution and whole body imaging. MRI is already in clinical use for injury and disease diagnosis on the anatomic scale. In combination with an efficient labeling method, MRI allows imaging in real-time at the cellular and even molecular level [Thorek et al., 2006].

2.6.1 Use of superparamagnetic iron oxide particles for MR imaging

Superparamagnetic iron oxide (SPIO) particles can be used to label cells in order to distinguish them from the surrounding tissue. Furthermore, based on the simple detection of these particles by light and electron microscopy, a correlation between MR imaging and conventional histology is possible to validate SPIO-enhanced MRI in preclinical studies. SPIO particles have been applied as magnetic contrast agents for over 20 years. They provide the targeted cell with a large magnetic moment that creates substantial disturbances in the local magnetic field, leading to a rapid dephasing of protons, including those not directly in the vicinity of the targeted cell [Bulte et al., 2004a]. This results in a strong decrease in the transverse relaxation time constant T_2^* and labeled cells become detectable as hypointense dark spots in T_2^* -weighted MR images. SPIO particles are biocompatible because of their biodegradable iron oxide core and their appropriate surface coating which allows intracellular incorporation and degradation using normal biochemical pathways for iron metabolism [Bulte and Kraitchman, 2004].

SPIO-based imaging of macrophage activity was the initial and is still the most significant clinical application in this field, in particular for tumor staging of the liver and lymph nodes [Harisinghani et al., 2001; Anzai et al., 2003]. As a valuable tool in preclinical research, various non-phagocytic cells, including MSCs, were previously labeled in culture with SPIO particles [Arbab et al., 2003a; Daldrup-Link et al., 2003; Jendelová et al., 2003; Frank et al., 2004; Rivière et al., 2005]. SPIO labeling was demonstrated to have no negative influence on the viability of magnetically labeled MSCs [Bos et al., 2004; Ju et al., 2006; Terrovitis et al., 2006]. Investigations on the proliferation rates of SPIO-labeled MSCs, however, showed in some studies no influence [Arbab et al., 2004; Ittrich et al., 2005], whereas other studies reported a slight inhibition [Bos et al., 2004; Terrovitis et al., 2006]. Furthermore, the differentiation of MSCs, especially the chondrogenic differentiation, has been controversially discussed in previous studies. No alteration in the differentiation capacity of human MSCs was demonstrated by Arbab et al. [2004, 2005b]. In contrast, Kostura et al. [2004] showed similar results concerning adipogenic and osteogenic differentiation, but a marked inhibition of chondrogenesis in human MSCs, using the same SPIO particles.

The particle size, as well as the surface coating material, has an influence on the cellular uptake of the particles [Wilhelm et al., 2003; Matuszewski et al., 2005; Sun et al., 2005]. SPIO particles with a diameter more than 60 nm are incorporated to a higher degree in different cell lines than ultrasmall SPIO (USPIO) particles with a diameter of approximately 10 to 40 nm, using particles with carboxydextran as a coating material [Matuszewski et al., 2005; Sun et al., 2005]. Dextran is the most common used coating, although a wide variety of SPIO particles with other coating materials have been developed showing different uptake efficiencies [Gupta and Gupta, 2005]. However, dextran-coated particles are only poorly incorporated into the cell because of a relatively inefficient fluid-phase endocytosis pathway. Therefore, several strategies have been developed to optimize SPIO particle uptake including the improvement of surface coating by functionalization with specific ligands, such as antibodies, transferrin, or the membrane-translocating signal peptide HIV-1 Tat [Lewin et al., 2000; Bulte et al., 2001; Ahrens et al., 2003]. Another possibility to improve particle incorporation is the use of transfection agents, which form highly-charged complexes with the SPIO particles, facilitating the interaction with anionic sites on the cell membrane thereby stimulating endocytosis [Arbab et al., 2003a; Frank et al., 2003; Montet-Abou et al., 2007].

2.6.2 Labeling of cells with very small superparamagnetic iron oxide particles (VSOPs) for cellular MR imaging

The so called very small superparamagnetic iron oxide particles (VSOPs) used in the present study have a total diameter of 11 nm including an iron oxide core of 5 nm (Fig. 3) [Pilgrimm, 2003]. They are coated with citrate bearing negative surface charges.

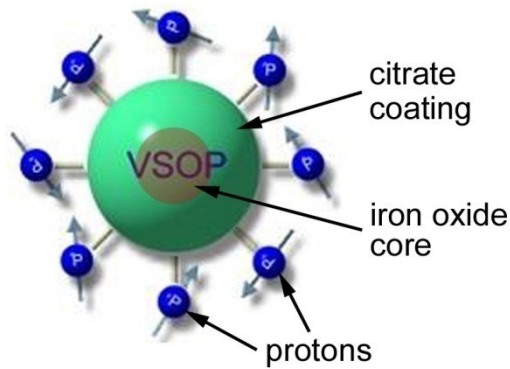


Fig. 3 Schematic figure of VSOP.

Protons are in close contact with the iron oxide core due to the small diameter of the citrate coating.

Modified from www.ferropharm.de.

Citrate is a natural occurring substance in mammals, which can be metabolized by them, thus providing high biocompatibility. In contrast to transfection agent-supported particle uptake, those anionic nanoparticles are probably incorporated by the cells via adsorptive endocytosis, mediated by strong and non-specific electrostatic interactions of the particles with cationic sites on the plasma membrane [Wilhelm et al., 2003]. A previous study has been proven that the use of VSOPs led to a pronounced incorporation of label into cells compared to conventional dextran-coated USPIO particles [Fleige et al., 2002]. So far, VSOPs were successfully employed to label and monitor embryonic stem cells in the rat brain [Stroh et al., 2005] and spleen-derived mononuclear cells in the ischemic mouse brain [Stroh et al., 2006]. In contrast to other SPIO particles, no addition of transfection agents is necessary, which are mostly not clinically approved and possibly capable to alter cell function. The small particle size of VSOPs should minimize possible negative effects on the stem cell function of hMSCs, especially on the chondrogenic differentiation capacity.

2.7 Objective of the study

In attempting to use stem cells as an alternative for chondrocytes in articular cartilage repair, the development of well-defined and efficient protocols for directing stem cell differentiation into the chondrogenic lineage *in vitro* is of utmost importance. To provide a three-dimensional surrounding where the cells can differentiate and incorporate new extracellular matrix molecules, hMSCs were seeded in a collagen type I hydrogel, which is already in clinical use for ACT. The transplantation of well-differentiated hMSCs in a 3D matrix is also likely to result in higher engraftment efficiency and better integration within recipient cartilaginous tissues.

A recent study from our group has already shown that hMSCs embedded in a collagen type I hydrogel are able to undergo chondrogenic differentiation [Nöth et al., 2007]. However, histological analyses revealed only dotted staining around individual cells and no homogeneous cartilage-specific protein accumulation throughout the constructs. The purpose of this study was therefore first to improve the culture conditions of hMSCs in collagen hydrogels both in terms of cellular survival and proliferation and differentiation into the chondrogenic lineage. In

detail, the effects of cell density and variations in culture media compositions were evaluated. These investigations should respond to the question whether hMSC are really able to produce a fully differentiated cartilaginous construct comparable to those derived from articular chondrocytes.

Additionally, after the establishment of optimized culture conditions for the fabrication of an hMSC-based incompletely developed engineered tissue, this construct could be employed as an *in vitro* model to predict the responses of such a tissue to mechanical stimulation. To address this issue, the second objective was to investigate the potential of a specific bioreactor system to induce chondrogenic differentiation of hMSCs in collagen hydrogels without additional chondrogenic supplements, i.e. TGF- β . If an impact of chondrogenesis in immature tissue engineered constructs due to mechanical stimulation would be demonstrated, this information could provide further knowledge which may benefit future approaches to the engineering of hMSC-based constructs for articular cartilage tissue repair.

To complete the development of a stem cell-based therapy, the localization of the transplanted cells is of great importance. Therefore, the third objective of this study was to visualize magnetically labeled hMSCs embedded in collagen hydrogels with the use of high-resolution MRI. To exclude a possible influence of the labeling procedure on cellular activity, a systematic evaluation of the viability, proliferation and differentiation capacity of VSOP-labeled hMSCs compared to unlabeled cells was performed. With this labeling technique, the non-invasive assessment of the transplanted cell distribution and migration in the target tissue, can be analyzed.

3 Materials and methods

3.1 Materials

3.1.1 Consumables

20-gauge needle	B. Braun, purchased from A. Hartenstein GmbH, Würzburg, Germany
Cell culture flasks (175 cm ²)	Greiner Bio-One GmbH, Frickenhausen, Germany
Cell culture flasks (25 cm ² , 150 cm ²)	TPP, purchased from Biochrom AG, Berlin, Germany
Cell culture plates (6-, 12-, 24-, and 96-well)	Greiner Bio-One GmbH, Frickenhausen, Germany
96-well assay plates	Corning, purchased by Schubert&Weiss GmbH, Munich, Germany
Cell strainers (70 µm)	BD Falcon, purchased from A. Hartenstein GmbH, Würzburg, Germany
Centrifugation tubes (15 ml, 50 ml)	TPP, purchased from Biochrom AG, Berlin, Germany
Lab-Tek Chamber Slides, Permanox, (2-, 4-, and 8-well)	Nunc, purchased from A. Hartenstein GmbH, Würzburg, Germany
Microscope slides	Marienfeld Laboratory Glassware, purchased from A. Hartenstein GmbH, Würzburg, Germany
Microscope cover slides	Marienfeld Laboratory Glassware, purchased from A. Hartenstein GmbH, Würzburg, Germany
Pasteur pipettes	A. Hartenstein GmbH, Würzburg, Germany
PCR tubes	Biozym, Hess. Oldendorf, Germany
Pipette tips	Brandt, purchased from Laug & Scheller GmbH, Kürnach, Germany
Plastic pipettes, serological	Sarstedt AG & Co., Nümbrecht, Germany
poly-L-lysine coated microscope slides	Menzel-Gläser, purchased from A. Hartenstein GmbH, Würzburg, Germany
Reaction tubes (1.5 ml)	Sarstedt AG & Co., Nümbrecht, Germany
Scalpel	Bayha, purchased from A. Hartenstein GmbH, Würzburg, Germany
Sterile filter (0.2 µm)	Carl Roth GmbH & Co. KG, Karlsruhe, Germany
UVettes	Eppendorf AG, Hamburg, Germany

3.1.2 Chemicals and reagents

2-propanol	Carl Roth GmbH & Co. KG, Karlsruhe, Germany
3-isobutyl-1-methylxanthine (IBMX)	AppliChem, purchased from A. Hartenstein GmbH, Würzburg, Germany
4',6-diamidino-2-phenylindole-dihydrochlorid (DAPI)	Invitrogen, Karlsruhe, Germany
β-mercaptoethanol	AppliChem, purchased from A. Hartenstein GmbH, Würzburg, Germany
Acetic acid	Merck KGaA, Darmstadt, Germany
Acetone	AppliChem, purchased from A. Hartenstein GmbH, Würzburg, Germany
Agar	Merck KGaA, Darmstadt, Germany
Agarose multi-purpose	Bioline GmbH, Luckenwalde, Germany
Alcian blue	Sigma-Aldrich Chemie GmbH, Schnelldorf, Germany

Alizarin red S	Chroma-Gesellschaft Schmidt & Co., Stuttgart, Germany
Aluminum sulfate	Merck KGaA, Darmstadt, Germany
Aluminum potassium sulfate	Merck KGaA, Darmstadt, Germany
Ammonia	Merck KGaA, Darmstadt, Germany
Amyl acetate	Merck KGaA, Darmstadt, Germany
Antibody dilution buffer	DCS, Hamburg, Germany
Aquatex®	Merck KGaA, Darmstadt, Germany
Boric acid	Merck KGaA, Darmstadt, Germany
Bovine serum albumin fraction V (BSA)	AppliChem, purchased from A. Hartenstein GmbH, Würzburg, Germany
Chloral hydrate	Merck KGaA, Darmstadt, Germany
Chloroform	Carl Roth GmbH & Co. KG, Karlsruhe, Germany
Citric acid	Merck KGaA, Darmstadt, Germany
Dexamethasone	Sigma-Aldrich Chemie GmbH, Schnelldorf, Germany
Dimethylsulfoxide (DMSO)	AppliChem, purchased from A. Hartenstein GmbH, Würzburg, Germany
dNTP Mix	Bioline GmbH, Luckenwalde, Germany
Dulbecco's phosphate buffered saline (PBS) powder	Biochrom AG, Berlin, Germany
Entellan	Merck KGaA, Darmstadt, Germany
Eosin	Merck KGaA, Darmstadt, Germany
Ethanol	AppliChem, purchased from A. Hartenstein GmbH, Würzburg, Germany
Ethanol, denatured	Carl Roth GmbH & Co. KG, Karlsruhe, Germany
Ethidium bromide	AppliChem, purchased from A. Hartenstein GmbH, Würzburg, Germany
Ethylendiamintetraacetic acid (EDTA)-Tetrasodium salt hydrate	Calbiochem, purchased from A. Hartenstein GmbH, Würzburg, Germany
Fluoromount-G™	SouthernBiotech, purchased by Biozol, Eching, Germany
Glycerol 2-phosphate disodium salt hydrate	Sigma-Aldrich Chemie GmbH, Schnelldorf, Germany
Glycerol gelatine	Sigma-Aldrich Chemie GmbH, Schnelldorf, Germany
Hematoxylin	Carl Roth GmbH & Co. KG, Karlsruhe, Germany
Horse serum	PAA Laboratories GmbH, Pasching, Austria
HPLC water	Carl Roth GmbH & Co. KG, Karlsruhe, Germany
Hydrochloric acid	Merck KGaA, Darmstadt, Germany
Hydrogen peroxide	Merck KGaA, Darmstadt, Germany
Indomethacin	Sigma-Aldrich Chemie GmbH, Schnelldorf, Germany
Insulin from bovine pancreas	Sigma-Aldrich Chemie GmbH, Schnelldorf, Germany
Iron multi-cation standard VI ITS-plus	Merck KGaA, Darmstadt, Germany
L-ascorbic acid 2-phosphate sesquimagnesium salt	Sigma-Aldrich Chemie GmbH, Schnelldorf, Germany
LE agarose	Biozym Scientific GmbH, Hessisch-Oldendorf, Germany
Levamisole	DakoCytomation GmbH, Hamburg, Germany
Methanol	AppliChem, purchased from A. Hartenstein GmbH, Würzburg, Germany
Mouse serum	PAA Laboratories GmbH, Pasching, Austria
Nitric acid, 65%, ultrapure	Merck KGaA, Darmstadt, Germany
Nuclear fast red	Merck KGaA, Darmstadt, Germany
Oilred O	Merck KGaA, Darmstadt, Germany
Osmium tetroxide	Sigma-Aldrich Chemie GmbH, Schnelldorf, Germany
Paraffin	Carl Roth GmbH & Co. KG, Karlsruhe, Germany

Paraformaldehyde	Merck KGaA, Darmstadt, Germany
PBS Dulbecco w/o Ca ²⁺ , Mg ²⁺	Biochrom, Berlin, Germany
PBS Dulbecco with Ca ²⁺ , Mg ²⁺	PAA Laboratories GmbH, Pasching, Austria
Pepsin	Sigma-Aldrich Chemie GmbH, Schnelldorf, Germany
peqGOLD 100 bp DNA Ladder Plus	PEQLAB Biotechnologie GmbH, Erlangen, Germany
Potassium ferrocyanide	Merck KGaA, Darmstadt, Germany
Proline	Sigma-Aldrich Chemie GmbH, Schnelldorf, Germany
Random hexamers	GE Healthcare, Munich, Germany
Sodium chloride	AppliChem, purchased from A. Hartenstein GmbH, Würzburg, Germany
Sodium hydroxide solution	AppliChem, purchased from A. Hartenstein GmbH, Würzburg, Germany
Sodium iodate	Merck KGaA, Darmstadt, Germany
Sodium pyruvate	Sigma-Aldrich Chemie GmbH, Schnelldorf, Germany
Transforming growth factor β -1 (TGF- β 1)	R&D Systems, Wiesbaden, Germany
Tris(hydroxymethyl)-aminomethan (Tris base)	AppliChem, purchased from A. Hartenstein GmbH, Würzburg, Germany
Trizol	Invitrogen, Karlsruhe, Germany
Trypan blue	Sigma-Aldrich Chemie GmbH, Schnelldorf, Germany
Tween 20	Merck KGaA, Darmstadt, Germany
VSOP C200	Ferropharm, Teltow, Germany
WST-1 reagent	Roche Diagnostics GmbH, Mannheim, Germany
Xylole	Merck KGaA, Darmstadt, Germany

3.1.3 Cell culture media and additives

DMEM/Ham's F-12 with L-Glutamine (3.2 g/l glucose)	PAA Laboratories GmbH, Pasching, Austria
DMEM high glucose (4.5 g/l) with L-Glutamine	PAA Laboratories GmbH, Pasching, Austria
Fetal bovine serum (FBS)	PAA Laboratories GmbH, Pasching, Austria
Fetal bovine serum (FBS)	Gibco, purchased from Invitrogen, Karlsruhe, Germany
Penicillin/streptomycin 100x	PAA Laboratories GmbH, Pasching, Austria

Additive stock solution

L-ascorbic acid 2-phosphate sesquimagnesium salt (50 mg/ml)

in distilled water, sterile filtered, stored in aliquots at -20 °C

Dexamethasone (1 mM)

in ethanol, stored in aliquots at -80 °C

Glycerol 2-phosphate disodium salt hydrate (1 M)

in distilled water, sterile filtered, stored in aliquots at -20 °C

Indomethacin (100 mM)

in DMSO, stored in aliquots at -20 °C

Insulin from bovine pancreas (1 mg/ml)

in 0.05% acetic acid, sterile filtered, stored in aliquots at -20 °C

3-isobutyl-1-methylxanthine (IBMX, 500 mM)

in DMSO, stored in aliquots at -20°C

Proline (40 mg/ml)

in distilled water, sterile filtered, stored in aliquots at -20°C

Sodium pyruvate (100 mg/ml)

in distilled water, sterile filtered, stored in aliquots at -20°C

TGF-β1 (10 µg/ml)

in 4 mM hydrochloric acid containing 1 mg/ml BSA, stored in aliquots at -20°C for up to 3 months

3.1.4 Components for the fabrication of collagen hydrogels

The following components for the fabrication of collagen hydrogels were provided by Arthro Kinetics AG (Esslingen, Germany):

- collagen type I stock solution, extracted from rat tails and dissolved in acetic acid at a concentration of 6 mg/ml collagen type I, pH = 4.0
- gel neutralization solution consisting of HEPES-buffered, double concentrated DMEM/Ham's F-12
- gel neutralization solution consisting of HEPES-buffered, threefold concentrated DMEM/Ham's F-12

Prior to use, 20% FBS were added to the gel neutralization solution consisting of double concentrated DMEM/Ham's F-12 (termed "2x GNS Ham F1").

30% FBS were added to the gel neutralization solution consisting of threefold concentrated DMEM/Ham's F-12 (termed "3x GNS").

3.1.5 Antibodies**Tab. 1 Antibodies used for the phenotypic characterization of hMSCs**

Clone	Antigen	Concentration of use
TÜK4	CD14 (lipopolysaccharide receptor)	1.15 µg/ml
BIRMA-K3	CD34 (early hematopoietic stem cell marker)	3.5 µg/ml
DF1485	CD44 (hyaluronate receptor)	2 µg/ml
T29/33	CD45 (leukocyte common antigen)	4.8 µg/ml
F15-42-1	CD90 (Thy-1)	4 µg/ml
SN6h	CD105 (TGF-β receptor endoglin)	5.25 µg/ml

All these antibodies were purchased from DakoCytomation GmbH (Hamburg, Germany). The antibodies were diluted in antibody dilution buffer.

The primary antibody for collagen type II (clone II-4C1) was purchased from Acris (Hiddenhausen, Germany), and was used at a concentration of 714 ng/ml.

3.1.6 Enzymes

2.5% Trypsin (10x concentrate)	PAA Laboratories GmbH, Pasching, Austria
Collagenase NB4	Serva Electrophoresis, Heidelberg, Germany
BioScript Reverse Transcriptase	Bioline GmbH, Luckenwalde, Germany
MangoTaq DNA polymerase	Bioline GmbH, Luckenwalde, Germany

3.1.7 Primers

All primer sets were already established in the laboratory. Whenever possible, they were designed to span different exons to exclude false positive detection of DNA contaminants in the RNA specimens.

Tab. 2 Sequences of primer sets used for gene expression analyses and expected product sizes

Primer sequences	Product size (bp)	Sequence ID ^a	T _A ^b (°C)
Housekeeping gene			
eukaryotic translation elongation factor 1 alpha 1 (EF1α)	235	NM_001402	54
sense: 5'-AGGTGATTATCCTGAACCATCC-3'			
antisense: 5'-AAAGGTGGATAGTCTGAGAAGC-3'			
Adipose-specific genes			
lipoprotein lipase (LPL)	276	NM_000237	51
sense: 5'-GAGATTTCTCTGTATGGCACC-3'			
antisense: 5'-CTGCAAATGAGACACTTTTCTC-3'			
peroxisome proliferator-activated receptor, gamma 2 (PPARγ2)	351	NM_015869	51
sense: 5'-GCTGTTATGGGTGAAACTCTG-3'			
antisense: 5'-ATAAGGTGGAGATGCAGGCTC-3'			
Bone-specific genes			
alkaline phosphatase (ALP)	454	NM_000478	51
sense: 5'-TGGAGCTTCAGAAGCTCAACACCA-3'			
antisense: 5'-ATCTCGTTGTCTGAGTACCAGTCC-3'			
bone sialoprotein (BSP)	450	NM_004967	54
sense: 5'-AATGAAAACGAAGAAAGCGAAG-3'			
antisense: 5'-ATCATAGCCATCGTAGCCTTGT-3'			
collagen type I, alpha 2 (Col I)	461	NM_000089	52
sense: 5'-GGACACAATGGATTGCAAGG-3'			
antisense: 5'-TAACCACTGCTCCACTCTGG-3'			
secreted phosphoprotein 1 (OP)	483/ 525	NM_000582/ NM_001040058	51
sense: 5'-ACGCCGACCAAGGAAAACCTC-3'			
antisense: 5'-GTCCATAAACCCACACTATCAG-3'			
Cartilage-specific genes			
aggrecan 1 (AGN)	392	NM_013227	54
sense: 5'-GCCTTGAGCAGTTCACCTTC-3'			
antisense: 5'-CTCTTCTACGGGGACAGCAG-3'			
biglycan (BGN)	213	NM_001711	53
sense: 5'-ACAGTGGCCTTTGAACCTGGA-3'			
antisense: 5'-TCATCCTGATCTGGTTGTGG-3'			
cartilage oligomeric matrix protein (COMP)	312	NM_000095	54
sense: 5'-CAGGACGACTTTGATGCAGA-3'			
antisense: 5'-AGGCTGGAGCTGTCCTGGTA-3'			

Primer sequences	Product size (bp)	Sequence ID ^a	T _A ^b (°C)
Cartilage-specific genes			
collagen type II, alpha 1 (Col II)	374	NM_033150	58
sense: 5'-TTTCCCAGGTCAAGATGGTC-3'			
antisense: 5'-CTTCAGCACCTGTCTCACCA-3'			
collagen type X, alpha 1 (Col X)	468	NM_000493	54
sense: 5'-CCCTTTTGGCTGCTAGTATCC-3'			
antisense: 5'-CTGTTGTCCAGGTTTTCTGGCAC-3'			
collagen type XI, alpha 1 (Col XI)	495	NM_080630	57
sense: 5'-ACTTCTGACTGCCTCTGCTC-3'			
antisense: 5'-GCTTTTGCCATGTGATTCTGCC-3'			
SRY (sex determining region Y) - box 9 (SOX9)	263	NM_000346	58
sense: 5'-ATCTGAAGAAGGAGAGCGAG-3'			
antisense: 5'-CAAGCTCTGGAGACTTCTGA-3'			
Matrix turnover-specific genes			
Matrix metalloproteinase 3 (MMP3)	388	NM_002422	55
sense: 5'-CACTTCAGAACCTTTCCTGGCATC-3'			
antisense: 5'-GCTTCAGTGTTGGCTGAGTG-3'			
Matrix metalloproteinase 13 (MMP13)	166	NM_002427	54
sense: 5'-AACATCCAAAACGCCAGAC-3'			
antisense: 5'-GGAAGTTCTGGCCAAAATGA-3'			
TIMP metalloproteinase inhibitor 1 (TIMP1)	165	NM_003254	57
sense: 5'-TGACATCCGGTTCGTCTACA-3'			
antisense: 5'-GCTAAGCTCAGGCTGTTCCA-3'			

^a reference sequence ID of the NCBI data base

^b annealing temperature T_A

Due to the existence of alternative splice variants of the secreted phosphoprotein 1 (OP) mRNA, two PCR products of different length can be generated.

3.1.8 Buffers and other solutions

Solutions for cell culture

1x PBS

9.55 g PBS Dulbecco w/o Ca²⁺, Mg²⁺
ad 1 l distilled water
pH adjusted to 7.4 and autoclaved

1x PBS/EDTA

9.55 g PBS Dulbecco w/o Ca²⁺, Mg²⁺
0.2 g EDTA tetrasodium salt hydrate
ad 1 l distilled water
pH adjusted to 7.4 and autoclaved

0.25% Trypsin

5 ml 2.5% trypsin (sterile)
ad 50 ml 1x PBS

1.25 U/ml Collagenase

in PBS with Ca²⁺, Mg²⁺
sterile filtered, stored in aliquots at -20 °C

Solutions for molecular biology10x TBE

108 g Tris base
55 g boric acid
9.05 g EDTA tetrasodium salt hydrate
ad 1 l distilled water
pH adjusted to 8.3 and autoclaved

Solutions for histology4% phosphate-buffered paraformaldehyde (PFA)

4 g paraformaldehyde were dissolved in about 75 ml 1x PBS, heated on a magnetic stirrer to 55-60°C and left on this temperature for 5 min. Sodium hydroxide was added until the solution became clear (approximately 100 to 150 µl). After cooling down to room temperature, the pH was adjusted to 7.4 and the solution was filled up to 100 ml with 1x PBS.

Hemalaun solution

6 g hematoxylin
1 g sodium iodate
250 g aluminum potassium sulfate
250 g chloral hydrate
5 g citric acid
ad 5 l distilled water

1% eosin solution

1 g eosin
ad 100 ml distilled water and one drop of acetic acid

0.5% oilred O stock solution

0.5 g oilred O
ad 100 ml 99% 2-propanol
0.3% oilred O working solution was prepared by mixing 6 parts stock solution with 4 parts distilled water, incubated over night and filtrated before use.

1% alizarin red S staining solution

0.25 g alizarin red S dye
ad 25 ml distilled water and 250 µl 25% ammonia

Nuclear fast red solution

5 g aluminum sulfate were dissolved in 100 ml distilled water and boiled on a magnetic stirrer. After addition and dissolution of 0.1 g nuclear fast red the solution was cooled down to room temperature and filtrated before use.

Solutions for immunohistochemistryWashing buffer

Stock solution: 10xTBS (0.5 M), pH 7.6

60.6 g Tris base
87.66 g sodium chloride
ad 1 l distilled water

pH adjusted to 7.6 and autoclaved

Working solution: 1x TBS (0.05 M), pH 7.6

1:10 dilution of 10x TBS, supplemented with 0.5% Tween 20

Blocking solution

1 g BSA
2.5 ml horse serum
ad 50 ml 1x TBS

1 M Tris-HCl, pH 2.0

121.14 g Tris base
ad 1 l distilled water
pH adjusted to 2.0 by addition of hydrochloric acid

3.1.9 Kits

BioGenex Super Sensitive™ Link-Label IHC Detection System	DCS, Hamburg, Germany
Caspase-Glo® 3/7 Assay	Promega, Mannheim, Germany
Live/Dead Viability stain	Mobitec, Göttingen, Germany
Nucleospin® RNA II isolation kit	Macherey-Nagel GmbH & Co. KG, Düren, Germany

3.1.10 Equipment

Accu-jet pipettor	Brand, purchased from A. Hartenstein GmbH, Würzburg, Germany
Autoclave H+P varioclave steam sterilizer	Thermo Electron GmbH, Oberschleißheim, Germany
AxioCam MRc digital camera	Carl Zeiss Jena GmbH, Jena, Germany
BioPhotometer	Eppendorf AG, Hamburg, Germany
Bruker Avance 500 MRI system	Bruker BioSpin GmbH, Rheinstetten, Germany
Centrifuge Heraeus Biofuge pico	Thermo Electron GmbH, Oberschleißheim, Germany
Centrifuge Heraeus Labofuge 400	Thermo Electron GmbH, Oberschleißheim, Germany
CO ₂ incubator Heraeus B5060	Thermo Electron GmbH, Oberschleißheim, Germany
Electron microscope EM10	Carl Zeiss Jena GmbH, Jena, Germany
Electrophoresis power supplies	Bio-Rad Laboratories GmbH, Munich, Germany
Freezer Bosch Economic (-20 °C)	Bosch GmbH, Gerlingen-Schillerhöhe, Germany
Freezer IIShin (-80 °C)	Nunc GmbH & Co. KG, Wiesbaden, Germany
Glassware	Schott, purchased from A. Hartenstein GmbH, Würzburg, Germany
Heating block	Boekel Scientific, purchased from A. Hartenstein GmbH, Würzburg, Germany
Hemocytometer Neubauer	Marienfeld Laboratory Glassware, purchased from A. Hartenstein GmbH, Würzburg, Germany
Hot air sterilizer Heraeus	Thermo Electron GmbH, Oberschleißheim, Germany
Horizontal mini gel electrophoresis system EasyCast Model B2	Owl Separation Systems, Portsmouth, USA
Laboratory dishwasher	Miele & Cie. KG, Gütersloh, Germany
Laminar airflow cabinet HERA safe	Thermo Electron GmbH, Oberschleißheim, Germany
Luminometer	Berthold Detection Systems, Pforzheim, Germany
Magnetic stirrer and heater	A. Hartenstein GmbH, Würzburg, Germany
Mass spectrometer Varian	Varian, Darmstadt, Germany
Micro-pipettes	ABIMED Analysentechnik GmbH, Langenfeld, Germany

Microscopes: Axiovert 25, Axioskop, and Axioskop 2 MOT	Carl Zeiss Jena GmbH, Jena, Germany
Microtome RM2125RT	Leica, Wetzlar, Germany
pH-meter inolab pH level 1	WTW, purchased from A. Hartenstein GmbH, Würzburg, Germany
Photometer SLT Spectra Classic	Tecan Deutschland GmbH, Crailsheim, Germany
Refrigerator Fresh Center	Bosch GmbH, Gerlingen-Schillerhöhe, Germany
Thermal cycler PTC-200	MJ Research, purchased from Biozym Scientific GmbH, Hessisch Oldendorf, Germany
Thermal printer	Seico, purchased from -ltf- Labortechnik GmbH & Co. KG, Wasserburg, Germany
Vacuum pump system	Vacuubrand, purchased from A. Hartenstein GmbH, Würzburg, Germany
Vortexer Vortex-Genie 2	Scientific Industries, purchased from A. Hartenstein GmbH, Würzburg, Germany
Water bath WB7	Memmert, purchased from A. Hartenstein GmbH, Würzburg, Germany

3.1.11 Software and online sources

AxioVision 4.4.1.0	Carl Zeiss Jena GmbH, Jena, Germany
Bio 1D/Capt MW software	LTF, Wasserburg, Germany
Bio Profile software	LTF, Wasserburg, Germany
Magellan 3.00	Tecan Deutschland GmbH, Crailsheim, Germany
Office Excel 2007	Microsoft Deutschland GmbH, Unterschleißheim, Germany
Office Word 2007	Microsoft Deutschland GmbH, Unterschleißheim, Germany
Photoshop Elements 4.0	Adobe, purchased from University of Würzburg, Germany
<i>e!</i> Ensembl Human	http://www.ensembl.org/Homo_sapiens
NCBI Blast	http://www.ncbi.nlm.nih.gov/BLAST
NCBI Pubmed	http://www.ncbi.nlm.nih.gov/entrez/query.fcgi?DB=pubmed

3.2 Methods

3.2.1 Isolation and culture of human mesenchymal stem cells (hMSCs)

Isolation of hMSCs was performed after the approval of the Institutional Review Board of the University of Würzburg. The cells were isolated from the femoral head of patients undergoing total hip arthroplasty, using a protocol first described by Haynesworth et al., 1992, and modified by Nöth et al., 2002b.

Briefly, harvested trabecular bone plugs were transferred to 50 ml centrifugation tubes containing stem cell medium (SCM) consisting of DMEM/Ham's F-12 supplemented with 10% fetal bovine serum (FBS), 100 U/ml penicillin, 100 µg/ml streptomycin, and 50 µg/ml L-ascorbic acid 2-phosphate. After centrifugation at 250 x g for 5 min the supernatant was discarded to remove any fatty components. To release marrow cells, bone plugs were subsequently washed by vortexing. The dispersed cells were filtered through a cell strainer to hold back bone fragments and collected in a fresh tube. This procedure was repeated for a total of five times to extract the remaining cells. Cell number and viability of the collected cells were determined with a hemocytometer and cells were plated at a density of 3×10^6 cells/cm² into cell culture flasks and cultivated at 37°C in a humidified atmosphere with 5% CO₂. After 2 to 3 days of cultivation non-adherent blood cells were removed and attached hMSCs were washed twice with PBS. The culture medium (SCM) was changed every 3 to 4 days. After 10 to 14 days of cultivation, when the cells reached 70 to 80% confluency, they were detached by incubation with PBS/EDTA for 5 min following addition of 0.25% trypsin-EDTA and incubation for 2-3 min at 37°C. To inactivate the trypsin, the same volume of SCM was added.

3.2.2 Phenotypic characterization of hMSCs

HMSC cultures were routinely observed on an inverted phase-contrast microscope. Photomicrographs were taken with a digital camera, using AxioVision software.

The expression of specific cell surface markers on hMSCs was analyzed in almost every cell preparation. The antibodies employed, their specified antigens and the used concentrations are listed in Table 1 (see section 3.1.5).

Cells were detached at the end of primary culture by trypsin-EDTA treatment, replated at 3,000 cells per well in chamber slides, and cultivated for 3 days in SCM. To detect surface antigens, cells were fixed with ice-cold ethanol/acetone (1:1) for 10 min, rinsed with washing buffer, blocked for non-specific staining with blocking solution and incubated overnight with the respective primary antibody at a concentration previously established by titration. Negative controls were incubated with mouse serum as a substitute for the primary antibody. Immunoreactivity was detected using BioGenex Super Sensitive™ Link-Label IHC Detection System, which is based on the streptavidin-biotin technology. The Link, a biotinylated secondary antibody, reacts with the Label, which is composed of streptavidin labeled with the enzyme alkaline phosphatase. This entire antibody-enzyme complex is then visualized by the incubation with a chromogenic substrate for alkaline phosphatase, Fast Red. According to the manufacturer's instructions, washed slides were incubated with the Link followed by incubation with the Label for 20 min at room temperature, respectively. Washing steps of 3 x 5 min were performed between each incubation step. Slides were then incubated with Fast Red until adequate color development was seen (usually within 5 min). Levamisole was added to the chromogenic substrate to block endogenous alkaline phosphatase. To stop the

reaction slides were washed in distilled water. The specimens were counterstained for 9 min with hemalaun and mounted in aqueous mounting medium.

3.2.3 Labeling of hMSCs with very small superparamagnetic iron oxide particles (VSOPs)

3.2.3.1 Labeling protocol

Cell labeling with VSOP C200 was always performed at the end of primary culture. The iron oxide particles were added to the culture medium at a concentration of 1.5 mM and the cells were incubated for 90 min at 37°C and 5% CO₂, according to the manufacturer's instructions. No additional transfection agent was used. After incubation, hMSCs were washed three times with PBS to remove excess VSOPs. The labeled cells were collected by trypsinization, passed through a cell strainer to exclude cell clusters, counted with a hemocytometer, and used for further experiments.

3.2.3.2 Detection of iron oxide particles within VSOP-labeled hMSCs

Particle incorporation was assessed using different methods.

Prussian blue staining.

To confirm successful VSOP labeling, an aliquot of hMSCs was stained with iron-specific prussian blue after each labeling experiment. Labeled and unlabeled hMSCs were seeded on poly-L-lysine coated slides and allowed to adhere overnight. Cells on slides were then fixed with 4% PFA for 10 min, washed with distilled water, incubated with 1% potassium ferrocyanide in 1% hydrochloric acid for 30 min, washed again and counterstained with nuclear fast red for 5 min [Ittrich et al., 2005].

Fluorescent dye-labeled VSOPs.

Particle incorporation was further demonstrated using fluorescent dye-labeled VSOPs. Labeling of hMSCs with FITC-labeled iron oxide particles was performed as described for unmodified VSOPs. An aliquot of labeled cells was seeded on poly-L-lysine coated slides and allowed to adhere overnight. The next day the adherent cells were fixed with ice-cold ethanol/acetone (1:1) for 10 min and incubated with 1 µg/ml DAPI for 5 min in the dark for nucleus staining. The cells were then washed three times with PBS for 5 min and finally mounted in Fluoromount-G. The uptake of fluorescent dye-labeled particles was visualized with a 63x oil-immersion objective using the Axioskop 2 MOT microscope equipped with an AxioCam MRc digital camera. Fluorescence from green (FITC) and blue (DAPI) channels were collected and processed into final two-color images.

Transmission electron microscopy (TEM).

The preparation of the samples for TEM was performed by the group of Prof. Krohne (Division of Electron Microscopy, Theodor-Boveri-Institute, University of Würzburg). VSOP-labeled and unlabeled hMSCs were seeded on microscope cover slides and allowed to adhere overnight. Cells on slides were fixed with 2.5% glutaraldehyde in 50 mM cacodylate buffer (pH 7.2) for 30 min, rinsed three times in 50 mM cacodylate buffer, and postfixed in 2% osmium tetroxide for 90 min at 4°C. Samples were then rinsed with distilled water, stained with 2% uranyl acetate overnight, washed with distilled water, dehydrated using a graded series of ethanol, passed through propylene oxide, and embedded in epoxy resin (Epon 812). The embedded samples were cut into ultrathin sections of 60 nm thickness and examined under the EM 10 microscope.

Quantification of cellular iron content.

The iron content per cell was determined using inductively coupled plasma - mass spectrometry (ICP-MS) against standard solutions of 500 and 1,000 ppm iron in 0.65% nitric acid. The cell suspensions with known cell density were centrifuged at 250 x g and the remaining cell pellet was resuspended in 500 μ l of 65% nitric acid and 10 μ l 30% hydrogen peroxide to lyse the cells. Subsequently, the solution was diluted with deionized water to a final concentration of 0.65% nitric acid.

The cellular iron content from different labeling experiments was expressed as mean \pm standard deviation (SD) and was verified by analysis of variance. The Mann-Whitney test was applied to identify significant differences. P values of less than 0.05 were considered statistically significant.

3.2.3.3 Cellular viability and apoptosis

Trypan blue viability test.

In each labeling experiment, the viability of VSOP-labeled and unlabeled cells was evaluated with a trypan blue dye exclusion test immediately after detachment of the cells. The cell pellet was resuspended in a known volume of SCM and cell number and viability were determined from an aliquot by mixing 50 μ l of cell suspension with 50 μ l of trypan blue and counted with a hemocytometer.

Apoptosis.

To detect if VSOP labeling led to cellular apoptosis, the Caspase-Glo[®] 3/7 Assay was used. This assay, based on luminescence, measures caspase-3 and -7 activities, key effectors in apoptosis in mammalian cells. VSOP-labeled and unlabeled cells were seeded at 10,000 cells per well in 96-well assay plates and cultivated for 24 h. Blank wells with only culture medium were included to measure background luminescence. After adding the Caspase-Glo[®] 3/7 Reagent, the cells were incubated in the dark for 30 min at room temperature. The luminescence, proportional to the amount of caspase activity present, was measured with a plate-reading luminometer.

The quantitative data, corrected by subtraction of the background luminescence, were expressed as mean \pm SD and were verified by analysis of variance. The Mann-Whitney test was applied to identify significant differences. P values of less than 0.05 were considered statistically significant.

WST assay.

The metabolic activity as an indicator of cell viability of VSOP-labeled and unlabeled cells was analyzed using the reagent WST-1. This assay allows the spectrophotometric quantification of cell proliferation, cell viability, and cytotoxicity. WST-1 (4-[3-(4-Iodophenyl)-2-(4-nitrophenyl)-2H-5-tetrazolio]-1,3-benzene disulfonate) is a non-toxic tetrazolium salt, which is cleaved by mitochondrial dehydrogenases of metabolically active cells into water-soluble formazan, accompanied by a change of color from slightly red to dark red. Therefore, the amount of formazan dye formed is directly proportional to the metabolic activity of living cells and can be quantified by measurement of the absorbance at a wavelength of 450 nm.

HMSCs were seeded at 4,000 cells per well in 96-well cell culture plates and cultivated in SCM for 3 days. Some wells were left empty to serve as a control for the background absorption of the medium itself. At day 3 of cultivation, the medium in each well was replaced by WST-1 reagent at a final dilution of 1:10 in SCM. Absorbance was repeatedly measured every 20 min up to 60 min after addition of the WST-1 reagent. The mean extinction values \pm

SD were calculated from 10 wells for VSOP-labeled and unlabeled cells, respectively, and corrected by subtraction of the background absorbance mean value.

3.2.3.4 Proliferation assays

Proliferation curves in short-time culture.

To evaluate the proliferation capacity of hMSCs directly after VSOP labeling, both labeled and unlabeled hMSCs were seeded at 10,000 cells per well in 24-well cell culture plates and cultivated in SCM. A cell count was performed each following day for up to 12 days in 3 wells, respectively, and the number of living cells was determined using trypan blue. Mean \pm SD was calculated for each time point. The medium was changed every 3 to 4 days.

Proliferation curves in long-term culture.

To evaluate possible influences of intracellular iron in an extended culture period, the proliferative activity of both, unlabeled and VSOP-labeled cells were examined over several passages. Cells were seeded at 2.3×10^3 cells/cm² in cell culture flasks and cultured until they reached 70 to 80% confluency. At the end of each passage living cells were counted using trypan blue dye. From each passage 2.3×10^3 cells/cm² were reseeded in cell culture flasks and the procedure described above was repeated for 6 passages. The proliferation capacity was modeled by the standard exponential proliferation equation:

$$N = N_0 \times 2^n \Leftrightarrow \log N = \log N_0 + n \times \log 2 \Leftrightarrow n = \frac{\log N - \log N_0}{\log 2}$$

with N_0 being the number of seeded cells on day 0 (4×10^5 cells) and N the number of harvested cells at the end of a passage. The cell doubling time was determined by dividing the total number of days in culture by the number of doublings (n).

The cell population doubling times of 8 different hMSC preparations over 6 passages were expressed as mean \pm SD and were verified by analysis of variance. The Mann-Whitney test was applied to identify significant differences. P values of less than 0.05 were considered statistically significant.

3.2.3.5 Differentiation of hMSCs

To determine whether VSOP labeling has any effect on the differentiation potential, both labeled and unlabeled hMSCs were analyzed for their capacity to differentiate along the adipogenic, osteogenic, and chondrogenic lineage. For each lineage differentiation VSOP-labeled and unlabeled cells from at least three donors were used. On day 28 of cultivation, histological staining for extracellular matrix (ECM) production was performed and total cellular RNA was extracted to assess gene expression of differentiated cells.

Adipogenic differentiation.

Adipogenesis was induced in confluent monolayer cultures according to the method described by Pittenger et al., 1999, and modified by Nöth et al., 2002a. The adipogenic differentiation medium consisted of DMEM high glucose, 10% FBS, 100 U/ml penicillin, and 100 μ g/ml streptomycin which was supplemented with 100 μ M insulin, 500 μ M IBMX, 1 μ M dexamethasone, and 100 μ M indomethacin. Cells maintained in SCM served as a negative control. Medium changes were performed three times a week.

Osteogenic differentiation.

Confluent monolayer cultures were grown in osteogenic differentiation medium consisting of DMEM high glucose containing 10% FBS, 100 U/ml penicillin, 100 μ g/ml streptomycin,

50 µg/ml L-ascorbic acid 2-phosphate, 10 mM glycerol 2-phosphate, and 100 nM dexamethasone, according to Jaiswal et al., 1997. Cells maintained in SCM served as negative controls. The medium was changed three times a week.

Chondrogenic differentiation.

Chondrogenesis was induced using a high-density pellet cell culture system, modified from Johnstone et al., 1998. The serum-free chondrogenic differentiation medium (CDM) consisted of DMEM high glucose, 100 U/ml penicillin, 100 µg/ml streptomycin, 50 µg/ml L-ascorbic acid 2-phosphate, 40 µg/ml proline, 100 µg/ml sodium pyruvate, 100 nM dexamethasone, and ITS-plus (final concentration: 10 µg/ml bovine insulin, 5.5 µg/ml transferrin, 5 µg/ml sodium selenite, 4.7 µg/ml linoleic acid, and 0.5 mg/ml BSA). Aliquots of 2.5×10^5 cells were washed and resuspended in chondrogenic differentiation medium, centrifuged at $250 \times g$ and 10 ng/ml TGF-β1 were added. Pellets maintained in chondrogenic differentiation medium without addition of TGF-β1 served as negative controls. Medium changes were performed twice a week.

3.2.4 Fabrication and culture of hMSC collagen hydrogels

3.2.4.1 Fabrication of hMSC collagen hydrogels

Additionally to the gel neutralization solution (2x GNS Ham F1) provided by Arthro Kinetics AG other GNS were tested to evaluate the influence of different compositions on the proliferation and chondrogenic differentiation of hMSCs.

- “2x GNS HG F1” consisted of HEPES-buffered, double concentrated DMEM high glucose and 20% FBS.
- “2x GNS HG F2” consisted of HEPES-buffered, double concentrated DMEM high glucose and 20% FBS (another lot, provided by the Cell Systems Laboratory from the Fraunhofer Institute for Interfacial Engineering and Biotechnology, Stuttgart, Germany).

The collagen type I stock solution remained liquid at 4°C and gelled when neutralized to pH 7.0 and transferred to 37°C. Therefore, the gel fabrication was carried out on ice. Collagen hydrogels with different final collagen concentrations were fabricated.

To produce standard collagen hydrogels, a gel neutralization solution based on double concentrated medium and 20% FBS was used, leading to hydrogels with a collagen concentration of 3 mg/ml.

HMSCs were resuspended in 2x GNS at two times the required cell density of the final gels. An equal volume of collagen type I stock solution was added and both components were carefully mixed to avoid air inclusions. The appropriate volume of the collagen-cell suspension was transferred into cell culture plates to produce hydrogels with a thickness of 5 to 6 mm. The exact cell concentrations and volumes of the fabricated collagen hydrogels are specified later in context with the performed experiments. Polymerization was allowed for 20 min at 37°C in a 5% CO₂ humidified atmosphere. The collagen hydrogels were subsequently incubated in the appropriate culture medium with changes every 3 to 4 days.

To assay the contraction of the collagen hydrogels, the diameters of the hydrogels were measured weekly and expressed as the percentage of the original diameter.

For the MRI experiments, collagen hydrogels with a final collagen concentration of 4 mg/ml were fabricated, using 3x GNS.

The gel fabrication was performed by mixing two parts of collagen type I stock solution with one part of 3x GNS. VSOP-labeled hMSCs were suspended in 0.5 ml 3x GNS using three times the required cell density of the final gels. After adding 1 ml of collagen type I stock solution, the two components were carefully mixed to avoid air inclusions. The resulting collagen-cell suspension was poured into custom-made Teflon inserts in 12-well cell culture plates. After polymerization for 20 min 3 ml of SCM were added. The resulting collagen hydrogels had a diameter of 17 mm and a thickness of 6 mm. Collagen hydrogels with unlabelled cells were used as controls. HMSC collagen hydrogels were cultivated for a minimum of 3 days before MR imaging to allow air bubbles to disappear, which could give similar signal voids as the iron oxide particles.

3.2.4.2 Cell proliferation in hMSC collagen hydrogels

HMSC collagen hydrogels were fabricated in 24-well culture plates to produce hydrogels with a diameter of 16 mm and thickness of 5 mm. The cell proliferation was investigated with initial cell seeding concentrations of 3×10^5 and 4×10^5 hMSCs/ml gel. The hydrogels were cultivated in serum-containing SCM, in chondrogenic differentiation medium without addition of TGF- β 1 (CDM⁻), or in chondrogenic differentiation medium with TGF- β 1 (CDM⁺). Additionally, the influence of different GNS on the proliferation within the matrix was assessed. The media were replaced in parallel every 3 to 4 days.

To determine the cell number within the collagen hydrogels, cells were recovered at day 1, 7, 14, and 21 by collagenase digestion. Collagen hydrogels were minced into small pieces and incubated in 0.625 U/ml collagenase NB4 at 37 °C. As soon as the gels were completely solubilized, which takes approximately 1 to 2 hours, the resulting cell suspension was centrifuged at 250 x g and the number of viable cells was determined with a hemocytometer using trypan blue.

3.2.4.3 Chondrogenic differentiation of hMSCs in collagen hydrogels

HMSC collagen hydrogels were cultivated for up to 28 days in serum-free chondrogenic differentiation medium as described above (see section 3.2.3.5) with the addition of 10 ng/ml TGF- β 1 (CDM⁺). As a control, hydrogels were cultivated in SCM containing 10% FBS or in CDM⁻. The media were changed every 3 to 4 days. To define the optimal initial cell density for chondrogenesis of hMSCs within the collagen hydrogel, initial cell seeding concentrations ranging from 1×10^5 to 1×10^6 hMSCs/ml gel were tested. Additionally, the effect of different GNS was examined. At the end of culture, histological and gene expression analyses were performed.

3.2.5 Bioreactor cultivation of hMSC collagen hydrogels

To investigate the metabolic response of hMSCs to mechanical stimulation in three-dimensional culture, hMSC collagen hydrogels were cultivated in a custom-designed bioreactor under sterile culture conditions. The bioreactor cultivation was employed in cooperation with the group from Prof. Bader in Leipzig, who developed this bioreactor (Fig. 4).

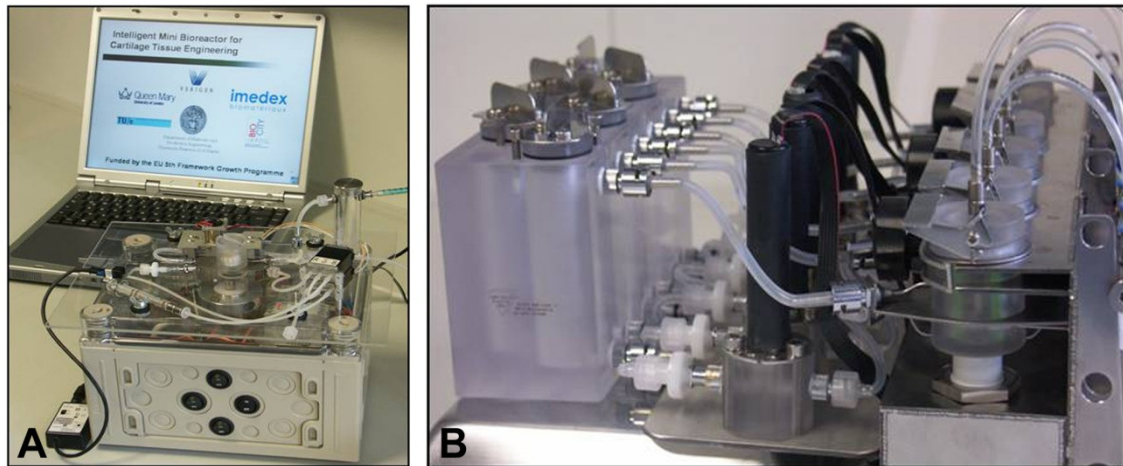


Fig. 4 Bioreactor system consisting of a control unit (A) and 6 individual cultivation chambers (B).

The main characteristic of this bioreactor system is the combination of a perfusion culture and cyclic mechanical compression. Perfusion permits an enhanced convection within the construct to deliver nutrients to and to remove waste products from the constructs and additionally applies shear forces to the cells. Mechanical loading is performed in a contactless manner via a magnetic field driven loading plate. The entire perfusion and stimulation device is designed for the operation within an incubator and consists of an autoclavable cultivation chamber with a perfused locating stage for the construct and a contactless actuator for mechanical loading (Fig. 5). Online monitoring of media temperature, volumetric flow rate, pH-value and the partial pressure of oxygen allows a continuous control of the culture environment. Additionally, samples for a manual offline analysis of glucose and lactose concentrations as indicators for the cell metabolism can be aseptically aspirated. In the bioreactor periphery, the culture medium is provided via a 50 ml medium reservoir. To achieve equilibrium with the gas environment of the incubator the recirculated medium from the reservoir passes a gas permeable silicone tubing gas exchanger.

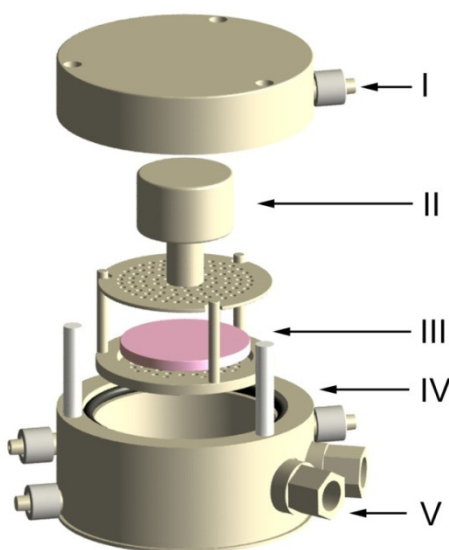


Fig. 5 Schematic figure of a cultivation chamber. Bioreactor device with a cover lid with an inlet/outlet port to maintain sterility (I), a magnetic mini-actuator with loading plate (II), the cultivation chamber comprising a locating stage for the construct (III), and a bioreactor vessel with three inlet/outlet ports for medium/gas change (IV) along with two sterile online sensor accesses for pO_2 and pH monitoring (V).

After assessment of the optimal culture conditions for hMSCs in the collagen hydrogels, constructs with a diameter of 34 mm, a thickness of 6 mm, and a defined initial cell seeding density were fabricated. They were pre-cultured for 10 days in 6-well cell culture plates under

free-swelling conditions to allow the cells to contract the hydrogel and synthesize new matrix to stiffen the gel. After this pre-incubation period, one construct was analyzed to determine gel diameter, cell number and viability. The hMSC collagen hydrogel constructs were transferred to the bioreactor to apply intermitted unconfined uniaxial compression. During the stimulation period of 8 hours the constructs were compressed for a single second every ten minutes. This results in a sinusoidal force profile showing per cycle one initial second of load with a maximum stimulation force of 4.2 kPa. These parameters of the loading protocol were chosen on the basis of previous studies allowing the hydrogels to recover to their initial height within 10 min. This course of mechanical stimulation was followed by a rest period of 16 hours. To secure a sufficient nutrient and oxygen supply, a dynamic medium change with a flow rate of 0.16 ml/min was applied. Control constructs were maintained under static, free-swelling conditions in 6-well cell culture plates. All constructs were further cultivated for 11 days at 37°C in a humidified atmosphere with 5% CO₂, with mechanical deformational loading applied daily to the constructs in the bioreactor. At the end of the culture period, the cell number and viability was assessed and the constructs were processed for histological and gene expression analyses.

3.2.6 High-field MR imaging

MR imaging studies of hMSC collagen hydrogels were performed at 11.7 T on a 500 MHz Bruker Avance 500 MRI system with a maximum gradient strength of 0.66 T/m. The constructs were transferred under sterile conditions into an 18-mm MR tube containing 2% agar at the bottom and SCM, and were then placed within a ¹H quadrature birdcage for imaging. The MR images were acquired using a 3D FLASH sequence. The applied parameters echo time T_E and repetition time T_R, and the nominal spatial resolution are specified in the figure legends. During the image post processing, a zero filling by a factor of two was applied in every dimension.

3.2.7 Histology and immunohistochemistry

At the end of cultivation, the pellets and the hMSC collagen hydrogels were harvested and fixed in 4% PFA for 2 h at room temperature. After fixation, the samples were dehydrated in a series of increasing ethanol concentrations and infiltrated with amyl acetate. Specimens were then embedded in paraffin and sectioned at a thickness of 4 μm. To prepare sections for histological and immunohistochemical staining, the paraffin sections were deparaffinized using xylene and rehydrated in a graded ethanol series.

3.2.7.1 Oil red O staining

To assess adipogenic differentiation, oil red O staining was performed to indicate intracellular lipid accumulation [Pittenger et al., 1999]. The cell monolayers were fixed with 4% PFA for 10 min, washed with distilled water and incubated in 60% 2-propanol for 5 min. Staining with 0.3% oil red O working solution was performed for 10 min at room temperature. Excess stain was removed by washing with 60% 2-propanol, followed by several changes of distilled water. The cells were counterstained for 2 min with hemalaun. Intracellular lipid vesicles stained light orange to red.

3.2.7.2 Alizarin red S staining

Osteogenic differentiation was assessed using alizarin red S staining to detect Ca_2HPO_4 deposition typically for mineralization of the extracellular matrix [Łączka-Osyczka et al., 1998]. Cell monolayers were fixed with ice-cold methanol for 10 min, washed with distilled water, and incubated for 2 min in the alizarin red S staining solution. Excess dye was removed by several washes with distilled water. Mineralized nodules appeared dark red to red brown.

3.2.7.3 Hemalaun&Eosin (H&E) staining

Sections were subjected to H&E as a general staining to evaluate tissue structure, cell morphology and distribution. All basophilic cell structures like the chromatin of the cell nucleus were stained blue from hemalaun, whereas eosin stained the acidophilic components like the cytoplasm and many tissue structures red.

Slides from distilled water were incubated in hemalaun for 9 min. Excess stain was removed by washing with distilled water, and the nucleus stain was differentiated in 0.25% hydrochloric acid/50% ethanol and blued in tap water for 10 min. After that staining in 1% eosin was performed for 1 min. Excess dye was removed by several washes with distilled water. The stained slides were dehydrated in a graded ethanol series and mounted.

3.2.7.4 Alcian blue staining

To detect negatively charged sulfated proteoglycans in chondrogenic differentiated cultures, alcian blue staining was performed [Lev and Spicer, 1964]. The slides from distilled water were first incubated with 3% acetic acid for 3 min and then stained with 1% alcian blue (pH 1.0) for 30 min. After removal of excess stain in distilled water they were counterstained with nuclear fast red for 5 min. Excess dye was removed by several washes with distilled water. The stained slides were dehydrated in a graded ethanol series and mounted.

3.2.7.5 Immunohistochemical staining for collagen type II

Chondrogenic differentiation and production of cartilage-specific collagen type II was detected using a monoclonal antibody specific for human collagen type II. The specimens were pretreated with pepsin (1 mg/ml in Tris-HCl, pH 2.0) for 15 min at room temperature for optimal antigen retrieval. After blocking nonspecific background staining, the sections were incubated with the primary antibody overnight at 4°C. Negative control slides were incubated with mouse serum as a substitute for the primary antibody. Immunohistochemical staining was detected colorimetrically using BioGenex Super Sensitive™ Link-Label IHC Detection System as described above (see section 3.2.2). The specimens were counterstained for 15 s with hemalaun and mounted in aqueous mounting medium.

3.2.8 Gene expression analyses

3.2.8.1 Total RNA isolation

For total cellular RNA extraction at day 28 from chondrogenic pellet cultures, adipogenic and osteogenic differentiated monolayer cultures, as well as their controls, Trizol reagent was used according to the manufacturer's instructions. The use of Trizol reagent allowed a sufficient separation of the extracellular matrix, especially in osteogenic differentiated cultures. Briefly, cells were homogenized in Trizol reagent and an additional centrifugation step at

3,500 x g at 4°C was included to remove any insoluble extracellular matrix material. The supernatant was transferred to a fresh tube and after addition of chloroform the mixture was separated in two phases by centrifugation at 3,500 x g at 4°C. The RNA in the upper aqueous phase was precipitated with 2-propanol and recovered by centrifugation at 3,500 x g at 4°C. The resulting RNA pellets were resuspended in lysis buffer (provided in the RNA isolation kit) containing 10 µl/ml β-mercaptoethanol and further purified by using Nucleospin® RNA II isolation kit, according to the manufacturer's protocol. Incubation in the lysis buffer generated appropriate binding conditions for adsorption of the RNA to the silica membrane of the mini spin column. Samples were on-column treated with DNase to remove possible genomic DNA contamination. Other contaminants like salts, metabolites and macromolecular cellular components were removed by multiple washing steps with appropriate buffers (provided in the RNA isolation kit). Total RNA was finally eluted in RNase-free water. The RNA samples were stored at -80°C.

For total RNA extraction from hMSC collagen hydrogels, the construct were minced into small pieces, frozen with liquid nitrogen for 1 min, transferred into lysis buffer and homogenized by aspiration through a 20-gauge needle. The homogenized solution was purified using Nucleospin® RNA II isolation kit as described above.

The RNA content was quantified spectrophotometrically at 260 nm. Since proteins absorb at 280 nm and contaminants like carbohydrates and peptides absorb at 230 nm, purity of RNA was estimated by the quotients E_{260}/E_{280} and E_{260}/E_{230} . Thereby, for pure RNA E_{260}/E_{280} should be 1.8 to 2.0 and E_{260}/E_{230} should be larger than 2.0.

3.2.8.2 cDNA synthesis

Equal amounts of total RNA from each sample were reverse transcribed into cDNA using random hexamers and Bioscript reverse transcriptase (RT) in a 20-µl mixture. Briefly, denaturing of secondary structures of RNA and annealing of 1 µg random hexamers was achieved by heating to 70°C and subsequent chilling on ice. The master RT reaction mix, containing 5x reaction buffer, 0.5 mM of each dNTP, and 50 U RT, was added and random hexamers were extended at 25°C prior to elongation of first strand cDNA species at 42°C. The reaction was stopped by incubation at 70°C and each sample was diluted with HPLC water to a final volume of 50 µl.

3.2.8.3 Reverse transcriptase polymerase chain reaction (RT-PCR)

PCR amplification of cDNA was performed using MangoTaq DNA Polymerase and the human-specific primer sets listed in Table 2 (see section 3.1.7). The housekeeping gene elongation factor 1α (EF1α) was always analyzed to monitor RNA loading. PCR was performed in a standard 30-µl volume reaction containing 1 µl of cDNA, 1x PCR buffer, 1.7 mM MgCl₂, 0.3 mM of each dNTP, 5 pmol of each sense and antisense primer, and 1 U MangoTaq DNA Polymerase.

The applied PCR reaction steps are listed below:

- 1) Initial denaturation: 94 °C 3 min
- 2) Denaturation: 94 °C 45 s
- 3) Annealing: 51 - 58 °C 45 s (depending on the primer pair)
- 4) Extension: 72 °C 1 min
- 5) Final extension: 72 °C 5 min
- 6) Cooling: 12 °C forever

Steps 2) - 4) were repeated 22 - 39 times depending on the intensity of the band for each PCR product.

3.2.8.4 Agarose gel electrophoresis

The amplified PCR products were electrophoretically separated on 1.5% agarose gels containing ethidium bromide and visualized using the Bio Profile software. Ethidium bromide intercalates into double-stranded DNA or RNA and fluoresces when exposed to UV light. Agarose gels were prepared in 0.5x TBE buffer and ethidium bromide was added to the warm liquid agarose solution to a final concentration of 5%. After gel polymerization, equal volumes of PCR products were directly loaded onto the agarose-ethidium bromide gel, since the respective buffer system already contained loading dyes. As marker for band sizes, a 100 bp DNA ladder containing DNA fragments of 100 – 3,000 bp was also loaded onto the gel. The intensity of individual bands was analyzed densitometrically with the Bio 1D/Capt MW software and the amount of PCR product for a single gene was normalized according to the corresponding EF1 α housekeeping gene PCR product.

4 Results

4.1 Characterization of hMSCs

Primary cultures of hMSCs appeared morphologically as a homogenous population of fibroblastic cells (Fig. 6). At day 4 of cultivation very few spindle-shaped cells attached to the culture plate and residual unattached round hematopoietic cells were observed. The adherent cells replicated rapidly and formed a confluent monolayer by day 10 to 14 of cultivation.

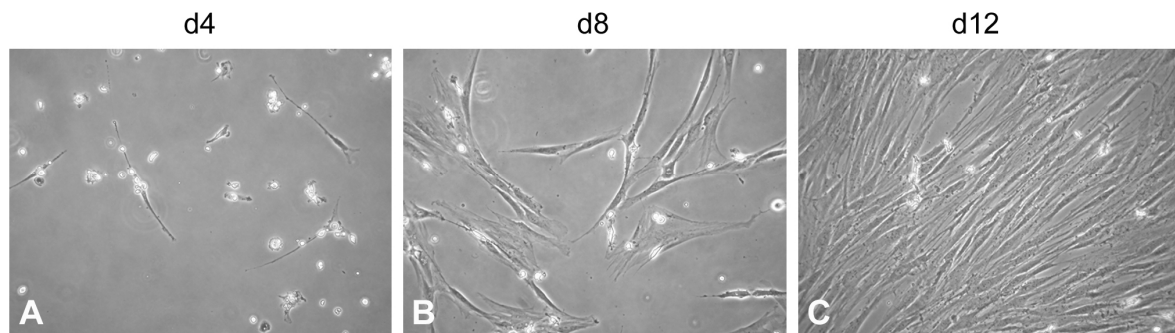


Fig. 6 Phase contrast photomicrographs of primary culture of hMSCs. An increase of adherent hMSCs showing a fibroblastic morphology could be observed from day 4 (A) to day 8 (B) up to day 12 (C) of cultivation. (200x)

When the cells reached 70 to 80% confluency, they were replated (passaged) to new cell culture flasks at a density of 2.3×10^3 cells/cm². As shown in Fig. 7, hMSCs retained their characteristic fibroblastic cell shape upon subcultivation. However, a distinct reduction in the growth rate was observed. Moreover, to exclude possible reduction of the differentiation capacity of hMSCs, only primary and first passages were used for all experiments.

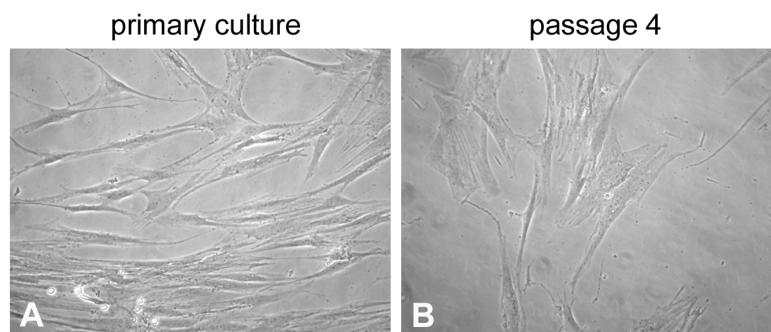


Fig. 7 Phase contrast photomicrographs of cultured hMSCs. The typical fibroblastic cell morphology of hMSCs at the end of primary culture (A) and in passage 4 (B) is shown. (200x)

To further characterize isolated hMSCs, the expression of specific cell surface antigens was analyzed at the end of primary culture. hMSCs showed a strong expression of CD44, a receptor for various ligands like hyaluronan and osteopontin, which plays a central role in the organization of the extracellular matrix in the marrow (Fig. 8A). The cells were also uniformly positive for CD90 (Thy-1), a marker for thymocytes and peripheral T lymphocytes (Fig. 8B),

and for CD105 (TGF- β receptor endoglin), dominantly associated with endothelial cells (Fig. 8C).

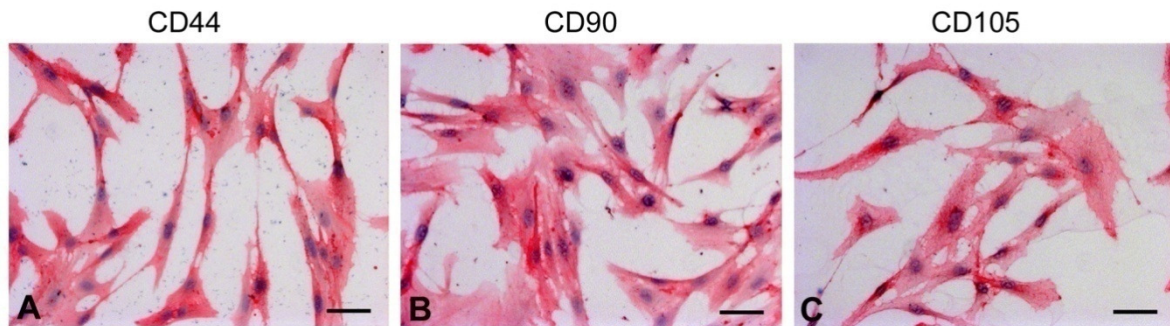


Fig. 8 Immunophenotyping of hMSCs. *hMSCs showed a strong expression of the cell surface markers CD44 (A), CD90 (B), and CD105. Bar = 50 μ m.*

In contrast, hMSCs lack typical markers of the hematopoietic lineage, including the lipopolysaccharide receptor CD14 (not shown), the early hematopoietic stem cell marker CD34 (not shown), and the leukocyte common antigen CD45 (Fig. 9A).

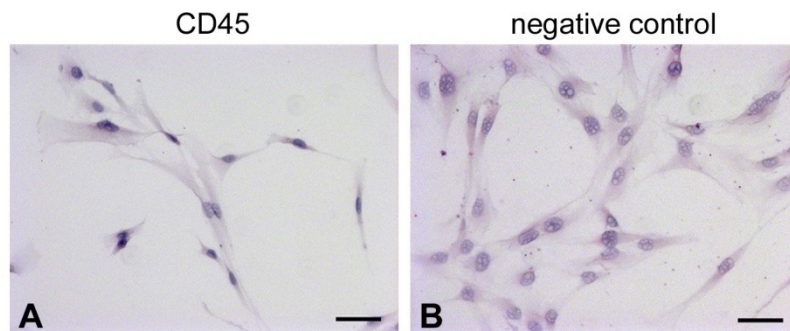


Fig. 9 Immunophenotyping of hMSCs. *hMSCs were negative for CD45 (A). Negative control demonstrates no unspecific staining (B). Bar = 50 μ m*

4.2 Fabrication and culture of hMSC collagen hydrogels

4.2.1 Contraction of hMSC collagen hydrogels

The contraction of standard collagen hydrogels, prepared with 2x GNS Ham F1, and with a collagen concentration of 3 mg/ml was monitored weekly up to day 21 of culture. A decrease in gel size was observed under all culture conditions, depending on the culture medium and the initial cell seeding density. The contracted hMSC collagen hydrogels nearly retained their rounded shape. Gels exposed to chondrogenic differentiation medium with TGF- β 1 (CDM⁺) showed always the highest contraction, resulting in a collagen disc with curled edges and an opaque, dense structure with a higher mechanical strength, as shown macroscopically in Fig. 10. In contrast, less contracted hMSC collagen hydrogels retained their translucent gel appearance. Gel contraction did not occur in unseeded collagen hydrogels.



Fig. 10 Macroscopic photograph of hMSC collagen hydrogels at day 21 of cultivation. Gels cultivated in CDM⁺ showed a more pronounced contraction compared to gels in SCM.

The amount of gel contraction was highly dependent on the culture medium, because both serum and TGF- β 1 induced a dramatic decrease in gel size (Fig. 11). By day 21, gels cultivated in serum-containing SCM and initially seeded with 1×10^5 hMSCs/ml gel had contracted to $64.8 \pm 16.0\%$ of their original diameters, whereas those seeded with 5×10^5 hMSCs/ml gel contracted to $42.9 \pm 16.1\%$ (Fig. 11A and C). In chondrogenic differentiation medium without TGF- β 1 (CDM), the decreases in gel sizes were less pronounced and were determined to $74.2 \pm 4.3\%$ and $56.5 \pm 8.5\%$ of their original diameters, respectively (Fig. 11A and C). In contrast, the presence of TGF- β 1 in CDM⁺ stimulated the highest contraction of the three-dimensional collagen hydrogels, resulting in gel diameters of approximately 30%, independent from the initial cell seeding density. Particularly in SCM and CDM⁺, a higher amount of contraction at earlier time points was observed with increasing initial cell seeding concentrations, comparing hMSC collagen hydrogels with 1×10^5 cells/ml gel (Fig. 11A), 3×10^5 cells/ml gel (Fig. 11B) and 5×10^5 cells/ml gel (Fig. 11C).

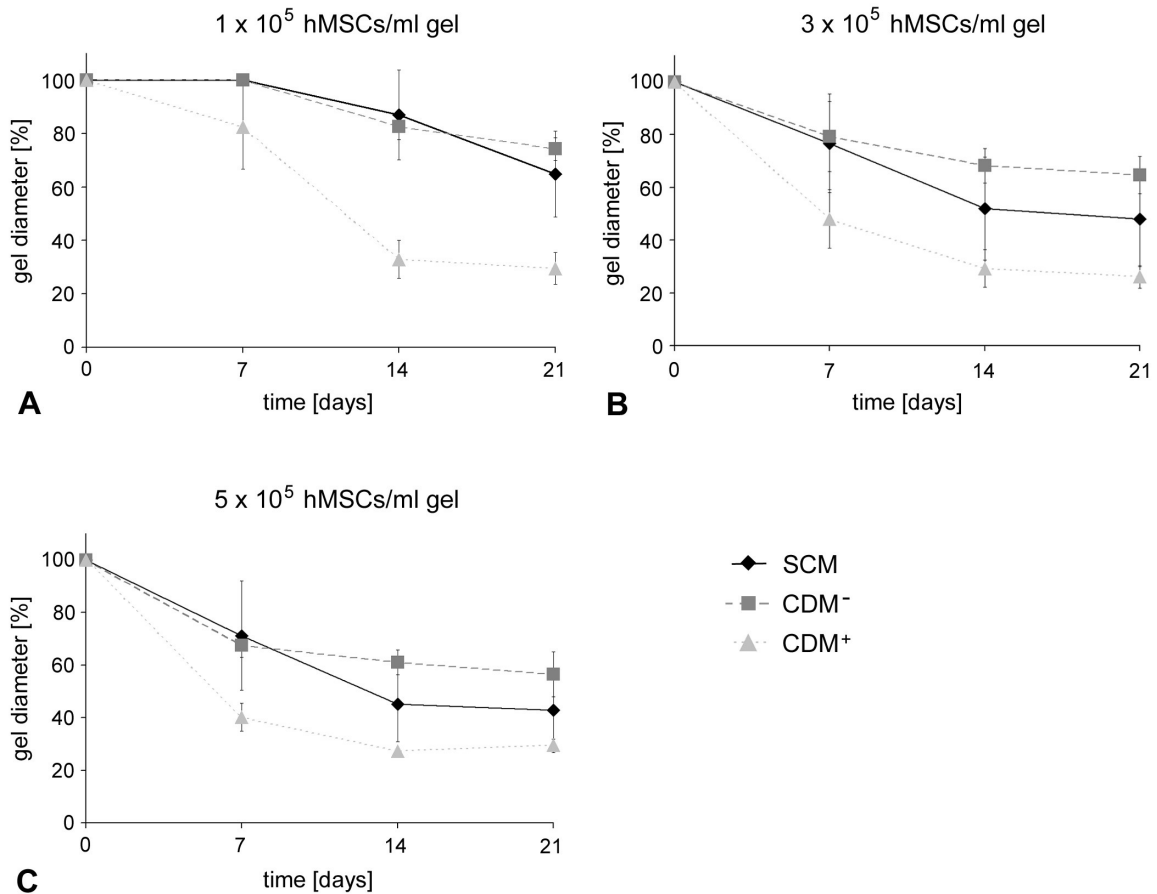


Fig. 11 Contraction of hMSC collagen hydrogels in different culture media. Independent from the seeded cell number, hMSC collagen hydrogels were most contracted under the influence of TGF-β1 (CDM⁺), followed by serum-containing SCM. Gels cultivated in CDM⁻ showed the lowest reduction of gel diameter (mean ± SD, n = 3).

In summary, Fig. 12 shows the time course of contraction of hMSC collagen hydrogels in SCM (Fig. 12A), CDM⁻ (Fig. 12B) and CDM⁺ (Fig. 12C) over 21 days of cultivation, fabricated with different initial cell seeding densities. In general, hMSC collagen hydrogels rapidly contracted within the first 14 days and then markedly slowed down their contraction over the rest culture period in all culture conditions. The rate of gel contraction by hMSCs was highly dependent on the number of cells incorporated into the collagen hydrogels. Enhanced gel contraction was observed with increasing initial cell seeding densities, showing high differences in the amount of contraction during the first two weeks of culture, especially in CDM⁻ (Fig. 12B). With increasing culture time, these differences became less important. Interestingly, gel contraction in CDM⁺ resulted at the same end point for all seeded cell numbers (Fig. 12C).

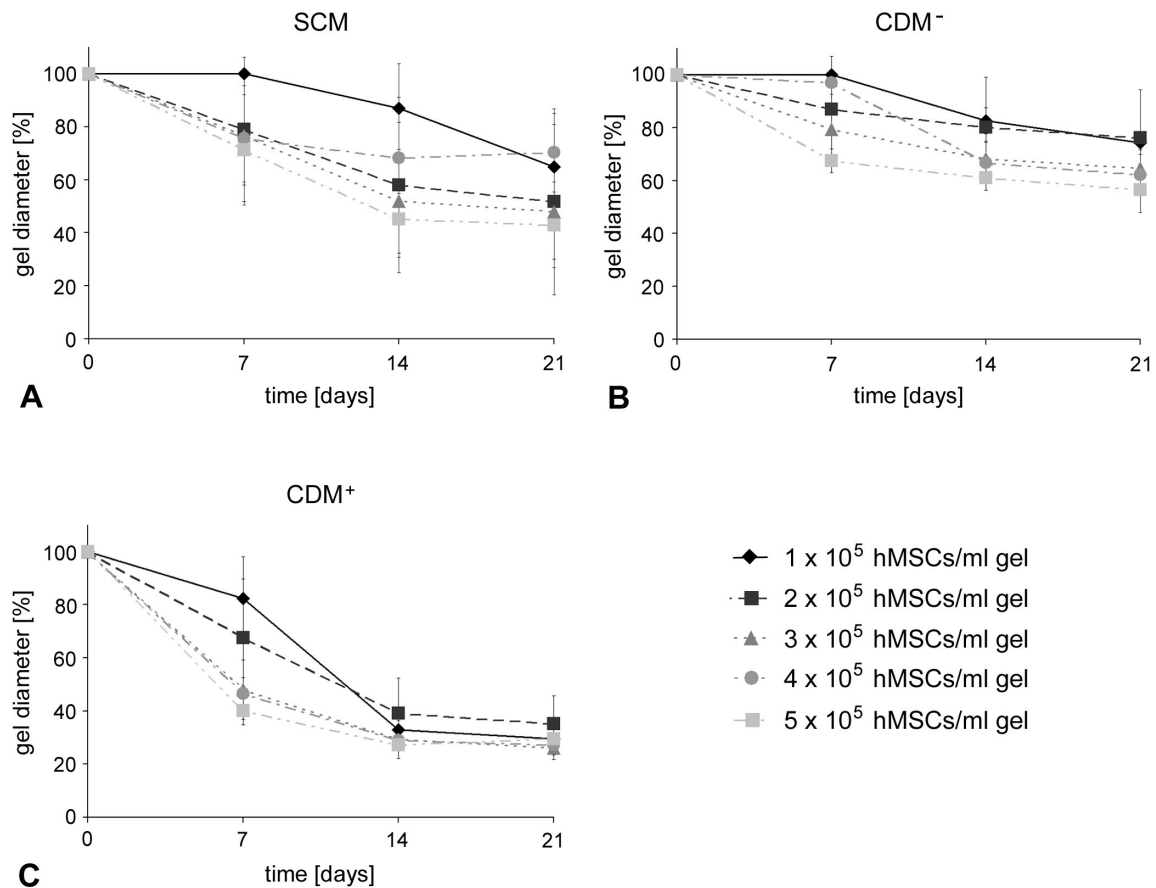


Fig. 12 Time course of hMSC collagen hydrogel contraction. After the drastic decrease in gel diameter over the first 14 days, the contraction reached nearly a plateau level, dependent on the culture conditions. Higher initial cell seeding densities resulted in smaller gel sizes (mean \pm SD, $n = 3$).

4.2.2 Cell proliferation in hMSC collagen hydrogels

The proliferation of hMSCs in standard collagen hydrogels, prepared with 2x GNS Ham F1, was monitored over 21 days in either SCM containing 10% FBS, the expansion medium used in monolayer culture, or in CDM⁻, a serum-free medium containing already some components necessary for chondrogenic differentiation, but no TGF- β 1 (Fig. 13). One day after fabrication of gels with 3×10^5 hMSCs/ml gel, a drastic decline in cell number to approximately the half of the initial cell seeding concentration was observed in both culture media, referring probably to the fabrication process itself, which includes rapid temperature changes and can cause short-time osmotic stress to the cells. Thereafter, hMSCs embedded in collagen hydrogels proliferated in both culture media up to day 7, reaching the initial cell seeding concentration. Surprisingly, in SCM the cells then gradually decreased in number over time to an end concentration of $1.8 \pm 0.2 \times 10^5$ hMSCs/ml gel. In contrast, in CDM⁻ the cell number remained nearly constant at a level of $3.7 \pm 1.3 \times 10^5$ hMSCs/ml gel throughout the culture. The high standard deviation refers to relatively large differences in the cell content of hMSC collagen hydrogels from different donors, ranging from 2.2×10^5 to 5.4×10^5 cells/ml gel at day 21.

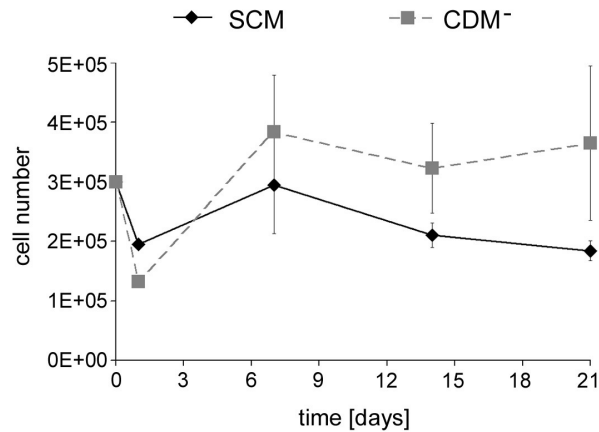


Fig. 13 Cell proliferation in hMSC collagen hydrogels in SCM and CDM. Collagen hydrogels were initially seeded with 3×10^5 hMSCs/ml gel. After 21 days of cultivation, the cell number in SCM was significantly lower compared to CDM (mean \pm SD, $n = 3$).

Histological staining using H&E demonstrated a homogenous cell distribution throughout the collagen hydrogel. HMSC collagen hydrogels cultivated in CDM (Fig. 14B) were more cellular than those cultivated in SCM (Fig. 14A), supporting the results of cell counting.

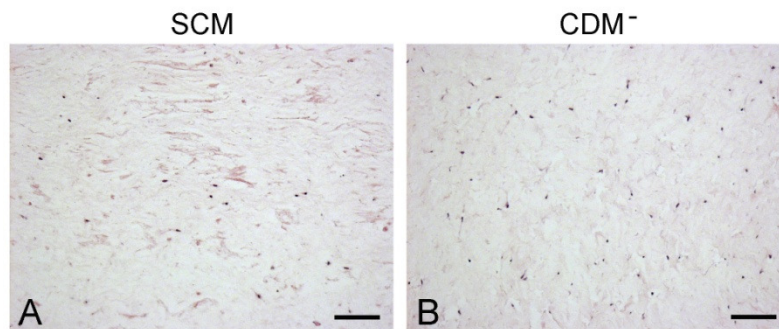


Fig. 14 Histological analysis (H&E staining) of hMSC collagen hydrogels cultivated in different media. Collagen hydrogels were seeded with 3×10^5 hMSCs/ml gel cultivated for 21 days in either SCM (A) or CDM (B). Cells were homogeneously distributed within the gels, with a higher cell number in gels cultivated in CDM. Bar = 100 μ m.

To evaluate if a higher initial cell seeding concentration led to a higher survival rate of hMSCs in collagen hydrogels cultivated in SCM, the cell seeding number was increased to 4×10^5 cells/ml gel. As shown in Fig. 15, a similar curve pattern was observed for both cell seeding densities. Maximum proliferation was again reached between day 1 and 7 and the cells then decreased in number continuously up to day 21. Interestingly, both cell seeding densities resulted in a similar cell number at day 1, and gels with the higher initial cell seeding concentration revealed lower cell densities at day 7 and thereafter. Therefore, more increase in the cell seeding concentration seemed to be meaningless.

On the other hand, a decrease in initial cell seeding number should facilitate the proliferation of hMSCs in collagen hydrogels. With regard to an adequate cell density necessary for chondrogenic differentiation (see section 4.2.3), the proliferation of hMSCs in collagen hydrogels with lower cell densities was not investigated.

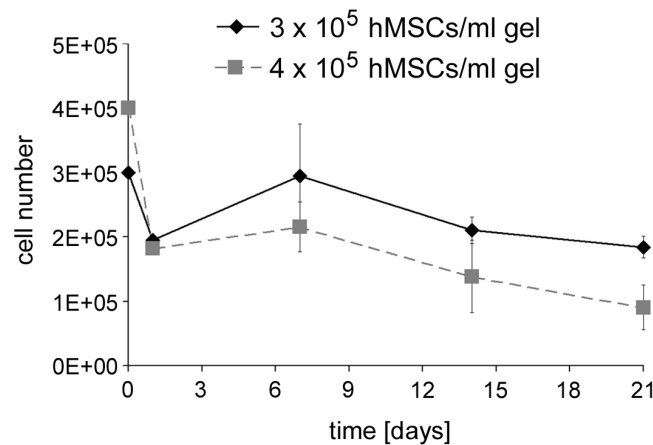


Fig. 15 Cell proliferation in hMSC collagen hydrogels with different initial cell concentrations. *HMSC collagen hydrogels were cultivated in SCM. After 21 days of cultivation, the cell number in gels with a higher initial cell density was significantly lower compared to gels with a lower initial cell density (mean \pm SD, $n = 3$).*

Additionally, to evaluate the behavior of hMSCs under conditions conducive to chondrogenic differentiation compared to expansion conditions, hMSC collagen hydrogels with 4×10^5 cells/ml gel were prepared. In the presence of TGF- β 1, the cell content of hMSC collagen hydrogels declined dramatically over 21 days of cultivation, suggesting that a certain amount of the cells did not differentiate and died (Fig. 16).

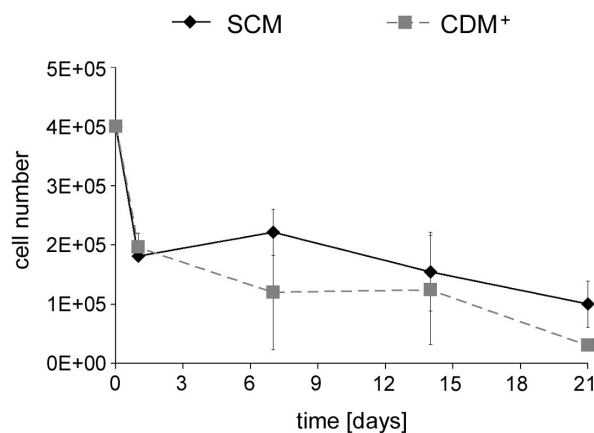


Fig. 16 Cell proliferation in hMSC collagen hydrogels in SCM and CDM+. *Collagen hydrogels were seeded with 4×10^5 hMSCs/ml gel. After 21 days of cultivation, the cell number in CDM+ was significantly lower compared to SCM (mean \pm SD, $n = 3$).*

To evaluate if the composition of the gel neutralization solution has an influence on the proliferation of hMSCs within collagen hydrogels, GNS differing in medium and FBS lot were tested. First, a GNS with DMEM high glucose instead of DMEM/Ham's F-12 was used, with no changes of the other components. DMEM high glucose was chosen with regard to the chondrogenic differentiation, where this medium was used as the differentiation medium. As shown in Fig. 17, a similar behavior of hMSCs in the collagen hydrogels could be observed

for both GNS, independently from the culture medium used. Again, the cell number at day 21 of cultivation was distinct lower in SCM (Fig. 17A) compared to CDM⁻ (Fig. 17B).

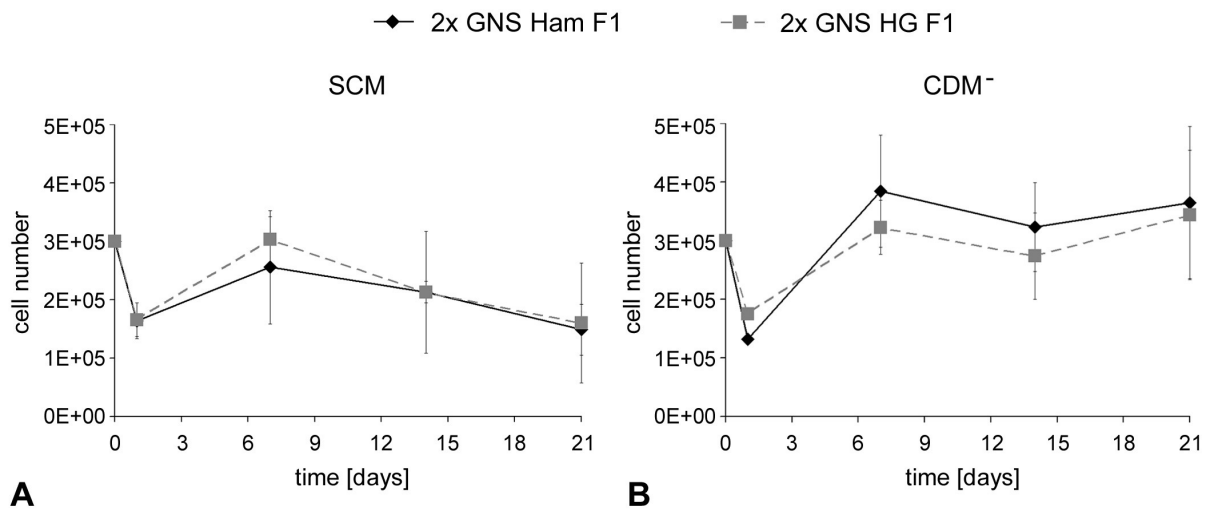


Fig. 17 Influence of the GNS composition on the proliferation of hMSCs in collagen hydrogels. Collagen hydrogels were seeded with 3×10^5 hMSCs/ml gel and were cultivated either in SCM (A) or in CDM⁻ (B). Over the whole culture period, no differences in the cell number in gels fabricated with different GNS were evaluated for both media (mean \pm SD, $n = 3$).

Additionally, 2x GNS HG F2, consisting of DMEM high glucose and a different lot of FBS, was tested in comparison to the standard 2x GNS Ham F1. As shown in Fig. 18, at the beginning of cultivation up to day 7 the cell numbers were comparable for both GNS. However, thereafter the typical decline of cell content in collagen hydrogels cultivated in SCM was observed for 2x GNS Ham F1, whereas in gels fabricated with 2x GNS HG F2 the cell number remained constant.

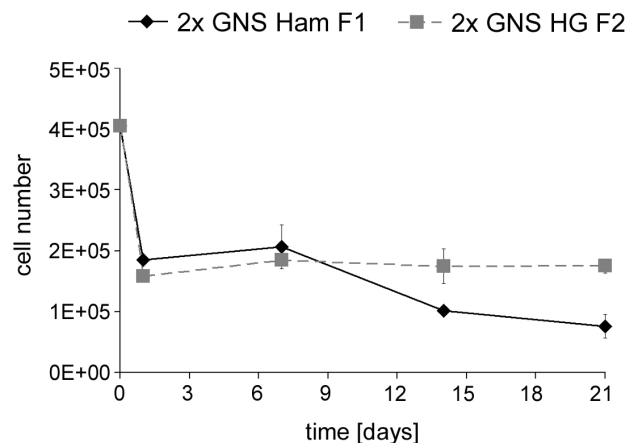


Fig. 18 Influence of the GNS composition on the proliferation of hMSCs in collagen hydrogels. Collagen hydrogels were seeded with 4×10^5 hMSCs/ml gel and cultivated in SCM. At the end of the culture period, significant higher cell numbers in gels fabricated with 2x GNS HG F2 were evaluated (mean \pm SD, $n = 2$).

The higher cell count in gels fabricated with 2x GNS HG F2 was confirmed by histological analysis at day 21 of cultivation. hMSCs were distributed throughout the collagen hydrogels,

presenting only few cells in gels fabricated with 2x GNS Ham F1 (Fig. 19A). In contrast, for 2x GNS HG F2 a distinct higher cell density could be observed (Fig. 19B). Additionally, gels fabricated with 2x GNS HG F2 showed more contraction, reaching half of the gel diameter at the end of the culture compared to gels with 2x GNS Ham F1. This pronounced contraction also contributed to the higher cell density seen in Fig. 19B.

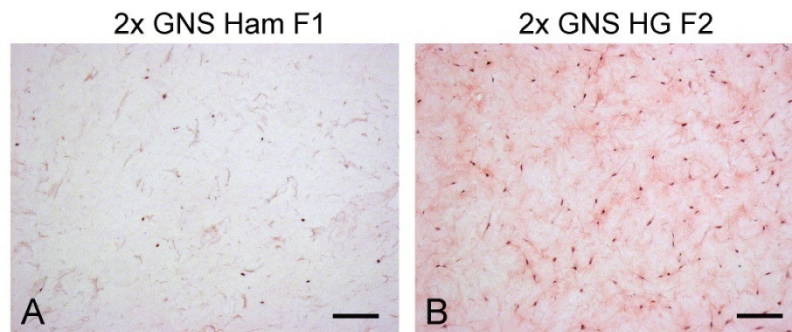


Fig. 19 Histological analysis (H&E staining) of hMSC collagen hydrogels fabricated with different GNS and cultivated in SCM. Collagen hydrogels were initially seeded with 4×10^5 hMSCs/ml gel. After 21 days of cultivation, gels fabricated with 2x GNS Ham F1 (A) showed a distinct lower cell density compared to gels fabricated with 2x GNS HG F2 (B). Bar = 100 μ m.

In CDM, a similar cell distribution could be detected compared to SCM at the end of culture in gels with different GNS. Both, hMSC collagen hydrogels fabricated with 2x GNS Ham F1 or 2x GNS HG F1 showed a homogenous cell distribution (Fig. 20A and B), but a distinct lower cell density compared to gels with 2x GNS HG F2 (Fig. 20C). Keeping in mind the absence of serum in the cultivation medium CDM, the lot of FBS as a component of the GNS seemed to have a crucial influence on the behavior of hMSCs in collagen hydrogels.

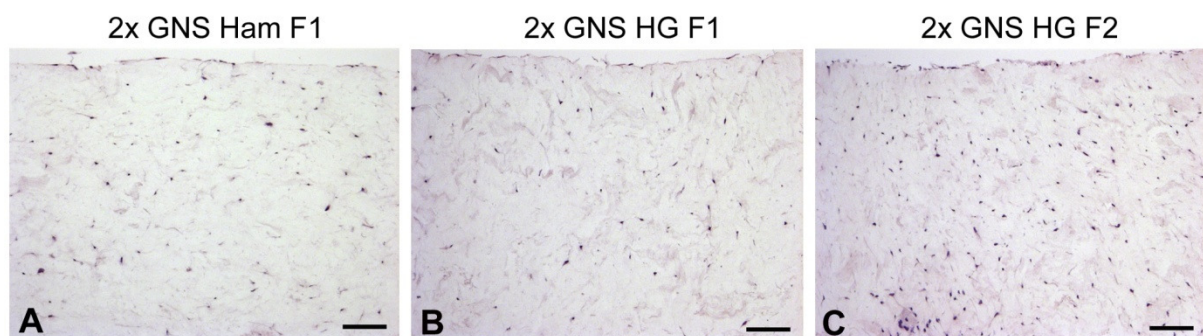


Fig. 20 Histological analysis of hMSC collagen hydrogels fabricated with different GNS and cultivated in serum-free CDM. Collagen hydrogels were seeded with 3×10^5 hMSCs/ml gel and analyzed after 21 days with H&E staining. HMSCs were evenly distributed throughout all constructs. Gels fabricated with 2x GNS Ham F1 (A) or 2x GNS HG F1 (B) showed a lower cell density compared to gels fabricated with 2x GNS HG F2 (C). Bar = 100 μ m.

4.2.3 Chondrogenic differentiation of hMSCs in collagen hydrogels

To promote chondrogenesis of hMSCs in a 3D matrix, hMSC collagen hydrogels were cultivated under conditions shown to induce chondrogenic differentiation in the standard pellet culture differentiation assay, using serum-free chondrogenic differentiation medium with 10 ng/ml TGF- β 1 (CDM⁺) [Johnstone et al., 1998]. The chondrogenic phenotype of hMSCs in collagen hydrogels was first verified using histological analyses (Fig. 21). Upon culture in CDM⁺ chondrogenesis could be confirmed by the accumulation of sulfated proteoglycans, evidenced by positive alcian blue staining (Fig. 21B), and the synthesis of collagen type II, evidenced by positive immunohistochemistry (Fig. 21D). In contrast, no cartilage-specific matrix deposition was observed in CDM⁻ (Fig. 21A and C).

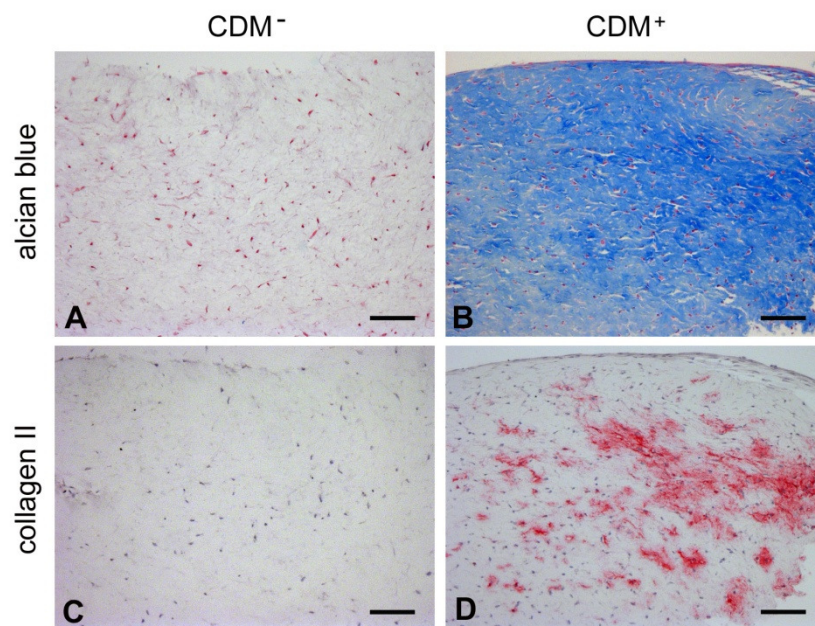


Fig. 21 Histological analysis of hMSC collagen hydrogels cultivated in either CDM⁻ or CDM⁺. Collagen hydrogels were seeded with or 3×10^5 hMSCs/ml gel and cultivated for 21 days in either CDM⁻ (A and C) or CDM⁺ (B and D). Alcian blue staining was negative in CDM⁻ (A), whereas in gels cultivated in CDM⁺ an ECM rich in sulfated proteoglycans could be detected (B). Immunohistochemical staining for collagen type II revealed no protein expression in CDM⁻ (C), whereas this cartilage-specific collagen was strongly deposited in CDM⁺ (D). Bar = 100 μ m.

In order to develop optimal differentiation conditions, parameters such as cell density and GNS composition were varied. First, the influence of different cell seeding densities on the chondrogenic differentiation of hMSCs in collagen hydrogels was examined after 28 days of culture by evaluating the expression levels of several cartilage-specific genes (Fig. 22). Standard collagen hydrogels were seeded with 1×10^5 or 3×10^5 hMSCs/ml gel, using 2x GNS Ham F1. Resulting from the proliferation studies (see section 4.2.2), higher cell seeding numbers were not investigated in these first experiments. HMSC collagen hydrogels cultivated in CDM⁻ expressed already basal levels of the early chondrocyte-related genes Col XI, AGN, and BGN and the chondrogenic transcription factor SOX9, regardless of the initial cell seed-

ing density. The mRNA level of COMP was distinct higher in gels seeded with the higher cell density. Surprisingly, a weak expression of Col II, the most important chondrogenic marker gene, was observed in the absence of TGF- β 1 in gels seeded with 3×10^5 hMSCs/ml gel, but not in gels with the lower cell density. There was no expression of Col IX and also no expression of Col X, the marker for hypertrophic chondrocytes. In the presence of TGF- β 1, however, all these genes were strongly up-regulated, to a similar degree for both analyzed initial cell seeding densities.

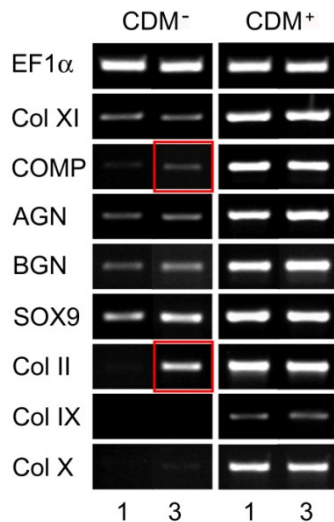


Fig. 22 Influence of the initial cell seeding density on the gene expression of hMSCs in collagen hydrogels. Collagen hydrogels were seeded with either 1×10^5 (1) or 3×10^5 (3) hMSCs/ml gel and cultivated in CDM or CDM⁺ for 28 days. The expression of several cartilage-specific genes could already be detected in CDM. However, a marked up-regulation was evaluated upon culture in CDM⁺.

Regarding the influence of different cell seeding densities on the chondrogenic differentiation of hMSCs in collagen hydrogels, Fig. 23 and Fig. 24 are showing the histological results of two different experiments with either 1×10^5 (Fig. 23A and B, Fig. 24A and B) or 3×10^5 hMSCs/ml gel (Fig. 23C and D, Fig. 24C and D). Areas at the margin of the hMSC collagen hydrogel, with a more fibrous appearance and stained positively for alcian blue (Fig. 23A), were often observed. There was obviously an accumulation of sulfated proteoglycans, but only negligible amounts of collagen type II could be detected (Fig. 24A). The light blue staining in the most part of the construct refers to the typical background staining known for collagen type I hydrogels, which is strengthened by the contraction of the gel. The strongest staining for cartilage-specific collagen type II in these experiments was detected in a construct seeded with 1×10^5 hMSCs/ml gel, as shown in Fig. 24B. Taking a closer look it could be ascertained, that the positive stained matrix revealed a complete different appearance compared to the rest of the hydrogel, and a distinct higher cell density. The cells in this area displayed a spherical morphology and appeared to be enclosed in lacunae, consistent with the chondrogenic phenotype. The cells were surrounded by a proteoglycan- and collagen type II-rich ECM. Considering hMSC collagen hydrogels seeded with the higher cell number, the histological staining showed on the one hand a complete lack of chondrogenic matrix secretion, indicated by negative staining for both, proteoglycans (Fig. 23C) and collagen type II (Fig. 24C). On the other hand, Fig. 23D and Fig. 24D show a construct with a similar appear-

ance to a pellet culture, with the formation of a proteoglycan- and collagen type II-rich ECM inside the hydrogel, and a more fibrous appearance at the periphery, stained only weakly positive for collagen type II (Fig. 24D).

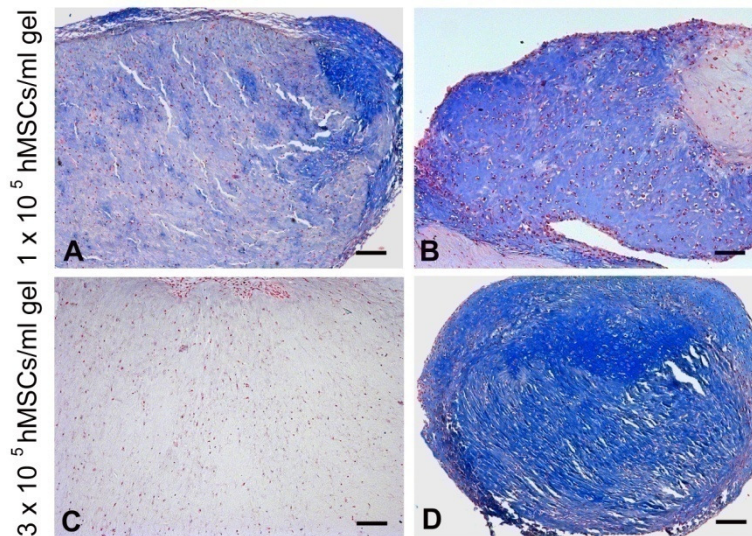


Fig. 23 Alcian blue staining of chondrogenic differentiated hMSC collagen hydrogels with different initial cell seeding densities. Collagen hydrogels were seeded with either 1×10^5 (A and B) or 3×10^5 hMSCs/ml gel (C and D) and cultivated for 21 days in CDM*. In both experiments with the lower cell number, distinct areas with positive staining could be detected (A and B), whereas in gels with the higher initial cell seeding density in one experiment no staining was observed (C), in contrast to the other experiment with an intense positive alcian blue staining (D). Bar = 150 μ m.

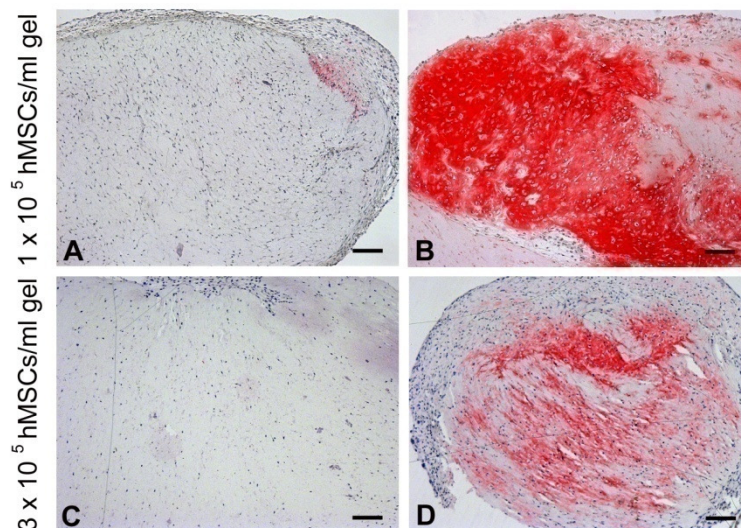


Fig. 24 Collagen type II immunostaining of chondrogenic differentiated hMSC collagen hydrogels with different initial cell seeding densities. Collagen hydrogels were seeded with either 1×10^5 (A and B) or 3×10^5 hMSCs/ml gel (C and D) and cultivated for 21 days in CDM*. The positive collagen type II staining was detected in corresponding areas to the alcian blue staining. Bar = 150 μ m.

Regarding the protein expression detected in histological staining, Tab. 3 summarizes the results obtained in all experiments performed with either 1×10^5 or 3×10^5 hMSCs/ml gel. Chondrogenic differentiation, indicated by the deposition of a proteoglycan-rich ECM (posi-

tive alcian blue staining) and cartilage-specific collagen type II, could not be realized in all experiments, neither with the lower nor the higher cell seeding concentration. In approximately 70% of the experiments a positive alcian blue staining was demonstrated for both cell numbers, whereas a higher percentage of hMSC collagen hydrogels initially seeded with 1×10^5 cells/ml gel revealed the accumulation of collagen type II.

Tab. 3 Overview of the histological results obtained in all experiments comparing the chondrogenic differentiation of hMSC collagen hydrogels with different initial cell seeding densities.

Seeded cell number/ml gel	Number of experiments performed	Number of positive alcian blue staining	Number of positive collagen type II staining
1×10^5	6 (100%)	4 (67%)	4 (67%)
3×10^5	17 (100%)	12 (71%)	8 (47%)

Gene expression analyses were also performed at different time points to compare the mRNA levels of several cartilage-specific genes (Fig. 25). Supporting the hypothesis of a mixed population of progenitor cells at different stages in primary hMSC cultures, at day 0 the expression of some cartilage-specific genes like Col XI, AGN, BGN, and SOX9, and the expression of the bone-specific genes Col I, ALP, OP, and BSP were detectable. In contrast to the results presented above (Fig. 22), in this particular experiment only low levels of COMP and AGN mRNA, and no Col II mRNA were expressed in CDM⁻. However, the expression of all chondrogenic genes was increased in the presence of TGF- β 1, more pronounced at day 21. The level of Col X mRNA also continued to increase with time in culture, indicating that hMSCs became hypertrophic when undergoing endochondral ossification. The development of a stable chondrogenic phenotype was further proved by analyzing the expression levels of several bone-specific marker genes. As shown in Fig. 25, ALP expression was no longer detectable upon cultivation in CDM⁻, whereas OP and BSP showed more or less constant mRNA levels. In CDM⁺ however, ALP, OP, and BSP were highly up-regulated at day 21 of culture. The mRNA level of Col I remained constant during the culture period, regardless of the medium, representing the constitutive expression of this gene already in undifferentiated, but also in chondrogenic differentiated hMSCs. These results suggest that hMSCs were capable of chondrogenic differentiation in collagen hydrogels, but showed additionally the expression of various osteogenic markers. However, no matrix mineralization was observed, indicated by negative alizarin red staining (not shown). The expression of bone-specific genes was not a result of culturing hMSCs in this particular 3D matrix, as hMSCs differentiated in the standard assay for chondrogenesis, in high-density pellet cell culture, showed a similar gene expression pattern (not shown).

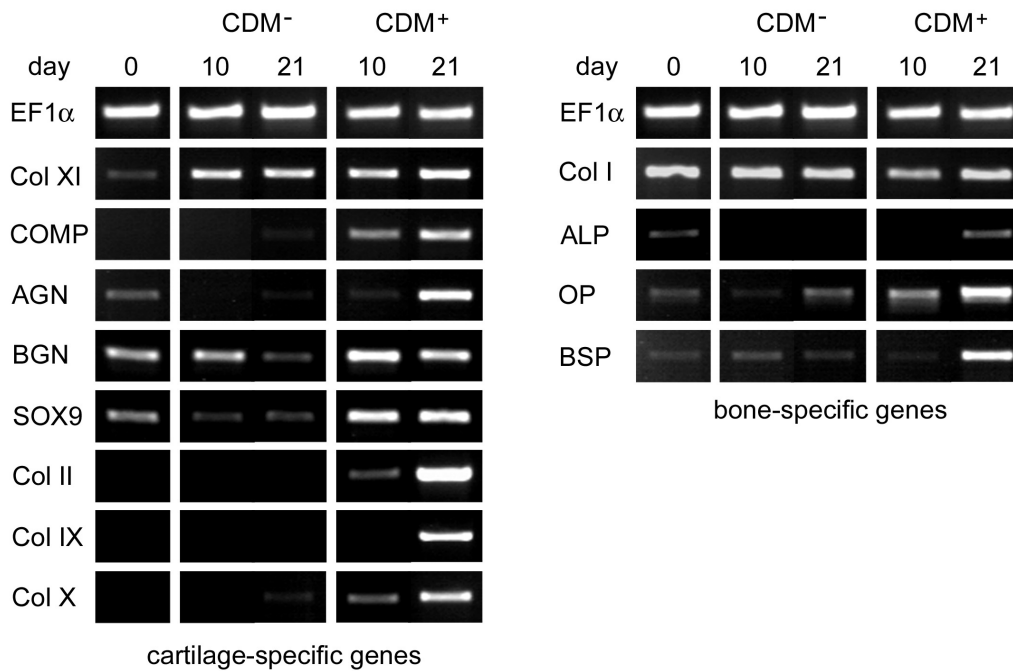


Fig. 25 Time sequence of the gene expression of hMSCs in collagen hydrogels cultivated in either CDM⁻ or CDM⁺. Collagen hydrogels were seeded with 3×10^5 hMSCs/ml gel and analyzed after 10 and 21 days of cultivation. Day 0 represents the gene expression levels of hMSCs at the end of primary culture, prior to embedding in collagen hydrogels. All analyzed cartilage-specific genes were expressed in CDM⁺ at day 21, but some were also detectable at day 0 and after 21 days cultivation in CDM⁻. Notably, also some bone-specific genes are already expressed at day 0 and are up-regulated in the presence of TGF- β 1.

Secondly, the influence of different GNS on the chondrogenic differentiation of hMSCs in collagen hydrogels was investigated. Fig. 26 shows the gene expression levels of various cartilage-specific genes after 28 days of cultivation in CDM⁺. hMSCs in collagen hydrogels, fabricated with different GNS, did express all these specific chondrogenic markers at comparable levels.

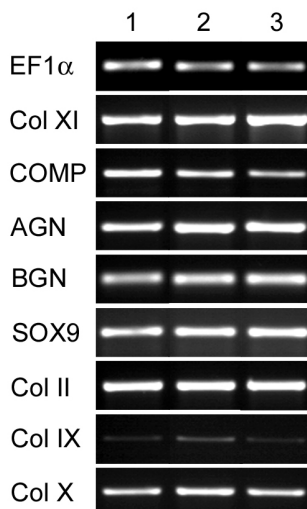


Fig. 26 Influence of the GNS composition on the gene expression of chondrogenic differentiated hMSC collagen hydrogels. Collagen hydrogels were seeded with 2×10^5 hMSCs/ml gel and cultivated in CDM⁺ for 28 days.

- 1: 2x GNS Ham F1
- 2: 2x GNS HG F1
- 3: 2x GNS HG F2

The expression of several cartilage-specific genes was similar in all GNS tested.

Histological staining of constructs of the same experiment as examined in Fig. 26 did confirm the gene expression analyses, except a slight diminished immunohistochemical staining for collagen type II in gels fabricated with 2x GNS HG F1. As shown in Fig. 27A-C, alcian blue staining revealed the accumulation of sulfated proteoglycans in the ECM of all constructs, with a homogeneous ECM structure in gels fabricated with 2x GNS HG F1 (Fig. 27B), whereas the use of 2x GNS Ham F1 or 2x GNS HG F2 resulted in the development of a more inhomogeneous, fibrous matrix (Fig. 27A and C, respectively). Immunohistochemical staining for collagen type II showed a similar staining pattern (Fig. 27D-F). hMSC hydrogels fabricated with 2x GNS HG F1 revealed only moderate dotted staining, evenly distributed throughout the matrix (Fig. 27E), whereas in gels with the other two GNS collagen type II was apparent more clearly but not homogeneously (Fig. 27D and F). The unstained areas in Fig. 27D and F contained no cells and therefore probably refer to swelled collagen fibers, incompletely dissolved by the fabrication of the collagen solution.

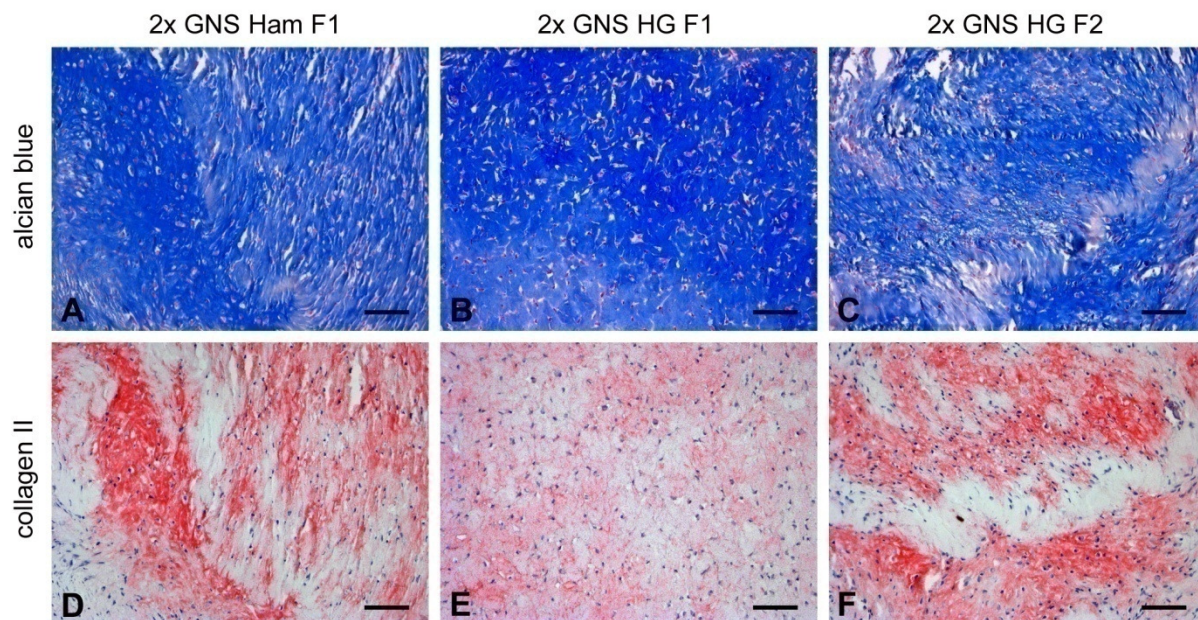


Fig. 27 Chondrogenic differentiation of hMSCs in collagen hydrogels fabricated with different GNS. Collagen hydrogels were seeded with 2×10^5 hMSCs/ml gel and cultivated in CDM⁺ for 28 days. Alcian blue staining revealed a proteoglycan-rich ECM in all constructs (A-C), showing a more homogeneous structure in gels fabricated with 2x GNS HG F1 (B). Collagen type II staining was more marked by the use of 2x GNS Ham F1 (D) and 2x GNS HG F2 (F), and showed only dotted staining in gels with 2x GNS HG F1 (E). Bar = 100 μ m.

In contrast to the results presented in Fig. 27, another experiment with a different lot of hMSCs revealed a complete different pattern of histological staining. As shown in Fig. 28, in hMSC collagen hydrogels fabricated with 2x GNS Ham F1 or 2x GNS HG F1, almost no cartilage-specific matrix accumulation could be detected (Fig. 28A,B,D,E). In a dramatic contrast to these staining, the use of 2x GNS HG F2 resulted in a pronounced chondrogenic differentiation of hMSCs within the hydrogel, with a intense alcian blue and collagen type II

staining throughout the gel, except a small area at the margins of the constructs (Fig. 28C and F). As a conclusion of this experiment, the culture medium used for the production of the GNS had no influence, whereas the use of a different FBS lot in combination with DMEM high glucose had a dramatic influence on the chondrogenic differentiation capacity of hMSCs in collagen hydrogels.

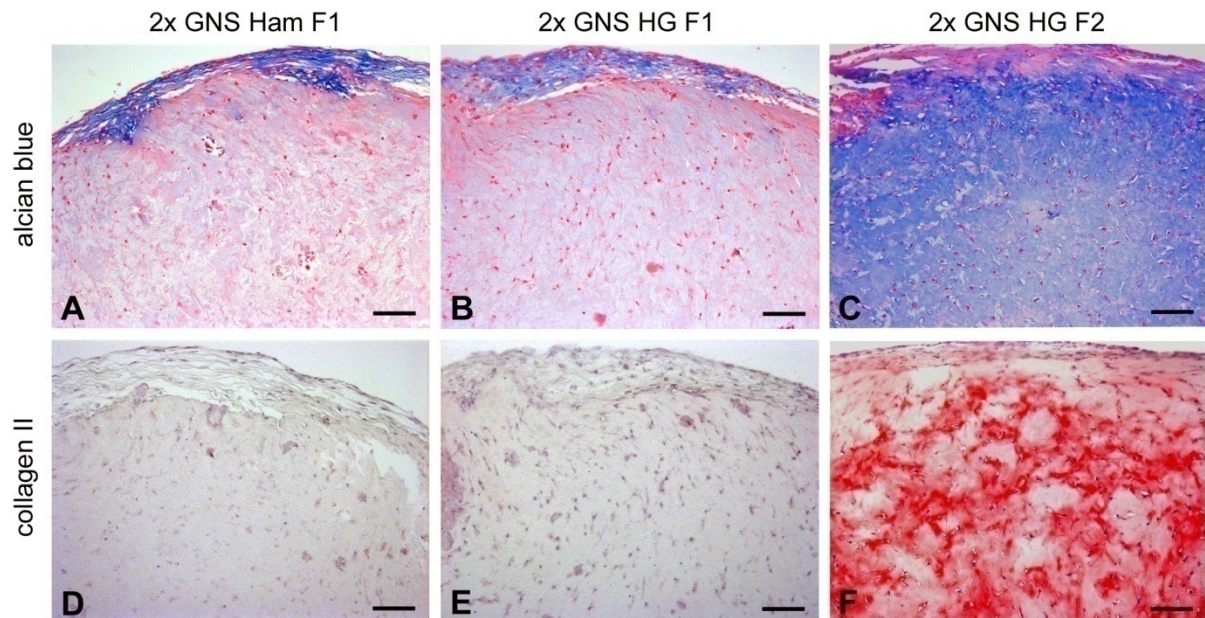


Fig. 28 Chondrogenic differentiation of hMSCs in collagen hydrogels fabricated with different GNS. Collagen hydrogels were seeded with 3×10^5 hMSCs/ml gel and cultivated in CDM⁺ for 28 days. Alcian blue staining revealed the deposition of proteoglycans only in a small area at the margins of the gels fabricated with 2x GNS Ham F1 (A) and 2x GNS HG F1 (B), whereas a homogeneous distribution of proteoglycans throughout the gel with 2x GNS HG F2 could be detected (C). Collagen type II staining was absent by the use of 2x GNS Ham F1 (D) and 2x GNS HG F1 (E), but was strongly positive for gels fabricated with 2x GNS HG F2 (F). Bar = 100 μ m.

Finally, one experiment was performed using 2x GNS Ham F1 and seeding cell numbers ranging from 1×10^5 to 1×10^6 hMSCs/ml into collagen hydrogels. RT-PCR analyses after 28 days of cultivation in CDM⁺ revealed for the early chondrocyte-related genes Col XI, COMP, AGN, and BGN almost no difference in the mRNA levels, whereas Col II, Col IX, and Col X showed a slight increase in gene expression with increasing cell number (Fig. 29). Nevertheless, even in collagen hydrogels with an initial cell seeding concentration of 1×10^5 hMSCs/ml gel all tested chondrogenic marker genes were expressed.



Fig. 29 Influence of the initial cell seeding density on the gene expression of chondrogenic differentiated hMSC collagen hydrogels. Collagen hydrogels were seeded with different cell numbers and cultivated in CDM⁺ for 28 days.

- 1: 1.0×10^5 hMSCs/ml gel
- 2: 2.5×10^5 hMSCs/ml gel
- 3: 5.0×10^5 hMSCs/ml gel
- 4: 7.5×10^5 hMSCs/ml gel
- 5: 1.0×10^6 hMSCs/ml gel

The expression of several cartilage-specific genes increased with increasing initial cell seeding density.

Histological analyses revealed a uniform distribution of the cells within the hydrogels and the development of a pericellular as well as an intercellular proteoglycan and collagen type II-rich extracellular matrix (Fig. 30 and Fig. 31).

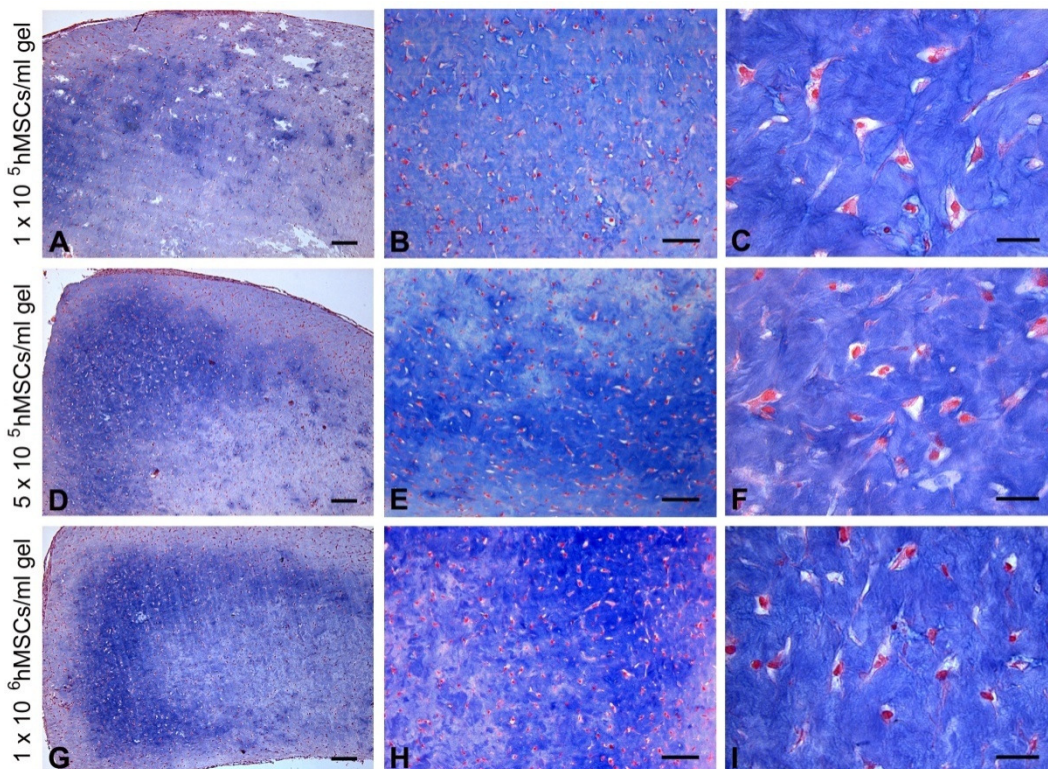


Fig. 30 Influence of the initial cell seeding density on the chondrogenic differentiation of hMSCs in collagen hydrogels. Collagen hydrogels were seeded with 1×10^5 (A-C), 5×10^5 (D-F), or 1×10^6 hMSCs/ml gel (G-I) and cultivated for 28 days in CDM⁺. As evidenced by alcian blue staining, in all constructs homogeneously distributed cells were embedded in a proteoglycan-rich ECM. Scale bars = 150 μ m (A,D,G), or 100 μ m (B,E,H), or 30 μ m (C,F,I).

On the surface of the hydrogels a dense layer of elongated cells was observed, consistent with findings from studies of MSCs in the pellet culture system [Mackay et al, 1998]. Interestingly, in the center and at the periphery of the construct areas with a lack of alcian blue and collagen type II staining were detected (Fig. 30A,D,G and Fig. 31A,D,G). The absence of newly synthesized matrix in the center of the hydrogels could be attributed to an insufficient nutrient supply. However, a higher magnification of the positive stained areas displayed a majority of cells with a spherical morphology indicative for the chondrogenic phenotype (Fig. 30C,F,I, and Fig. 31C,F,I). Although some cells appeared less spherical, they were also surrounded by a dense cartilage-specific ECM.

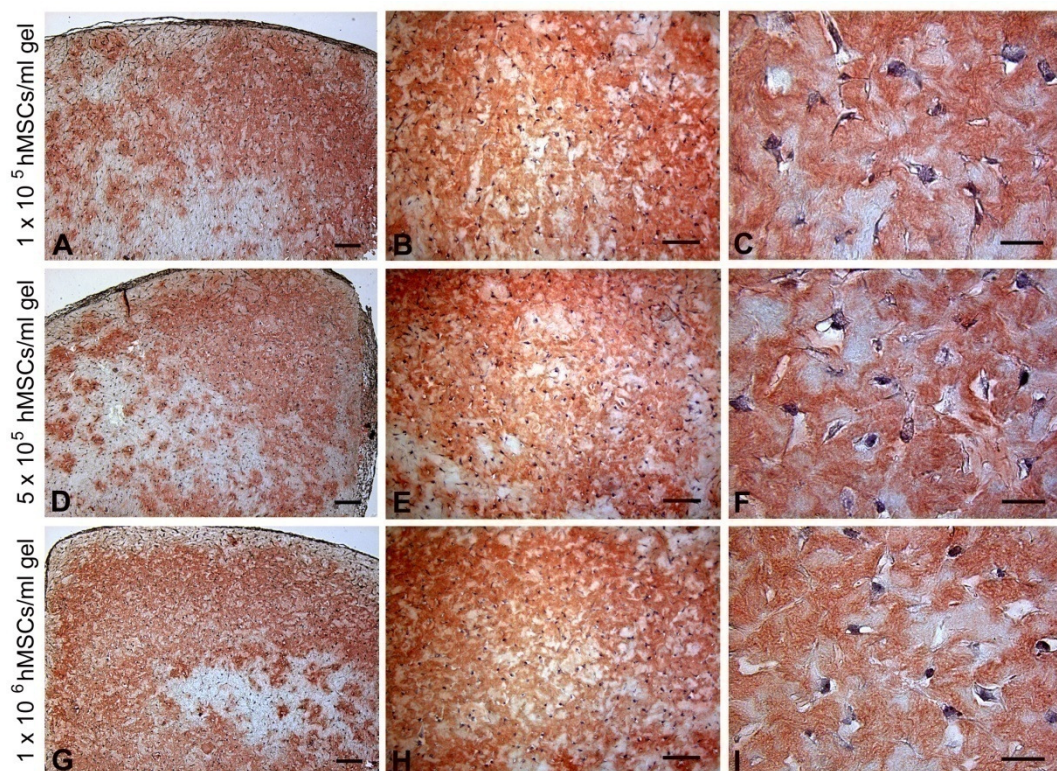


Fig. 31 Influence of the initial cell seeding density on the chondrogenic differentiation of hMSCs in collagen hydrogels. Collagen hydrogels were seeded with 1×10^5 (A-C), 5×10^5 (D-F), or 1×10^6 hMSCs/ml gel (G-I) and cultivated for 28 days in CDM*. As evidenced by immunohistochemical analysis, in all constructs most of the ECM was stained also for cartilage-specific collagen type II. Scale bars = $150 \mu\text{m}$ (A,D,G), or $100 \mu\text{m}$ (B,E,H), or $30 \mu\text{m}$ (C,F,I).

In conclusion, the partly inconsistent results presented above display probably the high donor variability influencing the development of a cartilaginous construct. Nevertheless, optimized hMSC collagen hydrogels for the bioreactor cultivation were fabricated with 2x GNS HG F2 and an initial cell seeding concentration of 3×10^5 cells/ml gel.

4.3 Mechanical stimulation of hMSC collagen hydrogels

4.3.1 Cellular behavior of hMSCs in collagen hydrogels during bioreactor cultivation

Constructs for the bioreactor cultivation were prepared by embedding 3×10^5 hMSCs/ml gel into collagen hydrogels, resulting in a total number of 1.8×10^6 hMSCs per gel. HMSC collagen hydrogels were first incubated in CDM⁻ for 10 days under free-swelling conditions. As presented already in section 4.2.1, during the cultivation process a distinct contraction of hMSC collagen hydrogels occurred dependent on the initial cell seeding concentration and the culture medium used. An initial cell concentration of 3×10^5 hMSCs/ml gel was used due to the results presented in sections 4.2.2 and 4.2.3. As the culture medium CDM⁻ was chosen because of the lowest amount of gel contraction and the highest survival of cells compared to SCM and CDM⁺. TGF- β 1, as the most important inducer of chondrogenic differentiation was deliberately omitted in the culture medium in order to detect explicitly the effects of mechanical stimulation on hMSCs without the strong influence of a cytokine. In the pre-culture period of 10 days, the contraction of hMSC collagen hydrogels was nearly completed. In contrast to the marked reduction in gel diameter during the contraction of cell seeded hydrogels, preliminary experiments showed almost no decrease of the height of hMSC collagen hydrogels over a culture period of 14 days.

Prior to transfer into the bioreactor, hMSC collagen hydrogels revealed a gel diameter of $66.9 \pm 1.6\%$ of their original diameter and a cell number of $1.4 \pm 0.3 \times 10^6$ per gel (Tab. 4). Viability staining clearly showed a majority of viable cells densely populated within the collagen hydrogel (Fig. 32). Some dead cells were also be detected, probably as a result of the transport of the constructs to the facility in Leipzig.

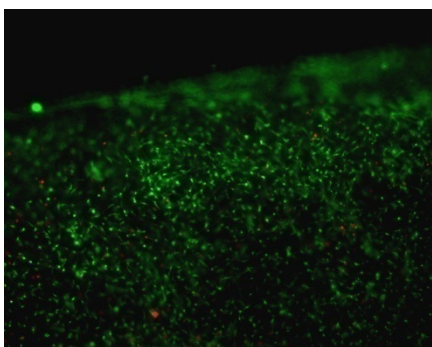


Fig. 32 Viability of hMSCs in collagen hydrogels after 10 days of cultivation in free-swelling culture. *Live/dead staining revealed that almost all cells in the construct were viable (green staining). Only a few dead cells (red staining) could be detected. (25x)*

A continuous control of the culture environment within the bioreactor system was performed during the whole culture period. Online monitoring of the oxygen partial pressure revealed a more or less constant pressure of 17%, the normally occurring level at 37°C (Fig. 33). Measurements of the pH-value showed slight cyclic variations in the range of 7.35-7.40, which is within normal physiology (Fig. 34).

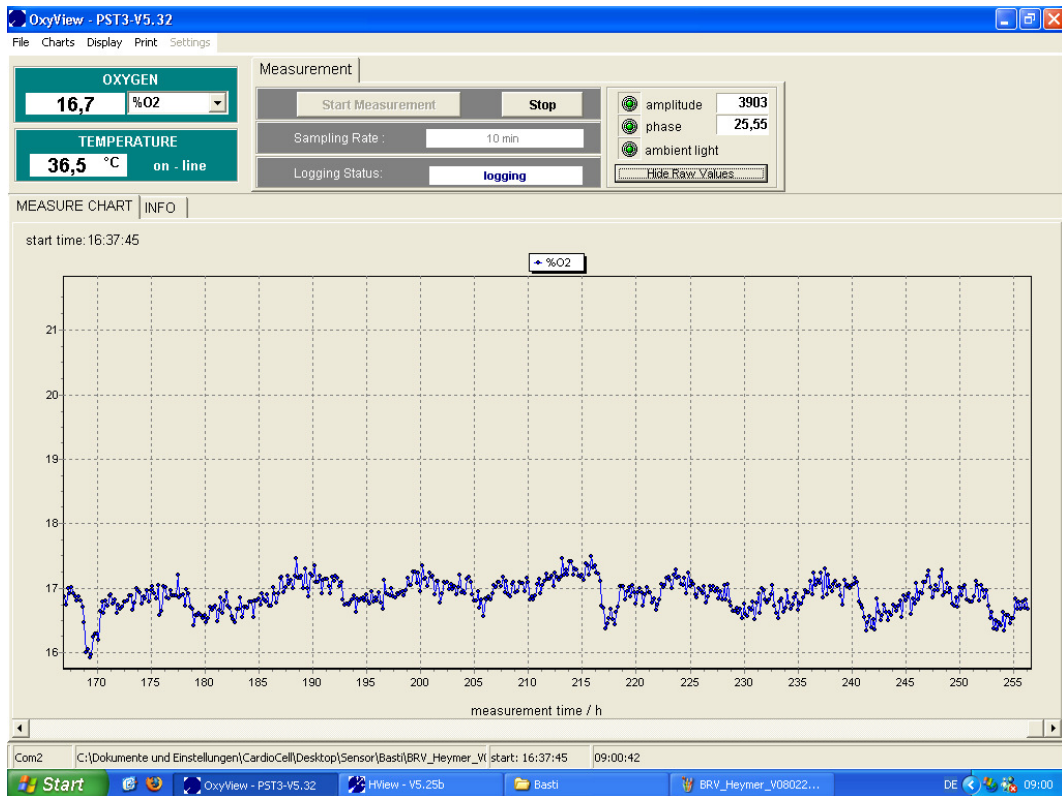


Fig. 33 Online monitoring of the partial pressure of oxygen. The course of oxygen partial pressure in the bioreactor system beginning at day 7 is shown. Measurements revealed always levels in the range of 17%.

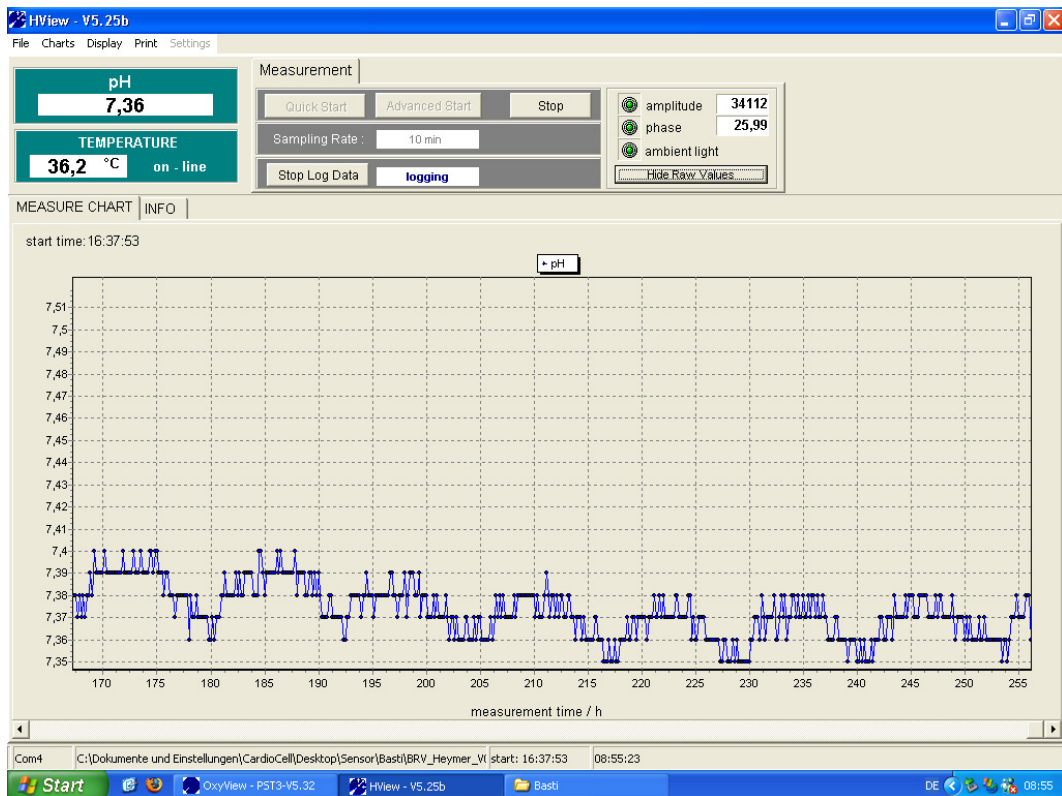


Fig. 34 Online monitoring of the pH-value. The course of pH-value in the bioreactor system beginning at day 7 is shown. Measurements revealed always levels in the physiological range of 7.3-7.4.

During the culture period, the gel diameter of mechanically stimulated constructs remained constant, whereas control cultures maintained under static, free-swelling conditions in 6-well cell culture plates showed a continued contraction (Tab. 4). The cell number at the end of culture was similar in stimulated and control constructs, revealing a slight increase compared to day 10. The live/dead assay provided proof of cell viability, showing living cells throughout the collagen hydrogel, in stimulated as well as in control cultures (Fig. 35). Only a few dead cells were visible.

Tab. 4 Summary of gel diameter and cell number of hMSC collagen hydrogels during 21 days of cultivation.

	day 0	day 10	control at day 21	load at day 21
gel diameter [%]	100.0 ± 0.0	66.9 ± 1.6	49.5 ± 4.8	68.8 ± 9.6
cell number [$\times 10^6$]	1.8 ± 0.0	1.4 ± 0.3	1.5 ± 0.1	1.5 ± 0.3

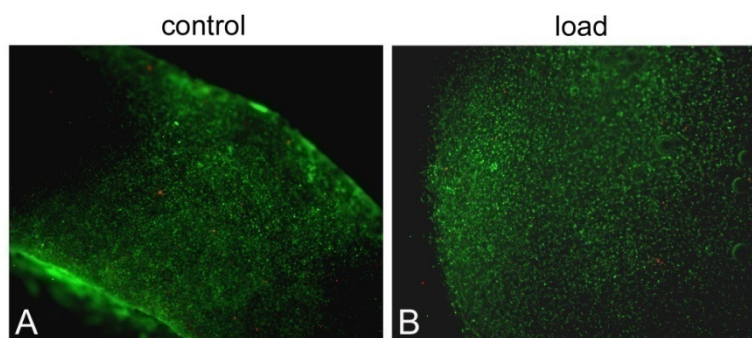


Fig. 35 Viability of hMSCs in collagen hydrogels after 21 days of cultivation. *Viable cells (green staining) were present in control (A) as well as in mechanical stimulated constructs (B). Only few dead cells (red staining) were detected. (25x)*

At the end of culture at day 21 histological analyses using alcian blue staining and collagen type II immunohistochemistry were performed in order to detect any potentially cartilage-specific matrix deposition. Similar for all analyzed constructs, hMSCs were homogeneously distributed throughout the collagen hydrogel. Control cultures maintained under static, free-swelling conditions in 6-well cell culture plates as well as mechanically stimulated constructs cultivated for 11 days in the bioreactor revealed no production of sulfated proteoglycans and collagen type II (Fig. 36A,B,D,E). Unfortunately, in all experiments performed almost no cartilage-specific protein deposition could be induced by the cultivation of hMSC collagen hydrogels in CDM⁺. As demonstrated in Fig. 36C, alcian blue staining was largely restricted to the vicinity of a few cells, and type II collagen expression was hardly ever apparent (Fig. 36F).

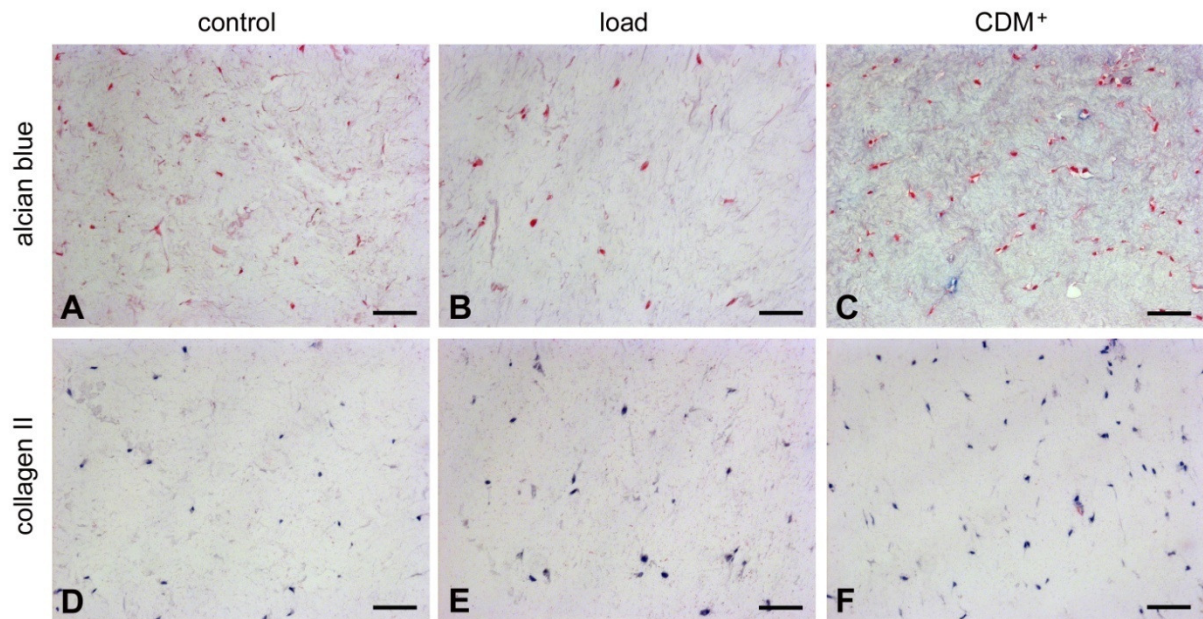


Fig. 36 Histological analysis of control (A and D), mechanically stimulated (B and E) and TGF- β 1-treated hMSC collagen hydrogels (C and F) after 21 days of cultivation. Alcian blue staining was negative in control (A) as well as in loaded constructs (B). Deposition of proteoglycans in hMSC collagen hydrogels cultivated in CDM⁺ appeared limited to only a view cells (C). Collagen type II staining was absent in control (D) and loaded construct (E), and was only weakly detected in the vicinity of one cell in the TGF- β 1-treated hMSC collagen hydrogel (F). Bar = 50 μ m.

4.3.2 Influence of mechanical stimulation on the gene expression of hMSCs in collagen hydrogels

Although histological analysis revealed no induction of chondrogenesis in mechanically stimulated hMSC collagen hydrogels, RT-PCR analyses of several cartilage- and bone-specific genes were performed to evaluate possible regulation on the mRNA level (Fig. 37). As already shown in Fig. 25, at day 0 the cartilage-specific genes Col XI, AGN, BGN, and SOX9, and the bone-specific genes Col I, ALP, OP, and BSP were expressed. Surprisingly, the expression of AGN disappeared during cultivation in CDM⁻ and was again strongly detected in CDM⁺. Regarding mechanically stimulated hMSC collagen hydrogels, the mRNA levels of two analyzed cartilage-specific genes were up-regulated, COMP and BGN. However, both genes were more expressed in CDM⁺, additionally to the other cartilage-specific genes. In this particular experiment the expression level of Col IX was only very low. All analyzed bone-specific genes were down-regulated upon culture in CDM⁻ and were distinct higher expressed in CDM⁺. In mechanically stimulated constructs, Col I and BSP were slightly up-regulated, whereas ALP and OP showed lower levels compared to the unloaded control constructs. To evaluate whether a degradation process was induced by mechanical stimulation, the gene expression levels of some matrix turnover-specific genes were assessed. After 21 days MMP3 was up-regulated in mechanically stimulated constructs, whereas similar expression levels of MMP13 and TIMP1 were detected in loaded and unloaded hMSC collagen

hydrogels. No induction of inflammation was confirmed by the absence of IL-1 β mRNA (not shown).

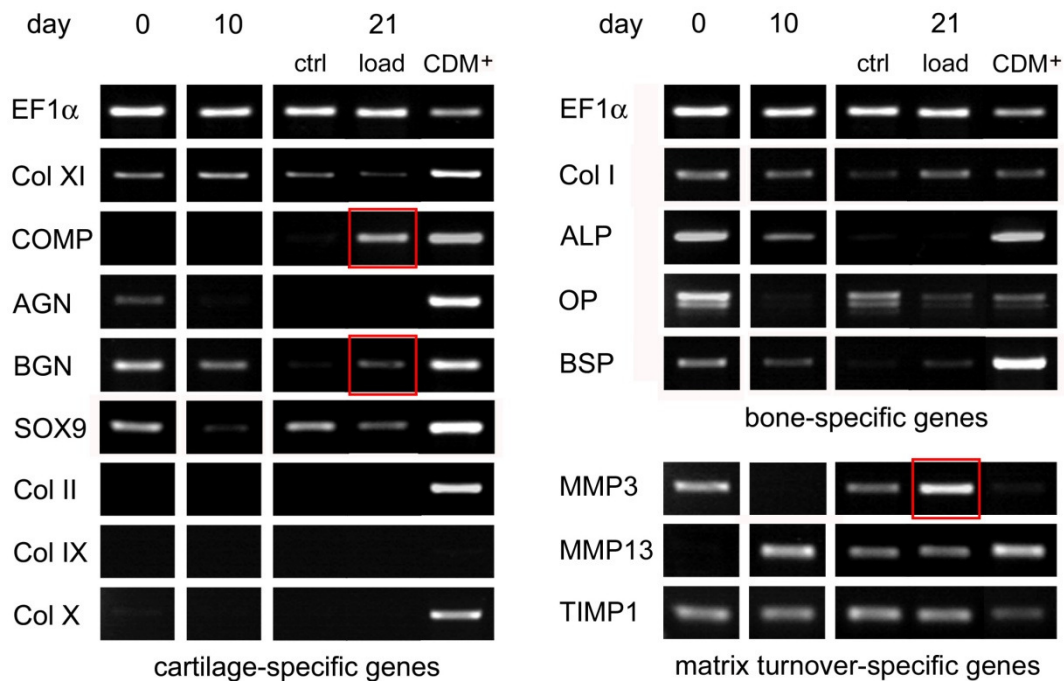


Fig. 37 Influence of mechanical stimulation on the gene expression of hMSCs in collagen hydrogels. *HMSC collagen hydrogels were analyzed prior to transfer into the bioreactor at day 10 and at the end of culture on day 21. Day 0 represents the gene expression levels of hMSCs at the end of primary culture, prior to embedding in collagen hydrogels. All analyzed cartilage-specific genes were expressed in CDM⁺ at day 21, but some were also detectable at day 0 and day 10. In mechanically stimulated constructs (load) COMP and BGN were up-regulated compared to the unloaded controls (ctrl). Bone-specific genes were highly expressed in CDM⁺ and showed only slight differences in the expression levels between control and mechanically stimulated constructs at day 21. The matrix-degrading enzyme MMP3 was up-regulated upon mechanical stimulation whereas MMP13 and TIMP1 were similar expressed.*

4.4 Labeling of hMSCs with VSOPs for cellular MR imaging

4.4.1 Detection of iron oxide particles within VSOP-labeled hMSCs

Efficient labeling was confirmed after each labeling experiment using iron-specific prussian blue staining. The presence of various small iron oxide particles within the cytoplasm of VSOP-labeled hMSCs was indicated by distinct blue dots. As demonstrated in Fig. 38A, the rate of labeling per cell was variable, with some cells showing more intense staining than others. No positive staining could be detected in unlabeled control cells (Fig. 38B).

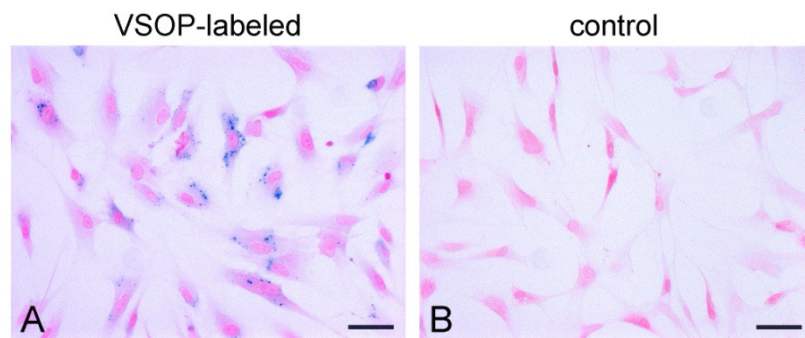


Fig. 38 Representative prussian blue staining of VSOP-labeled and unlabeled hMSCs. Intracytoplasmatic iron particles (blue) were only visible in VSOP-labeled cells (A), whereas unlabeled control cells showed no staining (B). Bar = 50 μm .

Particle incorporation was further demonstrated using fluorescent dye-labeled VSOPs. FITC-labeled iron oxide particles could be detected within the cytoplasm of the cells (Fig. 39A). Transmission electron microscopy of VSOP-labeled hMSCs also confirmed the presence of iron oxide particles inside the cells and clearly showed electron-dense clusters of magnetic particles exclusively in intracellular membrane-enclosed vesicles (Fig. 39B), indicating an endocytotic process of iron uptake.

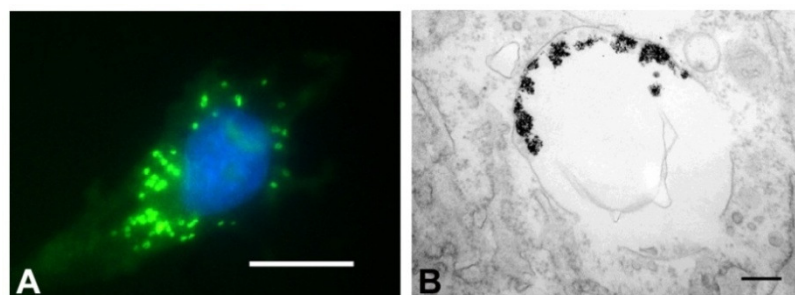


Fig. 39 Demonstration of iron oxide particles within the cytoplasm of VSOP-labeled hMSCs. (A) Fluorescence microscopy image of a single cell, showing green fluorescent VSOPs in the cytoplasm and blue nucleus from DAPI staining. Bar = 10 μm . (B) Representative TEM image showing accumulation of electron dense particles in endocytotic vesicles inside the cytoplasm. Bar = 0.25 μm .

Furthermore, to quantify the cellular uptake of iron oxide particles following VSOP labeling, ICP-MS was performed. The measurements revealed a significant higher average iron con-

centration of 4.59 ± 2.01 pg iron per cell in VSOP-labeled hMSCs (Fig. 40). The high standard deviation refers to relatively large differences in the iron content of labeled hMSCs from different donors. In contrast, unlabeled cells exhibited an iron content of 0.22 ± 0.15 pg per cell, which corresponds to the sum of the natural intracellular iron content.

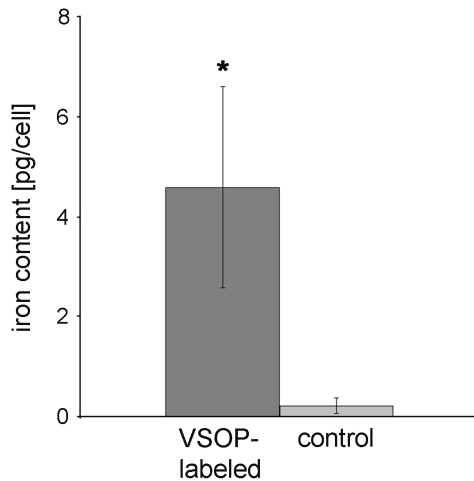


Fig. 40 Iron incorporation per cell as determined by ICP-MS. VSOP-labeled hMSCs exhibited a significant higher iron content per cell (mean \pm SD, $n = 8$, $p < 0.001$).

4.4.2 Influence of VSOP labeling on the cellular viability and apoptosis of hMSCs

Cellular viability, determined immediately after labeling with trypan blue, was not influenced by the labeling procedure. VSOP-labeled hMSCs exhibited a viability of $96.8 \pm 3.3\%$, unlabeled control cells a viability of $97.2 \pm 3.4\%$ (Fig. 41A). Furthermore, VSOP labeling of hMSCs did not result in increased apoptosis compared to unlabeled control cells. The measured luminescent signal, which is proportional to the amount of caspase activity, showed similar levels in both, labeled and unlabeled cultures (Fig. 41B).

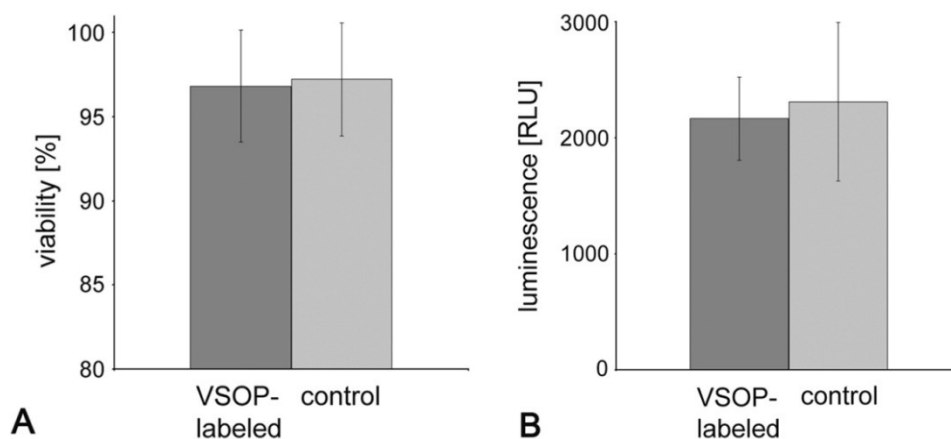


Fig. 41 Cellular viability and apoptosis of VSOP-labeled and unlabeled hMSCs. (A) Viability of VSOP-labeled and unlabeled hMSCs. Trypan blue exclusion test immediately after labeling showed no significant difference (mean \pm SD, $n = 42$). (B) Analysis of apoptosis of VSOP-labeled and unlabeled hMSCs 24 h after labeling. No induction of apoptosis in VSOP-labeled hMSCs could be detected compared to unlabeled cells (mean \pm SD, $n = 5$).

The metabolic activity as an indicator of cell viability of VSOP-labeled and unlabeled control cells, determined with the WST assay, was evaluated for three different donors. As shown in Fig. 42, in one hMSC population no difference could be detected, and in the other two populations VSOP-labeled hMSCs showed only a slight inhibition of cellular activity.

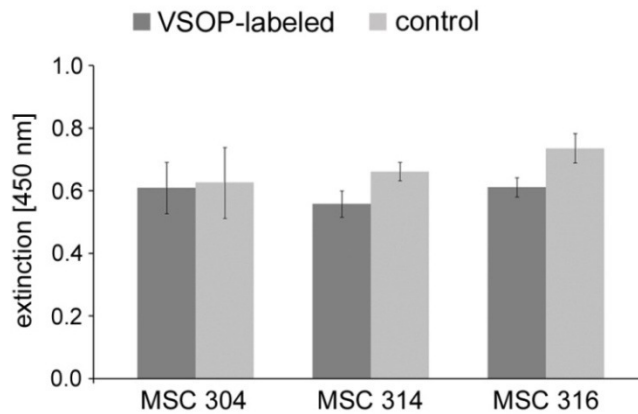


Fig. 42 Metabolic activity of 3 different hMSC populations after VSOP labeling. The WST assay revealed little or no inhibition of cellular activity of VSOP-labeled hMSCs compared to unlabeled control cells (mean \pm SD, $n = 10$).

4.4.3 Influence of VSOP labeling on the proliferation capacity of hMSCs

To evaluate whether VSOP labeling has any adverse effect on cellular proliferation, hMSCs from four different donors were examined in proliferation curves in the first passage, immediately after the labeling procedure. In three hMSC populations comparable growth rates of VSOP-labeled and unlabeled control cells could be assessed, as shown exemplary in Fig. 43A. However, VSOP-labeled hMSCs from one donor were slightly inhibited in their proliferation capacity (Fig. 43B).

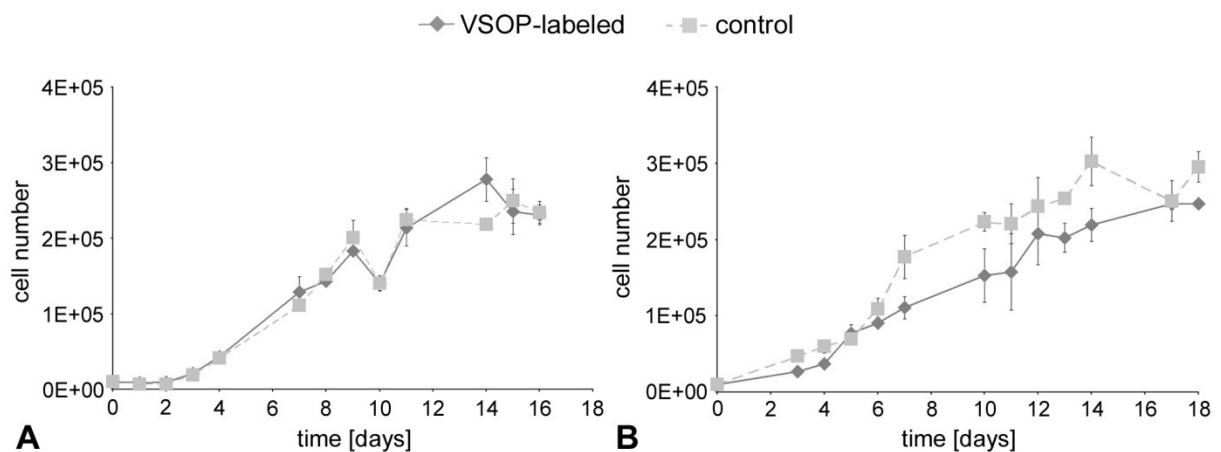


Fig. 43 Influence of VSOP labeling on hMSC proliferation in short-term culture. In 3 out of 4 experiments, the growth rates were not affected by the incorporation of VSOPs (A), whereas in one experiment a slight reduction of the cell proliferation rate was assessed (B). Mean \pm SD, $n = 3$.

The small differences between the proliferation curves in Fig. 43B were proved by determination of population doubling times during expansion of the cells over a longer period of time. As shown in Fig. 44, in long-term cultivation no loss of proliferative activity was detectable for VSOP-labeled cells compared to unlabeled control cells. The population doubling times, as determined over 6 passages of cultivation, showed no significant differences.

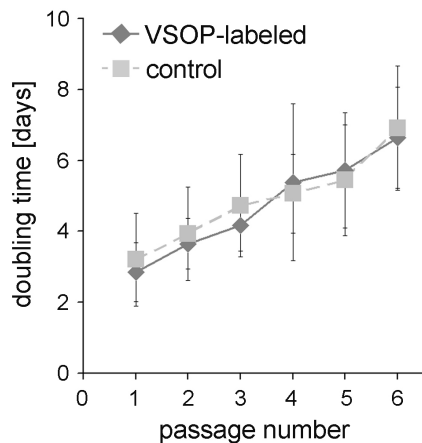


Fig. 44 Effect of VSOP labeling on the proliferation capacity of hMSCs. No differences in population doubling times were observed over 6 passages of cultivation (mean \pm SD, $n = 8$).

To determine the persistence of magnetic label upon cell division, the presence of iron in VSOP-labeled hMSCs was tracked histologically over several passages in monolayer culture (Fig. 45). Prussian blue staining revealed a distinct reduction of VSOP labeling after 5 to 9 cell divisions, relating to passages 2 to 3. This can be attributed to the splitting of iron oxide particles between the daughter cells but may also be a result of the cellular degradation of VSOPs.

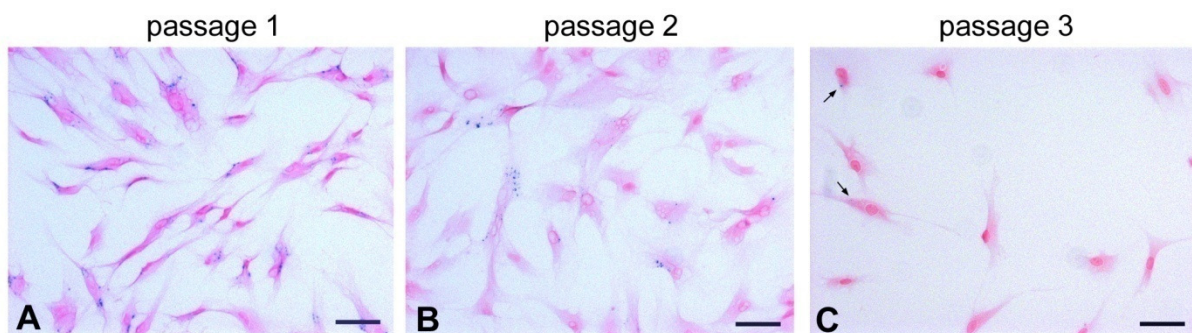


Fig. 45 Detection of intracellular iron oxide particles during expansion of hMSCs. Prussian blue staining clearly shows the presence of iron oxide particles as blue-colored dots in almost every cell at passage 1 immediately after VSOP labeling (A), but a distinct reduction of label in passage 2 (B). In passage 3, only scattered stained cells could be detected (C). Bar = 50 μ m.

4.4.4 Differentiation of VSOP-labeled hMSCs

To exclude possible adverse effects of the labeling procedure on the differentiation capacity of hMSCs, adipogenic, osteogenic, and chondrogenic differentiation assays were performed to prove multilineage differentiation of VSOP-labeled hMSCs. Differentiation into specific lineages was monitored with histological staining to detect accumulation of the extracellular matrix and by determination of lineage-specific mRNA levels.

Following adipogenic differentiation, positive oil red O staining at day 28 showed similar fat vacuole accumulation in both, VSOP-labeled and unlabeled control cells (Fig. 46A and B). Also, the gene expression levels of the adipogenic markers LPL and PPAR γ 2 in VSOP-labeled hMSCs and unlabeled cells revealed no differences after appropriate stimulation (Fig. 46C). Cells maintained in SCM as a negative control showed no intracytoplasmatic lipid vesicle staining (not shown).

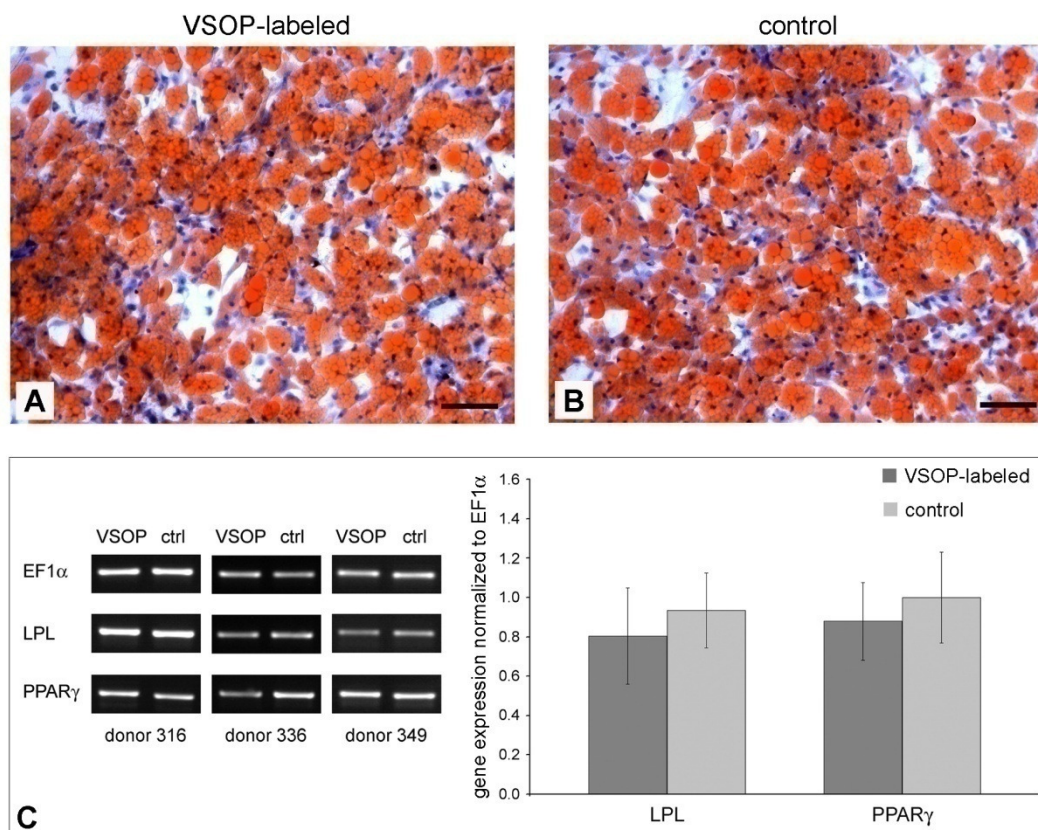


Fig. 46 Adipogenic differentiation of VSOP-labeled and unlabeled hMSCs. Oil red O staining revealed lipid vacuoles in VSOP-labeled (A) and unlabeled control hMSCs (B) following induction of adipogenesis (bar = 100 μ m). Analysis of gene expression showed the presence of LPL and PPAR γ 2 mRNA (C). Evaluation by densitometry exhibited no difference in the gene expression levels between adipogenic induced VSOP-labeled and unlabeled control cells (mean \pm SD, n = 3).

Osteogenic differentiation led to a strong matrix mineralization in VSOP-labeled as well as in unlabeled cultures at day 28, as shown histologically by alizarin red S staining (Fig. 47A and B). No positive staining was seen in negative control cells (not shown). Furthermore, VSOP-labeled and unlabeled cells exposed to osteogenic supplements revealed a similar gene expression pattern of the bone-specific markers ALP and BSP (Fig. 47C).

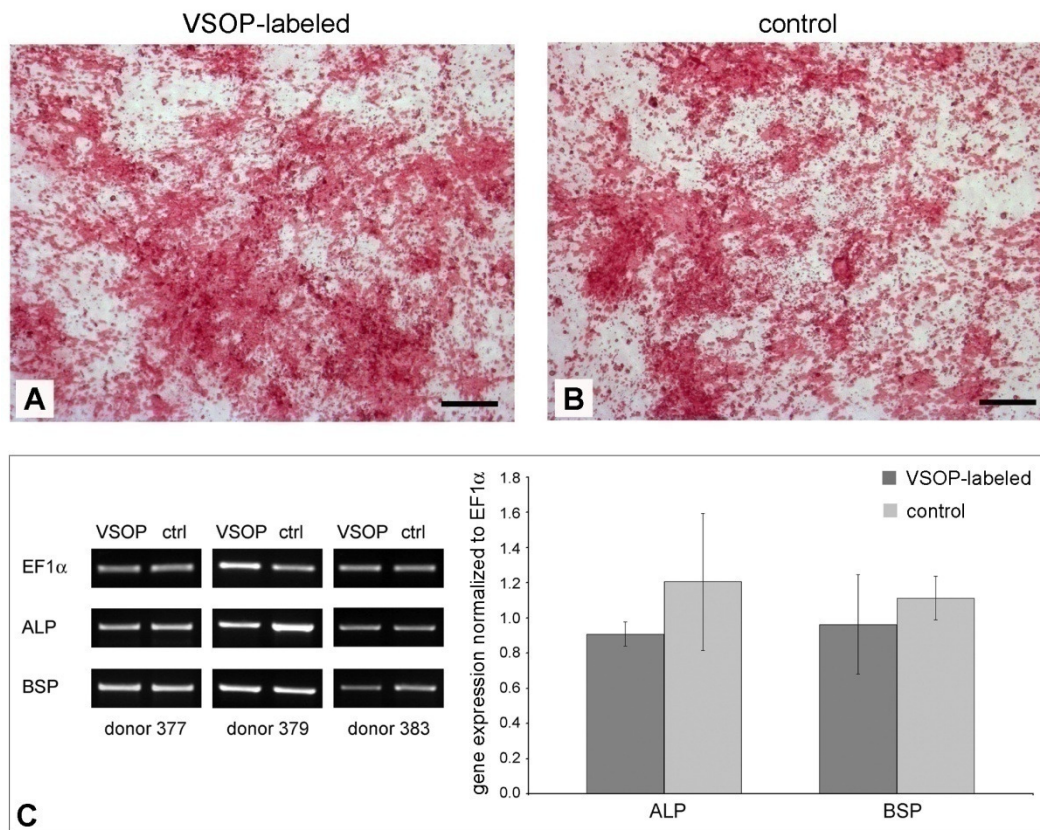


Fig. 47 Osteogenic differentiation of VSOP-labeled and unlabeled hMSCs. Alizarin red S staining showed similar calcium deposition in VSOP-labeled hMSCs (A) and unlabeled control cells (B) after induction of osteogenesis (bar = 100 μ m). Also, the mRNA expression of ALP and BSP were clearly detectable in both cultures (C). Analysis of the intensity of PCR products showed no differences in the gene expression levels of VSOP-labeled and unlabeled control cells (mean \pm SD, n = 3).

Chondrogenic differentiation in high-density pellet cell cultures over 28 days exhibited cells with a rounded chondrocyte-like morphology embedded in a cartilage-specific extracellular matrix. Alcian blue staining showed a homogeneous and in most cases similar distribution of sulfated proteoglycans in the ECM of both groups (Fig. 48A and B). In two out of six differentiation experiments, however, a slightly more intense staining in the pellets of unlabeled control cells was detected. This slight difference in staining intensity was also seen in the corresponding immunohistochemical staining for cartilage-specific collagen type II (Fig. 48C and D). In contrast, the analysis of the gene expression levels of the chondrogenic markers AGN and Col II revealed in all analyzed cultures no difference between VSOP-labeled and unlabeled hMSCs (Fig. 48E). Control pellet cultures cultivated without TGF- β 1 were considerably smaller and showed no evidence of chondrogenic matrix accumulation (not shown).

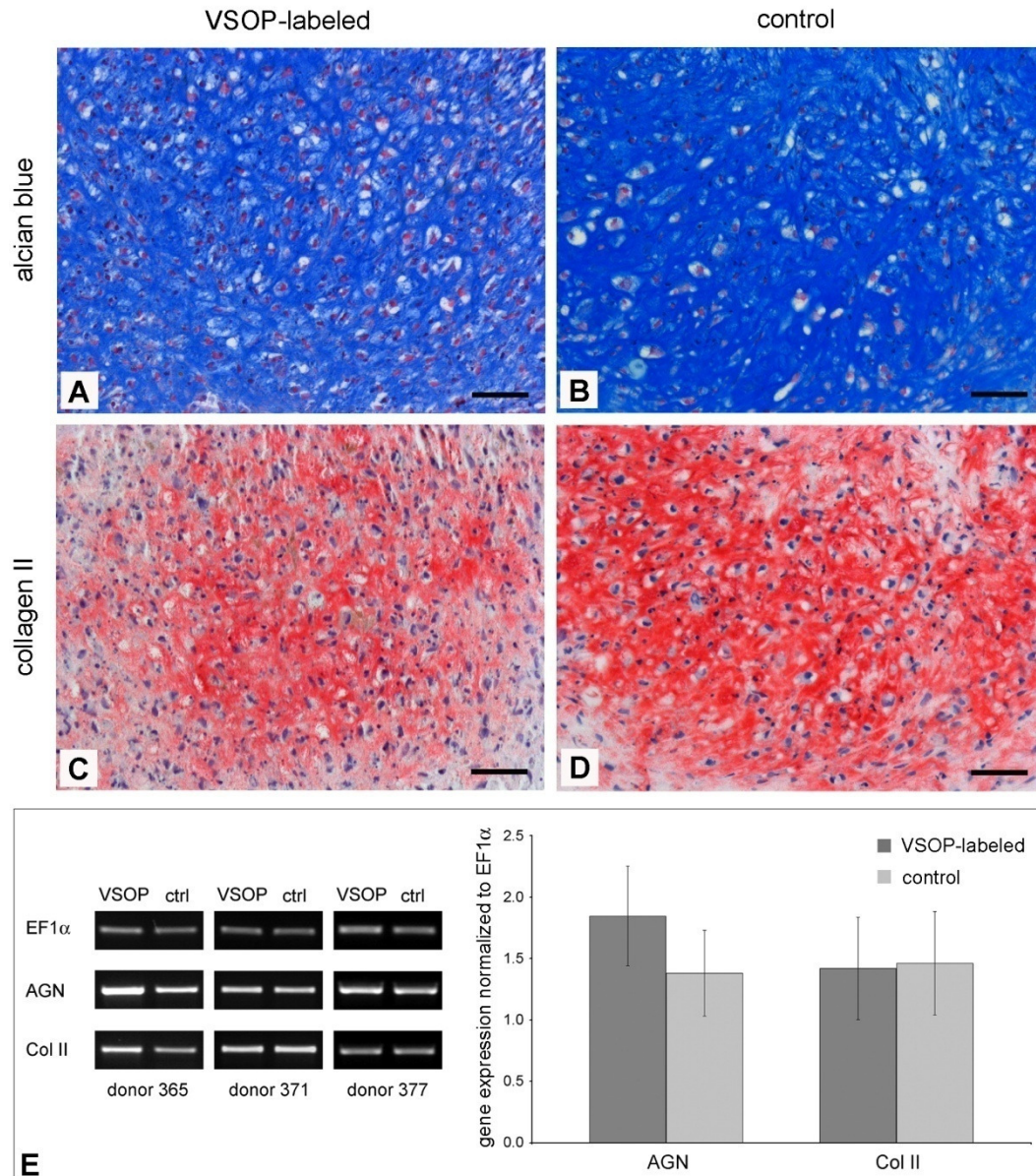


Fig. 48 Chondrogenic differentiation of VSOP-labeled and unlabeled hMSCs. Alcian blue staining revealed a proteoglycan-rich extracellular matrix in labeled (A) and unlabeled control pellets (B). Cartilage-specific collagen type II staining was observed in both, VSOP-labeled (C) and unlabeled cultures (D). Both staining were more pronounced in the unlabeled control cultures. Expression of AGN and Col II mRNA were visible in both, VSOP-labeled and unlabeled pellet cultures (E). No difference in the gene expression levels of these cartilage-specific genes could be evaluated (mean \pm SD, $n = 3$).

In summary, both VSOP-labeled and unlabeled control cells showed similar gene expression patterns and matrix staining after appropriate stimulation. Thus, labeling with VSOPs had no influence on the adipogenic, osteogenic, and chondrogenic differentiation capacity of hMSCs.

4.5 MR imaging of VSOP-labeled cells in collagen hydrogels

To visualize VSOP-labeled hMSCs in collagen hydrogels, high-resolution MR imaging at 11.7 T was performed. One major drawback in the detection of iron particles with ^1H -MRI is the similar signal void of iron oxide particles and potentially existing air bubbles. Therefore, to exclude false-positive signals, hMSC collagen hydrogels were cultivated for a minimum of 3 days before MR imaging to allow air bubbles to disappear.

4.5.1 Detection limit of MRI

In a first experiment, different concentrations of VSOP-labeled hMSCs were embedded in collagen hydrogels, cultivated for 5 days and imaged subsequently (Fig. 49). The presence of iron oxide particles was indicated by distinct hypointense spots in the MR images. In contrast, control collagen hydrogels with unlabeled cells were undistinguishable from the medium background and showed no iron specific loss of signal intensity. Isolated dark spots in these control gels and on their surface were attributed to the presence of some remaining air bubbles.

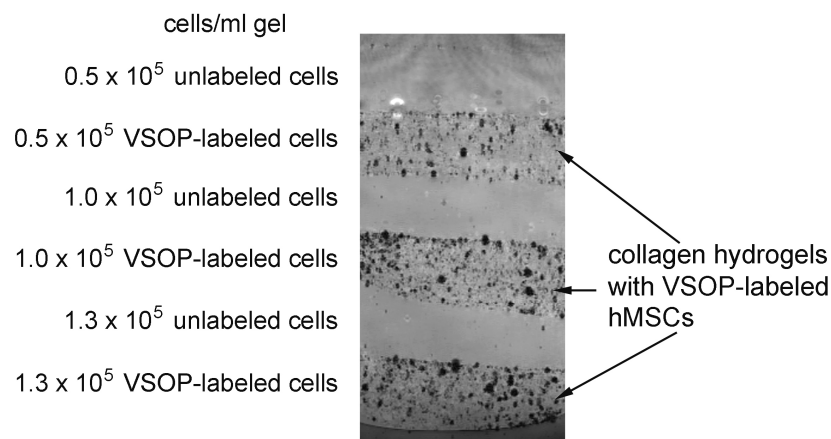


Fig. 49 MR imaging of hMSC collagen hydrogels. VSOP-labeled cells were detected by the typical signal decrease due to iron particles, present as dark spots. Control collagen hydrogels with unlabeled cells showed a homogeneous appearance without hypointense spots. 3D FLASH experiment, nominal spatial resolution: $78 \times 78 \times 208 \mu\text{m}^3$, $T_E = 20 \text{ ms}$, $T_R = 250 \text{ ms}$.

To confirm the MR data, histological analysis of the imaged hMSC collagen hydrogels was performed. As presented in Fig. 50, hMSCs were homogeneously distributed throughout the constructs. Prussian blue staining demonstrated the presence of iron oxide particles within VSOP-labeled hMSCs, whereas no positive staining could be detected in control collagen hydrogels.

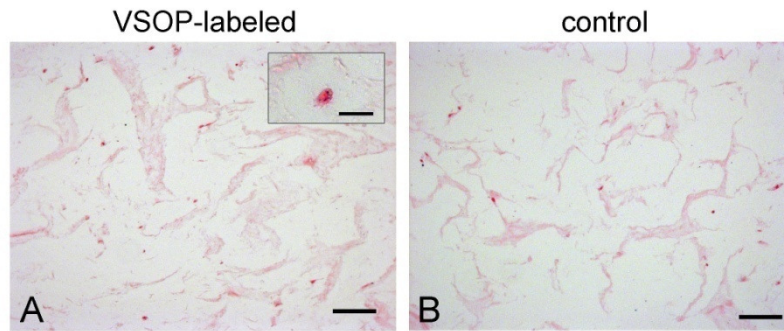


Fig. 50 Histological analysis of imaged hMSC collagen hydrogels. Prussian blue staining of hMSC collagen hydrogels with 1×10^5 cells/ml gel confirmed iron containing single cells, homogeneously distributed in the construct (A). The inset in (A) shows a higher magnification (bar = $20 \mu\text{m}$) of a single cell containing blue stained iron particles. Control collagen hydrogels with unlabeled cells showed no positive staining (B). Bar = $100 \mu\text{m}$.

As already demonstrated in Fig. 49, collagen hydrogels with 5×10^4 hMSCs/ml gel were clearly detectable in the MR images. To assess an *in vitro* MR detection limit for VSOP-labeled hMSCs in collagen hydrogels at 11.7 T, constructs with lower cell numbers of VSOP-labeled hMSCs were fabricated and cultured for 7 days in SCM before imaging. In order to make sure that almost no reduction of VSOP labeling due to cell proliferation occurs, all constructs were seeded with the equal total cell number, but differing in the fraction of labeled hMSCs. Preliminary experiments have shown that with an initial cell seeding density of 1×10^5 hMSCs/ml gel the cell number within collagen hydrogels remained nearly constant over a culture period of 7 days (Fig. 51). After the already in section 4.2.2 described decline in cell number at day 2 a slight proliferation of hMSCs with a maximum of one cell doubling could be observed. Resulting from the proliferation studies presented in section 4.4.3 comparable growth rates of VSOP-labeled and unlabeled hMSCs were assumed. Additionally, a distinct reduction of VSOP labeling appeared not till the 5th cell division (see section 4.4.3).

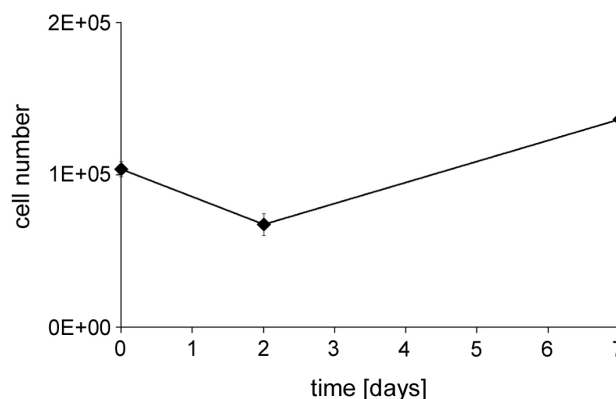


Fig. 51 Cell proliferation of hMSCs in collagen hydrogels seeded with 1×10^5 cells/ml gel and cultivated in SCM. After 7 days in culture, the cell number revealed no difference compared to the initially seeded cell concentration (mean \pm SD, $n = 3$). The high SD refers to relatively large differences between different donors.

Fig. 52 demonstrates an exemplary MR image containing three constructs with different concentrations of VSOP-labeled hMSCs and one control construct with only unlabeled cells. With the applied MR parameters a detection limit of 5×10^3 VSOP-labeled hMSCs/ml gel could be ascertained.

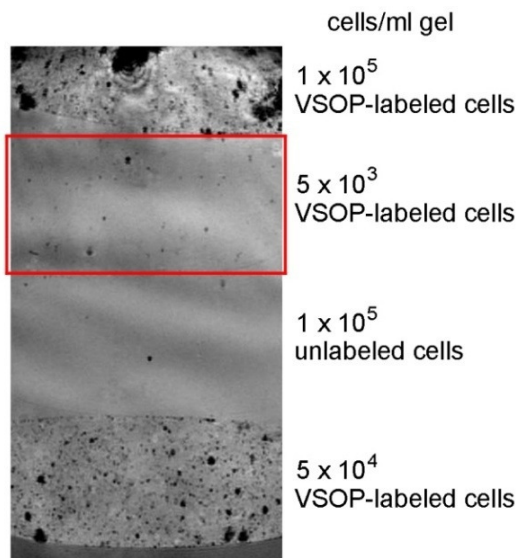


Fig. 52 Detection limit of VSOP-labeled hMSC collagen hydrogels at 11.7 T. With decreasing concentrations of VSOP-labeled hMSCs less hypointense spots were detected in the MR image. Collagen hydrogels with 5×10^3 hMSCs/ml gel were barely distinguishable from control gels with unlabeled cells. 3D FLASH experiment, nominal spatial resolution: $59 \times 78 \times 208 \mu\text{m}^3$, $T_E = 25$ ms, $T_R = 50$ ms.

4.5.2 Long-term MRI of VSOP-labeled hMSC collagen hydrogels

In order to examine the stability of VSOP labeling in hMSC collagen hydrogels, a long-term study was performed. After embedding 5×10^4 magnetically labeled hMSCs in collagen hydrogels and cultivation in SCM, where no proliferation takes place, Fig. 53 implicates that the cells could be detected with a MR spectrometer over 21 weeks. After 4 and 10 weeks a comparable distribution of dark spots in the VSOP-labeled constructs were observed in the MR images (Fig. 53A and B). However, with time in culture, a distinct reduction of these hypointense spots could be seen (Fig. 53C). Due to appropriate MR parameters and adjustment of the image contrast, controls with unlabeled cells were also visible in these MR images, but didn't exhibit the typical signal intensity decrease conditioned by VSOP.

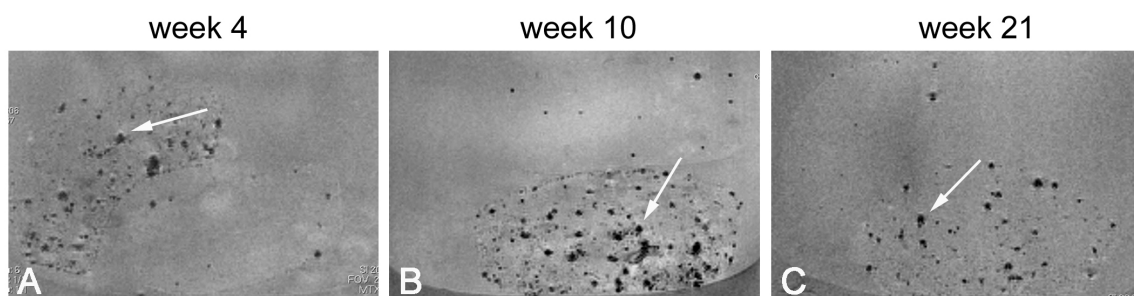


Fig. 53 Long-term detection of VSOP-labeled hMSC collagen hydrogels. MR images were acquired 4 (A), 10 (B), and 21 weeks (C) after fabrication of VSOP-labeled and control hMSC collagen hydrogels. The arrowheads point at signal intensity decreases probably due to the existence of VSOP-labeled hMSCs. 3D FLASH experiment, isotropic spatial resolution of $78 \mu\text{m}$, $T_E = 10$ ms, $T_R = 50$ ms.

To verify whether the detected dark spots in the MR images (Fig. 53) really refers to VSOP-labeled hMSCs, histological analyses of imaged hMSC collagen hydrogels were performed. At 4 and 10 weeks the MR data could be confirmed by the use of prussian blue staining, showing iron containing cells (Fig. 54A and B). After 4 weeks of culture, both, VSOP-labeled and unlabeled hMSCs were homogeneously distributed within the collagen hydrogels. After 10 weeks, however, in contrast to the MR findings, a distinct reduction in cell density was observed for both groups. The decrease in cell number became even more apparent at 21 weeks, where only a few unstained cells were seen at the margins of the construct, but surprisingly large positive stained areas in the center of the gel, referring probably to iron oxide particles deposited in the collagen matrix (Fig. 54C). The cell densities in the control constructs were comparable at each time point (Fig. 54D-F). The positive stained acellular areas at week 21 were related to the detected MR signals. One can speculate that the iron oxide particles were left in the collagen hydrogel as the cells died. Therefore it was investigated whether discrimination between living and dead cells in the MR images would be possible.

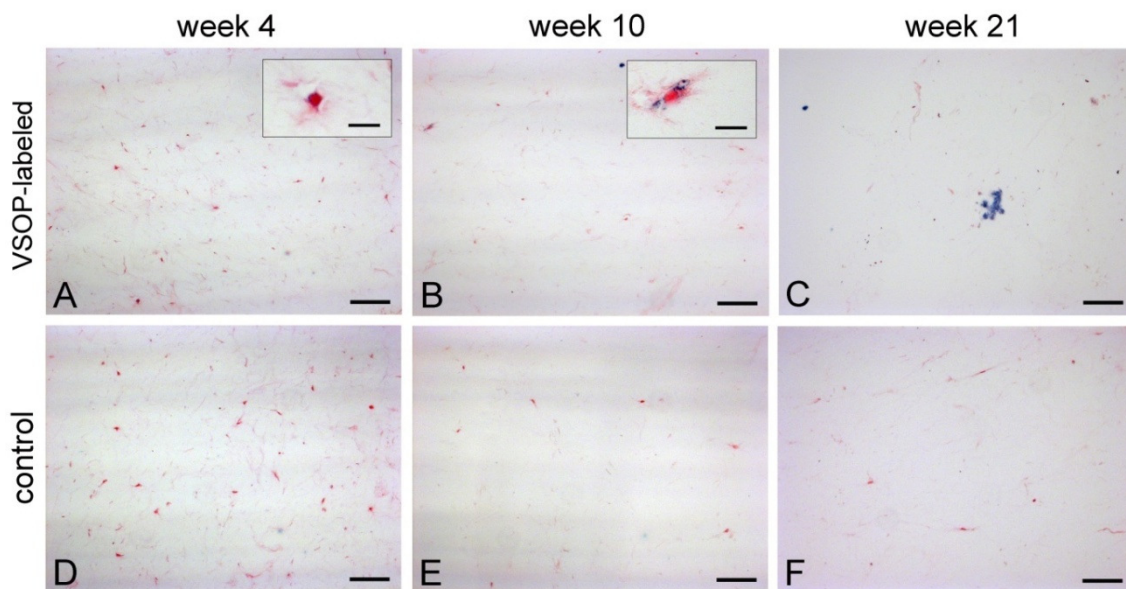


Fig. 54 Prussian blue staining of hMSC collagen hydrogels in long-term culture. *Confirming the MR data, after 4 and 10 weeks iron containing cells within collagen hydrogels could be detected (A and B, respectively), whereas controls showed no positive staining (D and E). After 21 weeks large positive stained areas were detected, but almost no cells (C). The decrease in cell number was also observed in the control constructs (F). Bar = 100 μ m, inset bar = 20 μ m.*

4.5.3 Discrimination of living and dead VSOP-labeled hMSCs in collagen hydrogels

In order to analyze the degree of VSOP labeling after cell death, images of collagen hydrogels with dead magnetically labeled hMSCs were acquired at different time points. To induce cell death in VSOP-labeled hMSCs, cells were subjected to repeated cycles of shock freezing in liquid nitrogen and thawing at 37°C before embedding them in collagen hydrogels. Un-

labeled controls were treated similarly. HMSC collagen hydrogels with a total cell number of 1×10^5 cells/ml gel were fabricated, containing 1×10^4 VSOP-labeled hMSCs.

MR imaging was first performed after 3 days of cultivation. As shown in Fig. 55A no differences between constructs with dead and living VSOP-labeled hMSCs could be assessed. At day 34, these constructs were again imaged. At this time, constructs with dead cells could be discriminated from those with living cells due to reduced hypointense spots in collagen hydrogels with embedded dead magnetically labeled hMSCs, compared to the living controls (Fig. 55B).

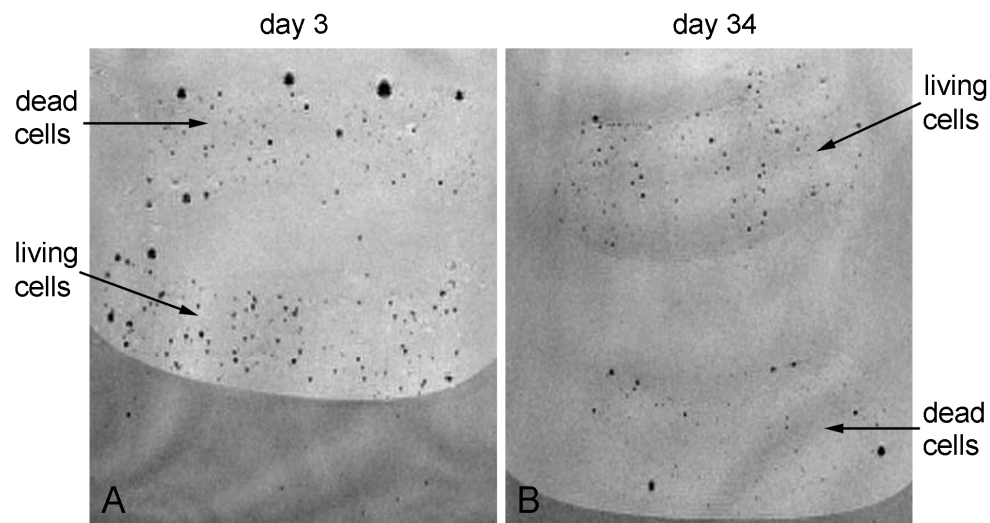


Fig. 55 MR imaging of collagen hydrogels with dead VSOP-labeled hMSCs. MR images were acquired at day 3 (A) and day 34 (B) after fabrication of VSOP-labeled and control hMSC collagen hydrogels. At day 3 a similar distribution of hypointense spots was visible (A). However, after 34 days of cultivation, constructs with dead VSOP-labeled cells revealed less dark spots compared to constructs with living cells (B). 3D FLASH experiment, isotropic spatial resolution of $78 \mu\text{m}$, $T_E = 20 \text{ ms}$, $T_R = 50 \text{ ms}$.

5 Discussion

Mesenchymal stem cells were selected as a cell source for tissue engineering of cartilaginous constructs based on their documented potential for expansion in culture and chondrogenic differentiation [Mackay et al., 1998; Pittenger et al., 1999]. The cells used in the present study were isolated from the femoral head of patients undergoing total hip arthroplasty and not from marrow aspirates from the iliac crest, the more common source of hMSCs. The isolated cells were routinely characterized by the expression of CD44, CD90, and CD105, and the lack of expression of markers for cells that are of hematopoietic origin, CD14, CD34, and CD45. This surface antigen expression profile, defined by positive and negative phenotype staining, is documented for non-hematopoietic bone marrow progenitor cells derived from marrow aspirates as well, even though no unique antibody profile for mesenchymal progenitor or stem cell exists [Conget and Minguell, 1999; Tuan et al., 2003; Barry and Murphy, 2004]. Furthermore, the ability of hMSCs to undergo selective differentiation was documented by adipogenic, osteogenic and chondrogenic differentiation in the appropriate culture media, shown in the unlabeled control cultures of the VSOP labeling studies. The presence of pluripotential mesenchymal progenitors in the bone marrow recovered from the femoral head was also confirmed by Suva et al. [2004], demonstrating similar characteristics of these cells compared to hMSCs derived from the bone marrow of the iliac crest in respect of phenotype, growth kinetics and multilineage differentiation potential. In all experiments performed, hMSCs were used in primary or first culture because of their documented progression in senescence and related sequential loss of the proliferation and differentiation capacity with increased culture time [Banfi et al., 2000; Muraglia et al., 2000; Stenderup et al., 2003].

5.1 Cellular behavior of hMSCs in collagen hydrogels

The extracellular matrix and interactions of hMSCs with their microenvironment play an important role in the differentiation of cartilage and bone [Sandell et al., 1994; DeLise et al., 2000]. Early in the differentiation process rapid changes in the ECM composition appear and may therefore promote this process, whereas those ECM components which are present in the differentiated tissue have a predominantly structural role. In this study, hMSCs were embedded in a collagen type I hydrogel prior to induction of chondrogenic differentiation. This biomaterial may be well suited as a delivery vehicle for hMSCs, taken into accounts that at the initial stage of chondrogenesis, prior to pre-cartilage condensation, collagen type I is prevalent in the embryonic mesenchyme [DeLise et al., 2000]. In rabbit full-thickness articular cartilage repair, the implantation of an acellular collagen type I hydrogel was shown to enhance initial cell recruitment and proliferation of MSCs [Kubo et al., 2007]. However, the application of the matrix alone did not result in a complete repair of the cartilage since no im-

provement of the histological grading score after the eighth postoperative week was observed. These findings suggest that the addition of cells and/or growth factors may be required to improve considerably the quality of the repair tissue. The use of a hydrogel permits a homogeneous cell distribution in a three-dimensional surrounding and a round cell shape, both important inducers of chondrogenic differentiation [Daniels and Solursh, 1991; Caplan et al., 1997].

5.1.1 Contraction of hMSC collagen hydrogels

However, important limitations for the use of cell-seeded collagen matrices for tissue engineering applications are the poor mechanical strength and the contraction of the matrices by the cells seeded within. Many different cell types, including chondrocytes, fibroblasts and MSCs, contract collagen matrices accompanied by an expulsion of water. The rate and extent of this contraction depends on the initial cell seeding density, cell proliferation within the gel, serum and collagen concentration, and the culture conditions [Bell et al., 1979; Zhu et al., 2000; Kinner and Spector, 2001; Redden and Doolin, 2003; Yokoyama et al., 2005]. The typical time course of contraction, with most contraction occurring during the first days of culture, was also observed in other studies [Kinner et al., 2002; Lewus and Nauman, 2005]. During the early culture period, hMSCs proliferated within gels cultivated in SCM or CDM⁻, suggesting a correlation between cell proliferation and gel contraction. In contrast, after one week of culture, the cell number remained nearly constant or gradually decreased, accompanied by a reduced contraction. This course of gel contraction was intensified with increasing cell seeding concentrations. Also, the presence of FBS in SCM led to a more pronounced contraction compared with the defined, serum-free CDM⁻. Especially the addition of TGF- β further increases the contractility normally observed in the presence of serum, as also presented by others for fibroblast-populated collagen gels [Montesano and Orci, 1988; Kobayashi et al., 2005]. The contraction of collagen matrices by MSCs is based on cell-generated forces and associated with an increased expression of α -smooth muscle actin [Kinner et al., 2002]. Gel contraction could be beneficial for the production of cartilaginous constructs using MSCs because it has the potential to dramatically increase the effective cell concentration. However, it may also limit nutrient diffusion through the matrix and induce apoptosis [Fluck et al., 1998; Kobayashi et al., 2005]. The occurrence of apoptosis was confirmed by the cell proliferation studies, which demonstrated a decline in cell number in hMSC collagen hydrogels cultivated in SCM or CDM⁺. However, apoptosis of hMSCs undergoing chondrogenesis *in vitro* in pellet culture was previously shown by Sekiya et al. [2002], similar to the *in vivo* observed apoptotic cell death in endochondral ossification during embryonic growth plate development [Kirsch et al., 1997]. Therefore, both gel contraction and chondrogenic differentiation could have contributed to the decrease in cell content.

The creation of more functional engineered tissues which preserve their shape after transplantation into cartilage defects *in vivo* is a condition precedent to prevent loss of implant-host tissue contact. Therefore, a strict control of the amount of contraction of hMSC collagen hydrogels is necessary before a potential clinical application. One possibility to decrease the marked contraction of a collagen hydrogel is the addition of short collagen fibers or the combination with a porous collagen sponge. But such a composite scaffold still exhibited a considerable cell-mediated contraction [Moriyama et al., 2001; Gentleman et al., 2004]. To further enhance the mechanical stiffness, chemical crosslinking may stabilize a collagen-based scaffold physically and metabolically, but possibly compromises the *in vivo* biocompatibility [Wallace and Rosenblatt, 2003]. Also, glycosaminoglycans, besides collagen a major component of hyaline cartilage, are of particular interest because of their ability to maintain hydration and give cartilage its characteristic property to withstand compressive load. The addition of cross-linked hyaluronan derivatives improved the structural mechanics of collagen hydrogels [Mehra et al., 2006], leading to a biomaterial, which resembles more the natural extracellular matrix of articular cartilage. Additionally, Varghese et al. [2007] could show in their study that the incorporation of chondroitin sulfate in a synthetic hydrogel provides a microenvironment that enhances the aggregation of MSCs and up-regulates cartilage-specific genes, similar to pre-cartilage condensation during limb development. Therefore, the addition of glycosaminoglycans might be crucial in the development of a biomaterial for cartilaginous tissue engineering.

5.1.2 Cellular survival in hMSC collagen hydrogels

An important objective of this study was to evaluate the behavior of hMSCs in collagen hydrogels under different culture conditions, performing cell proliferation studies and histological analyses. Surprisingly, under conditions favoring cell expansion in monolayer culture, by the use of SCM containing 10% FBS, a short proliferation period was observed up to approximately 3×10^5 hMSCs/ml gel at day 7. Thereafter, a gradual decrease in cell number was detected. This decline in cell number could be attributed to both cell apoptosis in contracting gels and migration of cells out of the matrix, confirmed by the partial presence of adherent cells attached to the bottom of the cell culture plates. In contrast, in the defined, serum-free medium CDM the cell number reached a higher level at day 7 of approximately 4×10^5 hMSCs/ml gel and remained nearly constant thereafter (Fig. 13). These results correlate with the histology, where fewer cells were found in SCM compared to CDM. An inhibition of cellular proliferation of MSCs in various collagen scaffolds was also reported in other studies [Meinel et al., 2004; Jäger et al., 2005; Lewus and Nauman, 2005]. The authors referred this to the limitation of nutrients, especially for non-differentiated MSCs, which are *in vivo* in close vicinity to vasculature with a high nutrient and oxygen supply. The influence of cell type on

the cell survival in tissue-engineered constructs was previously investigated by Emans et al. [2006] who demonstrated that chondrocytes survived to a higher degree following the transfer into an osteochondral defect compared to undifferentiated periosteum-derived progenitor cells. A higher viability of differentiated cells upon transplantation compared to undifferentiated cells was recently also shown by Ball et al. [2004]. These results suggest that the higher cell concentration in CDM⁻ in this study could be attributed to the beginning of the differentiation process of hMSCs under these conditions. This was confirmed by gene expression analyses, demonstrating Col II expression in hMSC collagen hydrogels cultivated in CDM⁻ (Fig. 22). The stop of proliferation in CDM⁻ could be further referred to the achievement of a distinct concentration threshold of cytokines, which are secreted by the cells in order to control the extent of cell division.

Surprisingly, increasing the initial cell seeding concentration didn't result in a higher cell density in hMSC collagen hydrogels cultivated in SCM at the end of culture. It is important to note that after one day of culture in almost every experiment a similar cell concentration was determined independent from the initial cell seeding number or the culture medium used. Thereafter, gels with the higher initial cell seeding density revealed considerable lower cell numbers suggesting a negative impact of the higher percentage of dead cells on the remaining viable cells. In contrast, Yoneno et al. [2005] reported a gradual increase in cell number in hMSC collagen hydrogels seeded with 5×10^5 cells/ml gel. Maybe this slight proliferation is related to the lower collagen concentration of these gels, possessing 0.6 mg/ml compared to 3 mg/ml in this study. Furthermore, the fabrication processes of the collagen type I stock solutions might differ as they are derived from different sources, resulting possibly in collagen hydrogels with different pore characteristics. These results suggest that a distinct optimal/maximal cell density was adjusted in hMSC collagen hydrogels dependent on the collagen matrix and the culture conditions and probably regulated by the release of specific cytokines.

To achieve a higher cell concentration within collagen hydrogels, possibly conducive for the chondrogenic differentiation of hMSCs, the composition of the gel neutralization solution was varied. The results showed that a marginally higher glucose concentration in the culture medium had no influence on cellular behavior. However, the use of a different lot of FBS resulted in a distinct higher cell concentration within collagen hydrogels, as evaluated in cell proliferation studies and histologically. The composition of serum is generally poorly defined, with a considerable degree of interbatch variations in e.g. growth factors and cytokines, even when obtained from the same manufacturer. Because of such lot-to-lot differences in various components the lot of FBS selected is already well-known as an important determinant of a rapid monolayer expansion of MSCs [Caplan, 2005]. Furthermore, also the differentiation ability of hMSCs might be influenced.

5.2 Chondrogenic differentiation of hMSCs in collagen hydrogels

5.2.1 Detection of cartilage- and bone-specific gene expression

Chondrogenesis is usually assessed demonstrating the gene expression of cartilage-specific markers, including AGN and Col II, and typically Col X as a marker of late stage chondrocyte hypertrophy. The time sequence of chondrogenic marker expression was analyzed by several authors, demonstrating somewhat different time points of up-regulation [Barry et al., 2001; Sekiya et al., 2002]. In contrast to most studies published, the expression of some cartilage-specific genes was weakly detected in undifferentiated hMSCs at the end of primary culture in this study. The constitutive expression of AGN was recently also presented by others, leading to the conclusion, that AGN message may not always be a good marker of chondrogenesis [Yokoyama et al., 2005; Mwale et al., 2006]. But one has to discriminate between the presence of mRNA and the translation into the protein, as posttranscriptional regulation may be an important mechanism of cartilage matrix synthesis [McAlinden et al., 2004]. Collagen type II, however, the predominant collagen in hyaline cartilage, is considered to be the most important and sensitive marker of chondrogenesis. However, an expression of this cartilage-specific marker was already observed in hMSC collagen hydrogels cultivated in CDM⁺, albeit not in every experiment performed. This surprising result has, to the best of my knowledge, never been reported in the literature. The expression of this cartilage-specific marker in CDM⁺ could be due to dexamethasone, which was part of this culture medium. Dexamethasone, a synthetic glucocorticoid, is not a specific chondrogenic differentiation factor, but was previously shown to facilitate chondrogenesis in a subset of rabbit marrow cell preparations [Johnstone et al., 1998]. This implies that dexamethasone may be a fundamental factor that triggers cartilage-specific gene expression in committed progenitor cells with chondrogenic capacity, which are present in the heterogeneous population of marrow-derived cultures. The addition of TGF- β 1 in CDM⁺ had a synergistic effect and further enhanced the process of chondrogenic differentiation and cartilage-specific matrix synthesis, with a distinct higher expression of Col II mRNA and the exclusive detection of the collagen type II protein immunohistochemically. COMP and Col IX are another two cartilage-specific markers, which have been previously shown as more sensitive for the differentiation state of articular primary chondrocytes after expansion in monolayer culture [Zaucke et al., 2001]. In the present study, however, COMP was partly expressed in CDM⁺, but the mRNA of Col IX was exclusively detected in chondrogenic differentiated hMSC collagen hydrogels after 21 days of cultivation.

Regarding Col X, an increasing number of studies have shown the mRNA expression of this marker already in undifferentiated hMSCs, but the synthesis of the protein in a proceeded stage of chondrogenesis following collagen type II secretion [Barry et al., 2001; Mwale et al.,

2006]. However, collagen type X, predominantly only associated with hypertrophic cartilage, has now been reported as a minor component of normal articular cartilage [Rucklidge et al., 1996]. The detection of Col X mRNA in chondrogenic differentiated hMSC collagen hydrogels demonstrates that these cells had a genotype of terminally differentiated hypertrophic chondrocytes. Increased amounts of collagen type X are also an indicator of osteogenic differentiation or osteoarthritic tissue [Kuettner, 1992]. In the present study, only the mRNA of Col X was proved. Whether the protein was also synthesized could have been checked by immunohistochemical analysis. But unfortunately no specific collagen type X antibody with no cross-reaction to collagen type I is commercially available.

The gene expression of Col I was not surprising referring to previous studies showing its persistent expression in chondrogenic differentiated MSCs [Barry et al., 2001; Mauck et al., 2006; Mwale et al., 2006]. A sequential synthesis of the collagen types I, II, and X by the same cells in pellet culture with a decrease of collagen type I and an increase of collagen types II and X with time is well known [Barry et al., 2001; Ichinose et al., 2005]. The presence of Col I mRNA may further be attributed to flattened cells of fibroblastic morphology at the surfaces of the constructs. This ubiquitous Col I gene expression complicates the interpretation of the development of a stable chondrogenic phenotype, since collagen type I is also a marker for dedifferentiated chondrocytes [Ochi et al., 2002]. Furthermore, collagen type I is a component of the fibrocartilaginous tissue that is usually generated by bone marrow cells recruited by penetrating subchondral bone [Newman, 1998]. Because this reparative fibrocartilaginous tissue was found to be functionally inferior to articular cartilage and degenerates over time, the efficiency of chondrogenic differentiation of hMSCs for clinical application has to be accurately investigated [Shapiro et al., 1993; Buckwalter, 2002].

In addition to cartilage-specific gene expression, several bone-specific marker genes were analyzed. The detection of specific osteogenic markers in monolayer primary hMSC culture was also reported by others, showing the presence of a significant level of osteogenic commitment in undifferentiated cells [Banfi et al., 2002]. During cultivation of hMSCs in collagen hydrogels in CDM, different osteogenic gene expression pattern could be observed. The mRNA levels of ALP and BSP decreased, whereas OP was down-regulated at day 10 and then again up-regulated at the end of culture. In contrast, when undergoing chondrogenesis within the collagen hydrogel, higher osteogenic gene expression levels, including ALP, were detected compared to constructs cultivated in CDM. This rise in the alkaline phosphatase activity is consistent with the differentiation of these cells into hypertrophic chondrocytes [Johnstone et al., 1998]. Up to now it is not fully understood what factors control the differentiation of articular cartilage chondrocytes that do not differentiate into hypertrophic chondrocytes with subsequent bone formation. Varghese et al. [2007] could show in their study, that the incorporation of the cartilage-specific ECM component chondroitin sulfate into a synthetic

hydrogel resulted in a down-regulation of Col X and *cbfa1* gene expression, indicating an important role of ECM components to inhibit further differentiation of MSCs into hypertrophic chondrocytes. Defining the control of hMSC differentiation to articular cartilage chondrocytes, as different from that for chondrocyte differentiation in endochondral bone formation may be critical for the successful regeneration of articular cartilage [Johnstone and Yoo, 1999].

5.2.2 Different patterns of matrix accumulation within chondrogenic differentiated hMSC collagen hydrogels

An important aim of this study was further the optimization of the preconditions to improve the chondrogenic differentiation of hMSCs and cartilage-specific matrix deposition in the collagen hydrogels. As matrix accumulation in constructs is dependent on the rate of protein production per cell and on the cell density, one could conclude that increasing cell density should increase the rate of matrix deposition. This was indeed observed for chondrocytes embedded in collagen hydrogels [Iwasa et al., 2003]. Examining the influence of different initial cell seeding densities on the chondrogenesis in hMSC collagen hydrogels, previous studies demonstrated proteoglycan deposition and Col II and X gene expression only in constructs seeded with cell numbers higher than 5×10^6 hMSCs/ml gel [Yokoyama et al., 2005; Yoneno et al., 2005]. Surprisingly, and in a marked contrast to the results presented here, the study by Yokoyama et al. [2005] showed histologically almost no cells in constructs fabricated with 1×10^6 hMSCs/ml gel. In the present study, however, cartilage-specific gene expression and matrix synthesis was already observed seeding 1×10^5 hMSCs/ml gel. With increasing cell number a slight increase in the gene expression levels of Col II, IX, and X was observed. Similarly, hMSC-seeded agarose constructs of higher initial cell seeding density exhibited more expression of the Col II gene [Huang et al., 2004b]. Since cellular contact and gap junction-mediated intercellular coupling play an integral role in mesenchymal condensation during the initial stages of chondrogenesis, the initial cell density has to be high enough to promote these two important issues of chondrogenic differentiation [Tacchetti et al., 1992; DeLise et al., 2000]. In contrast, very high cell concentrations at the beginning of culture might cause uncontrollable collagen hydrogel contraction and apoptosis in the center of the constructs. In the present work, based on the proliferation studies and the sometimes occurring gene expression of Col II already in CDM⁺ an optimal initial cell seeding concentration of 3×10^5 hMSCs/ml gel was defined.

In fact, it has been previously shown that the protein production per cell decreased with increasing cell density in chondrocyte-seeded alginate beads, possibly relying on a corresponding fall in the concentration of nutrients such as oxygen and glucose [Kobayashi et al., 2008]. As shown exemplary in Fig. 30 and Fig. 31, in some cases a proteoglycan- and collagen type II-rich peripheral zone was formed around an undifferentiated central zone. This

refers possibly to poor penetration of the medium components into the center of the construct, as nutrients were only supplied by diffusion to the cells. A decrease in diffusivity in hMSC-seeded constructs with increased culture time was previously shown by Leddy et al. [2004] referring both to new matrix synthesis and scaffold contraction. Actually in the present study, almost no differences in the distribution of proteoglycans and collagen type II in hMSC collagen hydrogels seeded with different initial cell seeding concentrations were ascertained. Additionally, it was noticed, that the cell density in constructs seeded initially with 1×10^5 hMSCs/ml gel seemed to be similar to constructs seeded with 1×10^6 hMSCs/ml gel after 21 days of cultivation. That final construct cellularity is relatively independent of cell seeding number was also shown by Vunjak-Novakovic et al. [1998] for chondrocyte-seeded PGA scaffolds. These results support the hypothesis that nutritional limits in the center of 3D constructs dictate the final cell density, and slow their metabolism and matrix production [Kobayashi et al., 2008]. Actually, a gradient of oxygen and other nutrients was demonstrated between the surface and the center of tissue-engineered constructs as well as articular cartilage, dependent not only on the tissue properties and geometries, but also on the cell density [Malda et al., 2004; Zhou et al., 2004]. Diffusional limitations in oxygen supply or low oxygen tension in the medium, resulting in an anaerobic environment in the center of a construct, can markedly suppress the *in vitro* chondrogenesis in both natural and engineered cartilage [Obradovic et al., 1999]. Moreover, some studies reported even apoptosis and cell death in the center of tissue-engineered constructs [Horner and Urban, 2001; Kobayashi et al., 2008]. In the present study, however, the nutrient supply in hMSC collagen hydrogels was sufficient to maintain cell viability, but may not be adequate to support matrix production. Numerous attempts have been undertaken to increase the protein production rate per cell, predominantly in chondrocyte-seeded constructs. Culture conditions such as stirring and perfusion are able to improve transport of oxygen and nutrients and removal of waste products at least initial in culture until accumulation of matrix proteins occurs accompanied by a decrease in the hydraulic permeability of the constructs [Vunjak-Novakovic et al., 1999; Pazzano et al., 2000; Davisson et al., 2002]. In the present work, perfusion was applied during mechanical loading studies to assure sufficient oxygen and nutrient supply.

Another phenomenon, the lack of cartilage-specific protein accumulation in a small area at the surface of the constructs was not related to nutrient limitation, but rather to a failure of differentiation of hMSCs which retained their flattened morphology (Fig. 28C and F). This dense superficial layer of cells was previously described for pellet cultures and chondrogenic differentiated hMSC collagen constructs as well [Mackay et al., 1998; Ponticciello et al., 2000; Nöth et al., 2007]. In contrast, some hMSC collagen hydrogels showed large cell masses on the periphery upon culture in CDM⁺, which were mostly stained positive for alcian blue, but rarely and weakly for collagen type II (Fig. 23, Fig. 24, and Fig. 28A and B). A similar pheno-

menon and the occurrence of chondrocyte clusters in agarose hydrogels was previously observed by Mauck et al. [2003]. They referred this change in local cell density to the mitotic effect of TGF- β 1. Additionally to this non-homogeneous matrix accumulation within individual constructs, large variations in the amount cartilage-specific matrix deposition in constructs from different donors were assessed.

5.2.3 Variations in the chondrogenic differentiation capacity of hMSC collagen hydrogels

Summarizing the histological results of numerous experiments performed (Fig. 23, Fig. 24, and Tab. 3), large variations in the differentiation capacity of hMSCs, becoming apparent in different amounts of cartilage-specific matrix deposition, were observed. This was not referred to the collagen hydrogel culture system, because in high density pellet cultures performed as a positive control using hMSCs from the same donor similar minor or pronounced matrix staining was assessed. These variations in chondrogenic differentiation could be due to several reasons. hMSCs in this work were predominantly obtained from elderly donors (> 60 years). Although a decreased proliferation potential and accelerated senescence were reported for cells of elderly individuals, donor age did not influence the differentiation potential of these cells [Justesen et al., 2002; Murphy et al., 2002; Stenderup et al., 2003]. Another impact on the differentiation ability of hMSCs might have been the result from the disease status of the donor. hMSCs in this work were isolated from the femoral head of patients undergoing total hip arthroplasty. Therefore, an osteoarthritic degradative affection cannot be excluded. However, the activity of hMSCs from OA patients is controversially described in the literature. A study by Murphy et al. [2002] demonstrated a reduced chondrogenic activity of hMSCs, whereas Kafienah et al. [2007] reported no differences in the biochemical composition of tissue-engineered cartilage constructs from OA hMSCs and bovine nasal chondrocytes. The sometimes occurring minor differentiation capacity of hMSCs in this study could indeed be referred to a inferior donor pool, but one has to keep in mind that the cells are derived from those patients who should be treated in the future with such stem cell therapies. Furthermore, a number of studies using hMSCs from healthy donors have shown a high degree of donor-to-donor variability in the growth properties and differentiation potential, which do not correlate with donor age, gender, or ethnic background [Phinney et al., 1999; Huang et al., 2005]. This again points to the heterogeneity of hMSC populations presenting cells at various stages of differentiation [Pittenger et al., 1999]. By demonstrating differences in both growth rate and osteoprogenitor quantity even in hMSC cultures established from multiple aspirates from the same donor, Phinney et al. [1999] concluded that cellular heterogeneity produced by the method of harvest is propagated within and among different donor populations during *in vitro* culture. Recent efforts to develop more efficient and reproducible hMSC

isolation procedures used separation protocols based on the expression of cell surface antigens, e.g. Stro-1 and CD105 [Majumdar et al., 2000; Dennis et al., 2002], optimization of culture conditions to resemble the *in vivo* microenvironment, e.g. low oxygen and ECM substrata [D'Ippolito et al., 2004; Mauney et al., 2004], and expansion of hMSCs in specific serum lots [Caplan, 2005; Shahdadfar et al., 2005]. The addition of fibroblast growth factor-2 to the culture medium during monolayer expansion has been shown to increase the percentage of multipotent progenitors [Muraglia et al., 2000; Stevens et al., 2004] and to enhance the chondrogenic differentiation [Tsutsumi et al., 2001; Solchaga et al., 2005]. These are important approaches in order to facilitate extensive proliferation without loss of differentiation potential to develop hMSC-based therapies for clinical application.

5.2.4 Enhancement of chondrogenesis

In this study, no alterations in the cell isolation procedure and expansion conditions were performed, but the differentiation conditions were attempted to optimize. The cell proliferation studies already showed differences in hMSC behavior in collagen hydrogels dependent on the gel neutralization solution used. Therefore, the influence of GNS composition on the chondrogenic differentiation was also investigated. The heterogeneity in the chondrogenic differentiation ability was also reflected in these results. One experiment revealed almost no differences in gene expression and protein synthesis (Fig. 27), whereas in another experiment only hMSC collagen hydrogels fabricated with 2x GNS HG F2 showed cartilage-specific matrix accumulation throughout the construct (Fig. 28). Interestingly, the best results were obtained with the same GNS which facilitated cellular survival in SCM and CDM⁻. Also it has to be pointed out that hMSCs were expanded in the same lot of FBS and after embedding in collagen hydrogels the only difference was up to the FBS lot differing between 2x GNS HG F1 and 2x GNS HG F2. Since further cultivation was performed in CDM⁺, the chondrogenic differentiation medium without FBS, the striking differences are difficult to explain. FBS may contain uncharacterized growth and differentiation factors, which were possibly bound to the collagen fibers of the hydrogel and could therefore influence the cells over a long period of time. To further optimize the composition of the GNS, TGF- β as important differentiation factor could be added. Yokoyama et al. [2005] compassed the best results with this strategy suggesting that this cytokine is required at an early phase of chondrogenesis.

Reviewing the literature, cartilage-like tissue was not consistently generated in the *in vitro* and *in vivo* studies published to date, including the present study [Wakitani et al., 1994; Solchaga et al., 1999; Nöth et al., 2007; Yamazoe et al., 2007]. Perhaps prolonged culture periods may be required to detect a higher degree of chondrogenic differentiation and mature matrix secretion of hMSCs in collagen hydrogels. Part of the rationale for the use of undifferentiated or partly differentiated cellular transplants is that the *in vivo* environment should

provide all of the signals that are required for the chondrogenic differentiation of the transplanted cells. However, it is possible that the signals that are present during development and growth of articular cartilage are no longer present in adults. Therefore, it could be of significant importance to apply a wide range of stimulatory signals already *in vitro*, including mechanical stimulation.

5.3 Mechanical stimulation of hMSC collagen hydrogels

To further optimize the culture milieu for chondrogenic differentiation the application of physical stimuli was performed. It has long been known that the supply of oxygen and soluble nutrients becomes critically limiting for the *in vitro* culture of 3D cartilaginous tissues under static conditions [Martin et al., 2004]. As a consequence, as also seen in some cases in this study, a less differentiated central zone with poor cartilage-specific matrix deposition was formed. Furthermore, increasing evidence suggests that mechanical forces, which are known to be important modulators of cell physiology, might increase the biosynthetic activity of cells in 3D constructs and, thus, possibly improve or accelerate tissue regeneration *in vitro*.

5.3.1 Establishment of culture conditions

The basic prerequisite for the use of a bioreactor system is the ability to maintain cellular viability when the constructs are placed within the apparatus. This could effectively been shown in this study as no significant differences were assessed in the viability and cell number in constructs cultured under dynamic compression compared with free-swelling controls. Therefore, the detected differences in the gene expression of hMSCs reflect changes in the metabolic activity per cell and are not referred to alterations in cell number or viability.

Before mechanical stimulation, hMSC collagen hydrogels were pre-cultured for 10 days under free-swelling conditions to allow matrix synthesis and deposition by the cells. Several studies using chondrocytes have already shown that the efficiency of mechanical stimulation strongly depends on the maturation of the matrix surrounding the cells [Buschmann et al., 1995; Davisson et al., 2002; Démariseau et al., 2003]. The presence of a narrow pericellular matrix was proposed to influence the deformation behavior of the chondrocyte suggesting a functional biomechanical role of the cell-associated matrix by the transmission of mechanical signals via this matrix to the cell membrane [Quinn et al., 1998; Guilak et al., 1999]. Additionally, the biomaterial used to fabricate a tissue-engineered construct can cause differences in the magnitude of mechanical stimuli experienced by the cells, based on the different physical characteristics of different matrices, e.g. sponges compared to hydrogels. Lee et al. [2003] reported an increase in protein and proteoglycan biosynthesis in chondrocyte-seed fibrous collagen type II sponges, but a massive loss of these newly synthesized matrix molecules

into the culture medium in compressed as well as in control (free-swelling) constructs. The collagen hydrogel used in the present study probably allowed a better retention of secreted ECM molecules within the construct.

5.3.2 Alterations in the gene expression of hMSCs in collagen hydrogels after mechanical stimulation

The bioreactor system used in the present study displayed a combination of perfusion culture and cyclic dynamic compression. Because of the simultaneous application of both stimuli the effect of each stimulus alone cannot be ascertained. Previous studies have demonstrated that fluid flow, resulting from perfusion or from cyclic loading, could be the most important biophysical stimulus for many different cell types including chondrocytes and MSCs [Glowacki et al., 1998; Buschmann et al., 1999; Davisson et al., 2002].

Obviously, the applied loading regime in the present study could not induce the chondrogenic differentiation of hMSCs in collagen hydrogels presented by a lack of gene expression of AGN and Col II. However, higher levels of COMP mRNA were observed. COMP, an abundant non-collagenous ECM protein, has been found to be highly expressed in both developing and mature cartilage as well as in tendon and ligaments. Importantly, COMP is known as a sensitive marker of chondrocyte differentiation [Zaucke et al., 2001]. COMP mRNA expression and protein production have been reported to be enhanced by dynamic compressive loading of both cartilage explants and chondrocyte-alginate constructs [Wong et al., 1999; Giannoni et al., 2003]. Therefore, the increase in COMP gene expression in the present study could be interpreted as a beginning of the differentiation process of hMSCs into the chondrogenic lineage.

Additionally, to exclude the initiation of a degradation process in response to mechanical overload, the expression levels of several matrix turnover-specific genes were evaluated. Reviewing the literature, the expression and regulation of matrix metalloproteinases (MMPs) were investigated extensively under excessive or abnormal loading conditions of the joint. Additionally, MMPs have been implicated to participate in controlling MSC differentiation [Mannello et al., 2006]. The regulation of MMP activation to maintain tissue homeostasis is a tightly controlled process in ECM turnover. Examples for such regulators are the tissue inhibitors of MMPs (TIMPs) which exhibit important matrix protecting functions by suppressing the enzymatic activity of nearly all MMPs. Loss of this regulation potentiates an imbalance of MMPs over their inhibitors and may lead to articular cartilage matrix degradation. MMP3 has been shown to be strongly expressed in normal and early degenerative cartilage and down-regulated in osteoarthritic cartilage. In contrast, MMP13 revealed increased expression levels and activities in late-stage OA contributing to catabolism and articular cartilage destruction [Aigner et al., 2003; Kevorkian et al., 2004]. Furthermore, MMP13 is the dominant proteolytic

enzyme in hypertrophic cartilage during endochondral ossification [Ortega et al., 2004]. The induction of MMP13 expression in human skin fibroblasts was previously attributed to the contact with collagen fibers, mediated via integrins [Ravanti et al., 1999], and was also reported in chondrocyte-seeded collagen hydrogels after 6 days of culture [Galois et al., 2006]. In the present study, mechanical stimulation led to a distinct higher expression of MMP3 suggesting a high matrix turnover. In contrast, MMP13 was first detected after 10 days of culture in collagen hydrogels and remained detectable, but no differences in the mRNA levels between loaded and control constructs were assessed. Also, the expression of the MMP inhibitor TIMP1 was unaffected. IL-1 β , a pro-inflammatory mediator of matrix degradation and a direct suppressor of Col II and AGN gene expression in chondrocytes, was not expressed in the present study, suggesting no induction of a degradative process. Whether the applied loading protocol really stimulated the onset of chondrogenesis in hMSC collagen hydrogels can't be answered based on the presented results. Furthermore, the response of hMSCs to mechanical stimulation may not be a general inhibition or stimulation of cellular activity, but an alteration of specific metabolic pathways. An aggravating factor is that no cartilage-specific protein deposition could be induced in hMSC collagen hydrogels cultivated in CDM⁺. However, chondrogenesis of hMSCs was clearly detected on the mRNA level with the expression of Col II. The possible reasons for the failure of cartilage-specific matrix accumulation were already discussed in section 5.2.3. To shed light on the metabolic processes which were induced by mechanical stimulation may be whole genome microarray analyses can give more information.

The failure of chondrogenic induction in the present study is in contrast to other studies which demonstrated an up-regulation of cartilage-specific genes in MSC-seeded hydrogels by mechanical stimulation alone, without the addition of TGF- β [Huang et al., 2004a; Mauck et al., 2007; Terraciano et al., 2007]. However, MSCs in these studies were all derived from young animals, whereas the cells used in the present study were from elderly human individuals. Regarding chondrocyte-seeded constructs, similar controversial reports exist about the effects of cyclic unconfined compression on the cell metabolism, with some studies showing an up-regulation of proteoglycan biosynthesis [Chowdhury et al., 2003; Kisiday et al., 2004], while others showing no alteration [Hunter et al., 2002; Démariseau et al., 2003]. Hunter et al. [2002] referred the non-responsiveness of the chondrocyte gene expression to the mechanical properties of the collagen hydrogel which is significantly softer and more permeable than other three-dimensional culture systems resulting in less fluid flow within this matrix. But just this interstitial fluid flow has been proposed as an important stimulus for chondrocytes [Buschmann et al., 1999].

The minor effects of cyclic loading in the present study may also be related to the low frequency (0.002 Hz) used. A recent study has shown that cyclic loading-induced stimulation of

chondrogenesis in limb bud cells embedded in agarose depends on loading frequency and duration. The application of small dynamic oscillations at frequencies of 0.15 Hz or lower had no effect on the differentiation of these cells into chondrocytes [Elder et al., 2001]. In articular cartilage explants, an increase in the biosynthesis of proteoglycans and proteins was shown already at frequencies of 0.002 Hz [Kim et al., 1994]. In the present study, a low frequency was chosen based on the collagen hydrogel material properties which are quite different from agarose or the natural articular cartilage ECM. At low frequency, the collagen hydrogel underwent oscillating cycles of full compression during the loading phase. To avoid a consolidation of the matrix, which could result in minor diffusion properties, a single compressive strain was applied every 10 min to allow the hydrogel to recover to the initial height. To enable the application of higher frequencies and with that higher stimulus, the mechanical properties of the collagen hydrogel should be enhanced. Furthermore, dynamic compression in the present study was performed for a time period of 8 hours, followed by free-swelling culture for 16 hours. In contrast to continuous cyclic loading, more complex stimulation protocols involving blocks of mechanical stimulation intermitted by blocks of free-swelling culture were previously shown to be more effective for the design of long-term loading studies [Angele et al., 2003; Chowdhury et al., 2003; Kisiday et al., 2004]. Additionally, clinical studies for joint repair have established a rehabilitation program after microfracture that includes the use of a continuous passive motion machine for 6 to 8 hours per 24 hours [Steadman et al., 2003]. This is thought to facilitate the transport of fluid, nutrients, and solutes within the joint, as well as stimulating cell metabolism.

Recent studies demonstrated synergistic interaction between growth factors and mechanical stimulation with beneficial effect on the tissue development of cartilaginous constructs, i.e., more than the linear summation of each stimulus individually [Mauck et al., 2003; Hung et al., 2004; Miyanishi et al., 2006]. However, in the present study, TGF- β 1 was deliberately omitted in the culture medium in order to detect explicitly the effects of mechanical stimulation on hMSCs without the strong influence of a cytokine.

Reviewing the literature suggests that cellular response to mechanical factors is highly sensitive to parameters such as the cell source, culture conditions, the addition of cytokines, as well as specific parameters of the mechanical regimen. These variations make it difficult to compare various cell mechanics studies.

Importantly, none of the studies published to date have engineered a hyaline-like tissue that fully regenerates the natural zonal organization, as well as the biochemical and biomechanical properties of native human articular cartilage, even after several months *in vivo*.

5.4 Labeling of hMSCs with VSOPs for cellular MR imaging

The development of new clinical cell therapies for articular cartilage repair requires methods to monitor these cells non-invasively and repeatedly. MR imaging of cells, labeled with a MR contrast agent *in vitro* prior to transplantation, offers a possibility to accomplish this task.

In the present study, a commercially available MR contrast agent, consisting of very small superparamagnetic iron oxide particles was used. These VSOPs have been developed as a blood pool contrast agent for MR angiography and were recently evaluated in a phase I clinical trial [Taupitz et al., 2004]. The development of labeling procedures with commercially available and clinically approved MR contrast agents allows a faster implementation of cell tracking techniques into clinical practice. In contrast to various previously described labeling methods [Arbab et al., 2003a; Jendelová et al., 2003; Arbab et al., 2004; Ittrich et al., 2005], cell labeling with VSOPs is very quick and easy to apply since it needs only an incubation time of 90 min and no additional reagents and techniques with their possibly adverse biological effects.

5.4.1 Intracellular iron content and its effect on cellular viability and proliferation

In order to assure the MR detectability of transplanted cells, the applied labeling protocol has to assure a sufficient iron uptake. First, prussian blue staining confirmed efficient labeling after each labeling experiment but a heterogeneous uptake of VSOPs was demonstrated between individual cells. This heterogeneity was also observed in other studies [Jendelová et al., 2003; Ju et al., 2006; Müller et al., 2007]. Second, the use of fluorescent dye-labeled VSOPs and TEM demonstrated a clear intracellular localization of iron oxide particles and not a loose association with the cell membrane. Third, the iron content of the VSOP-labeled hMSCs was determined with ICP-MS and yielded an average amount of 4.59 ± 2.01 pg iron per cell. This is a relatively low value, compared to other studies described in the literature which found up to 64.5 pg iron per cell [Frank et al., 2003; Bulte et al., 2004a; Ju et al., 2006], depending on the contrast agent, cell type and labeling protocol used [Arbab et al., 2003a; Sun et al., 2005]. Nevertheless, the labeled cells embedded in collagen hydrogels could be easily detected in the MR images. This was confirmed by histological analysis with iron specific prussian blue staining. The variability in the iron concentration per cell in the present study may be due to a varying endocytotic activity of individual cells and hMSCs from different donors. According to Stroh et al. [2004], the low iron content can be attributed to the relatively low VSOP concentration (82 μg of iron per ml) used for the labeling procedure.

In the context of efficient cell labeling, the effect of high intracellular iron content on the metabolism of the cells has to be considered. It is well known, that an intracellular iron overload

can induce free radical formation and oxidative stress, which may also lead to cytotoxicity and cell death [Emerit et al., 2001]. A transient increase of oxidative stress in rat macrophages immediately after labeling with VSOPs was indeed ascertained, but 24 h after incubation, this induction of oxidative stress could no longer be observed [Stroh et al., 2004]. Supporting these results, in the present study no increased rate of apoptosis 24 h after labeling hMSCs with low VSOP concentrations was assessed. However, using the WST assay to evaluate the metabolic activity three days after VSOP labeling, in 2 out of 3 labeled hMSC populations a slight inhibition of cellular activity was detected. An insignificant transient increase in the production of reactive oxygen species in SPIO-labeled hMSCs at day 3 was also observed by Arbab et al. [2003b] may be due to free iron released into the cytoplasm of the cells. In the present study, proliferation assays in short-time culture revealed in only 1 out of 4 labeled hMSC populations a slight reduction in the cell proliferation rates. Controversial results are also reported in other studies using different iron oxide particles, showing on the one hand no influence of SPIO labeling on the proliferation capacity [Arbab et al., 2004; Ittrich et al., 2005], on the other hand a slight inhibition [Bos et al., 2004; Terrovitis et al., 2006]. Interestingly, Terrovitis et al. [2006] showed a distinct inhibition of proliferation after 5 days of culture, and slight, but not significant differences in the proliferation rates after 9 days. Their histological analysis with iron specific prussian blue staining showed immediately after labeling a lot of SPIO particles occupying almost the whole cytoplasm of the cells. Maybe this high iron load led to the observed inhibition of proliferation in the first days after labeling. In contrast, such accumulation of high amounts of VSOPs in labeled hMSCs was only rarely observed in this study. Regarding long-term proliferation assays no cytotoxic effects due to the presence of intracellular iron oxide particles were indicated, neither in this study, nor in the study by Stroh et al. [2004]. Concerning the amount of intracellular iron during the proliferation of labeled cells, several studies have already demonstrated the dilution of the magnetic label upon cell division, as well as shown in this study [Ittrich et al., 2005; Terrovitis et al., 2006]. Prussian blue staining still reveals staining of most cells, but fewer iron within each cell, suggesting that the iron oxide particles are splitted between the daughter cells. Loss of label is certainly also related to the biodegradation of SPIO particles and the subsequent recycling of iron by the cells. Regarding long-term tolerability, Arbab et al. [2003b] revealed the long-term retention of intracellular iron in non-dividing hMSCs over 7 weeks with no increase in the production of reactive oxygen species. In the present study, however, only the time sequence of VSOP labeling reduction was determined. A better understanding of one possible mechanism of iron loss was provided by Arbab et al. [2005a] suggesting a fusion of SPIO-containing endosomes with lysosomes with subsequent degradation of dextran-coated SPIO particles at low pH.

5.4.2 No adverse effect of VSOP labeling on the differentiation ability of hMSCs

Human MSCs are possible candidates for future matrix-based cartilage repair technologies, where they are expected to differentiate into chondrocytes and regenerate missing cartilage tissue. Therefore, a possible adverse effect of the labeling procedure on their function has to be excluded. Since previous studies assessed the influence of magnetic labeling on the differentiation ability of MSCs predominantly by histological and immunohistochemical analyses, RT-PCR analyses were additionally performed in this study to evaluate possible changes also on the mRNA level. Concerning adipogenic and osteogenic differentiation, the results are in accordance with previous studies [Arbab et al., 2004; Kostura et al., 2004; Arbab et al., 2005b]. Both, VSOP-labeled and unlabeled cells showed similar matrix staining after appropriate stimulation. These qualitative results were confirmed by semi-quantitative analyses of the gene expression levels. This suggests that iron incorporation did not affect mesenchymal stem cells when undergoing these differentiation pathways.

The chondrogenic differentiation of hMSCs has been discussed controversially in previous studies, which present opposing results about the influence of magnetic labeling. At first, Arbab et al. [2004] reported no effect of Feridex[®] labeling on chondrogenesis of hMSCs. However, a critical revision of this publication assumed the failure of chondrogenic differentiation, based on the lack of glycosaminoglycan and collagen type II staining [Bulte et al., 2004b]. In contrast, Kostura et al. [2004] reported a marked inhibition of chondrogenesis in hMSCs following Feridex[®] labeling and referred this inhibition to the iron oxide particles themselves, rather than to the transfection agent. Both studies used the same MR contrast agent (Feridex[®], particle size of 80-150 nm), but different transfection agents. Arbab et al. [2005b] demonstrated in a second publication again no inhibition of chondrogenic activity in both, Feridex[®]-labeled and unlabeled hMSCs. The authors speculated that the failure of chondrogenic differentiation in the study by Kostura et al. [2004] referred to residual extracellular iron particle complexes on the surface of the cells.

In this study, a different type of SPIO particles and their influence on the chondrogenic differentiation ability of hMSCs was investigated. The results showed a very slight inhibition of cartilage-specific matrix accumulation in two out of six VSOP-labeled pellet cultures, as evidenced histologically, but no differences in the semi-quantitative analyses of the AGN and Col II gene expression could be detected. One could speculate that the reason for the inhibition at the protein level only but not at the mRNA level might be related to degradation products, released from VSOPs in endosomes, which interacts with enzymes involved in the protein synthesis in the cytoplasm of the cells.

In this study deliberately only one labeling condition was chosen, based on findings of previous studies, which used the same particles. It was shown that labeling of rat macrophages with a two-fold higher VSOP concentration led to a pronounced increase in oxidative stress

compared to the conditions applied here [Stroh et al., 2004]. Furthermore, no influence on the viability and differentiation capacity of embryonic stem cells was assessed, when using this labeling protocol [Stroh et al., 2005]. These findings suggest that a small particle size and/or a low iron content of the cells may minimize possible negative effects on the stem cell function of hMSCs, especially on the chondrogenic differentiation capacity. Moreover, the approximately 10-fold smaller particle size of VSOPs compared to Feridex[®] and the lower iron content of the labeled cells are two characteristics of this particular labeling technique, which is quite different from the study of Kostura et al. [2004], who showed a marked inhibition of chondrogenic differentiation of hMSCs. So far it cannot be assessed if the absence of a marked inhibition of differentiation is related to either the small particle size, the surface coating material, the low iron content of the cells, or the absence of a transfection agent. To understand the mechanism of a possible impact of SPIO labeling on stem cell function, comparative studies with different SPIO particles and/or increasing iron internalization have to be performed.

5.5 MRI of hMSC collagen hydrogels

The ability to track cells in a matrix is mandatory for the development of a successful monitoring technique. In the present study, hMSCs were embedded in a collagen type I hydrogel, which is already in clinical use for matrix-based ACT [Nöth et al., 2006; Andereya et al., 2007]. In a first step, different concentrations of VSOP-labeled hMSCs in the hydrogel could be visualized using high-resolution MRI at 11.7 T. This allows the statement that a sufficient amount of VSOPs was incorporated in the cells to act as an efficient cellular label for MRI experiments. The limits of detection are mainly dependent on the concentration of intracellular label and on the resolution of MRI, which is largely determined by the strength of the external magnetic field [Bulte and Kraitchman, 2004; Verdijk et al., 2006]. A condition precedent for the quantification of SPIO-labeled cells using MRI is a strong linear correlation between signal intensity loss and labeled cell numbers, assuming constant cellular iron content. This was indeed demonstrated in other studies, but importantly, the regression lines were different for different cell types, even with the same amount of intracellular iron [Rivière et al., 2005; Rad et al., 2007]. However, intercellular heterogeneity in SPIO loading occurs, as also seen in this study, because endocytosis is a biological process that exhibits cell-to-cell variability. Additionally, because of the use of different SPIO particles, labeling protocols and cell types, which lead to varying intracellular iron contents, and the subsequent imaging at different magnetic fields, a comparison with other studies is nearly impossible. There are a lot of reports about the detection threshold of labeled cells within a gel phantom *in vitro*, all using other conditions than applied in the present study [Terrovitis et al., 2006; Verdijk et al., 2006;

Schäfer et al., 2007; Zhang et al., 2007]. Summarizing the reported results, all studies demonstrated a higher detection threshold, ranging from 1×10^4 to 2.5×10^5 cells/ml. The cellular iron contents were distinct higher and lower magnetic fields were applied compared to this study. With a lower iron concentration per cell and/or a lower magnetic field strength the sensitivity of detecting labeled cells decreases accordingly [Verdijk et al., 2006]. Terrovitis et al. [2006] used a similar cell culture system as in the present study and reported at 1.5 T a detection limit of 1×10^5 SPIO-labeled hMSCs/ ml collagen gel. They applied a different kind of SPIO particles (Feridex[®]) and unfortunately, the iron concentration per cell was not assessed. In the present study, the intracellular iron concentration of VSOP-labeled hMSCs was relatively low, and a higher magnetic field was applied. The threshold cell concentration for an easy and distinct identification of labeled hMSCs in collagen hydrogels was determined to 5×10^3 VSOP-labeled cells/ml gel. This much lower value compared to other studies is probably attributed to the application of a higher magnetic field.

However the question, whether a single hypointense spot represents a single cell or small cell clusters, couldn't be answered. Difficulties arise from the magnetic susceptibility effect of the iron oxide label which affects a much larger region of the image than it is suggested by the actual volume of the cell. This results in a MR signal with substantially larger (up to 20-fold) area than the dimension of the cell [Heyn et al., 2006]. Heyn et al. [2005] also investigated the differences in image contrast for a given quantity of SPIO particles present in a single cell vs. distributed between two cells by studying voxels containing two cells with 1 pg iron/cell vs. voxels containing one cell with 2.3 pg iron/cell. The total iron content per voxel was approximately the same in each case, and the only main difference was the distribution of the SPIO particles. There was no significant difference between these two cases leading to the conclusion that the discrimination between one and two cells/voxel might not be possible. Furthermore, because negative contrast MR techniques lack specificity, other sources of magnetic field inhomogeneity can cause localized MR signal loss. Especially, discrimination between possibly remaining air bubbles and magnetically labeled cells can't be made. It was attempted to correlate the MR monitoring results with findings from conventional histology, but because of the tremendous differences in the resolution of both techniques and the disparity in the slice thicknesses it was so far not possible to overlay MR and histological images in the present study. In other studies, a direct optical validation was often performed by co-registering signal voids on MRI with fluorescent dye-labeled cells [Heyn et al., 2006]. However, these studies assumed that all fluorescent dye-labeled cells really contained SPIO particles. A better approach would be the use of fluorescent dye-labeled SPIO particles in order to correlate single hypointense spots with labeled cells. Actually, a number of other studies have indicated that MRI cell tracking of small numbers of labeled cells or even single labeled cells may be feasible [Heyn et al., 2006; Smirnov et al., 2006].

A long-term study was performed in order to evaluate the stability of VSOP labeling in hMSC collagen hydrogels *in vitro*. Compared with the study of Terrovitis et al. [2006], where Feridex[®]-labeled hMSCs could be detected over 4 weeks *in vitro* culture on a fibrous collagen scaffold, in the present study the persistence of VSOP labeling was satisfactorily proved over 10 weeks of culture. The stability of SPIO labeling in non-dividing hMSCs over 6 weeks *in vitro* culture was also confirmed by Arbab et al. [2003b]. In the present study, a considerable longer culture period was investigated. After 21 weeks the MR image still presented hypointense spots, but at a lower quantity. However, the dark spots in the MR image were correlated to free iron oxide particles deposited in the collagen matrix after cell death. In another experiment, where dead VSOP-labeled hMSCs were embedded in collagen hydrogels, similarly a reduction of the amount of hypointense spots was observed. Assuming the release of the incorporated particles after cell death one would expect the diffusion of iron out of the hydrogel. This was obviously not the case may be due to interactions of residual negatively charged surface coatings with amino groups from side chains of the collagen fibers. Summarizing these findings the conclusion that a hypointense spot really represents a viable VSOP-labeled cell or a cluster of viable VSOP-labeled cells can't be drawn.

In vivo, several studies have shown the persistence of magnetic label over up to 6 weeks [Bulte et al., 2001; Jendelová et al., 2003; Stroh et al., 2005]. Recently, also tissue-engineered constructs containing labeled cells were imaged after 10 weeks *in vivo* [Ko et al., 2007]. However, a discrimination of viable and non-viable cell transplants *in vivo* would be more complicated. If cell lysis occurs magnetic particles are likely been taken up by monocytes or macrophages. This failure in tracking the appropriate cells was indeed shown in several studies leading to false-positive findings by MRI and thus represents a major potential limitation of non-invasive stem cell imaging [Cahill et al., 2004; Amsalem et al., 2007].

In summary, it will be critical to develop robust strategies to distinguish single cells from clusters of cells, or label that is released from dead cells. Also, for cellular imaging, since labeling is not permanent and self-replicable like reporter genes, with dilution of label upon cell division, iron oxide detection may only be possible in tissue-engineered constructs in which no cell proliferation takes places.

5.6 Perspective

Mesenchymal stem cells can play an important role in the development of a clinically useful therapy for the treatment of articular cartilage defects. A small number of autologous MSCs may be isolated, expanded *in vitro*, embedded in a collagen hydrogel and introduced into articular cartilage defects. This provides the basis for the development of a repair technology that is capable to regenerate large areas of articular cartilage.

In general, hMSCs have the potential to differentiate into various cell types including chondrocytes. They can be easily isolated from the bone marrow without damaging healthy tissue. However, a number of issues must be taken into account in considering the adoption of hMSCs for articular cartilage repair and regeneration. As evident from this study, hMSCs show large and unforeseeable variations in their differentiation capacity. To possibly abolish this, a more reproducible hMSC isolation and cultivation protocol has to be developed in order to minimize the heterogeneity in the cell preparations. The characterization of a unique cell surface antigen on hMSCs may allow an exclusive separation of these stem cells from other cells of the bone marrow. Furthermore, the establishment of culture conditions that resemble more the *in vivo* microenvironment would possibly facilitate an extensive expansion without loss of the differentiation potential.

However, a great discussion raised in recent years which candidate cell type is better suited for cartilage repair in forming and maintaining hyaline cartilage, hMSCs or articular chondrocytes. Pelttari et al. [2006] recently pointed out that hMSCs undergo a typical endochondral sequence of differentiation, leading to the development of transient endochondral cartilage instead of stable hyaline cartilage. This was also shown in the present study with the expression of the hypertrophic and osteogenic markers Col X, ALP, OP, BSP, and MMP13 in chondrogenic differentiated hMSCs. Therefore, a more stringent analysis of the chondrogenic differentiation of hMSCs is necessary when considering the use of hMSCs for articular cartilage regeneration in clinical practice. Another study by Mauck et al. [2006] showed also minor cartilage-specific matrix accumulation and reduced mechanical properties in bovine MSC-seeded agarose gels compared to those with chondrocytes. Together, these results suggest that successful tissue engineering of cartilaginous constructs using MSCs will require the optimization of the *in vitro* culture and differentiation conditions to maintain the hMSC-derived chondrocytes in the pre-hypertrophic state and prevent them from undergoing terminal differentiation as seen in the growth plate. Therefore, it might be of significant importance to provide these cells with signals, such as an appropriate scaffold, e.g. inclusion of glycosaminoglycans, or bioactive factors, e.g. PTHrP, or appropriate mechanical stimuli to promote already *ex vivo* the development of a phenotype of permanent hyaline cartilage.

In the present study it was attempted to apply two of these signals to the cells by combining seeding hMSCs in a particular 3D environment with the application of a distinct mechanical

stimulation protocol. Obviously, cyclic dynamic compression in this experimental set-up was not able to induce chondrogenesis in hMSC collagen hydrogels. Further studies have to demonstrate whether other loading protocols, e.g. varying loading frequency and/or duration of loading, can promote chondrogenic differentiation. To make a clear statement which metabolic processes are really induced by different mechanical loading conditions whole genome microarray analyses are a helpful tool.

For a successful articular cartilage repair therapy, the stability of the tissue-engineered hMSC-derived cartilage construct has to be proved *in vivo* after transplantation in an articular cartilage defect in a joint environment. Any *in vivo* studies, in animal models as well as in humans, require the statement whether the transplanted cells really contribute to the repair process, i.e. the cells have to be monitored in the repair tissue. A reliable labeling technique using VSOPs has been developed in the present study. However, an additional important prerequisite for the translation of this method into clinical practice is the detection of VSOP-labeled hMSC collagen hydrogels on a clinical whole body MR scanner at 1.5 T, which is currently used as a clinical standard. Taken together, these investigations should reveal, whether a monitoring technique relying on MRI only is feasible to track cells after transplantation in the repair tissue.

6 References

- Adachi N, Ochi M, Deie M, Ito Y. (2005) Transplant of mesenchymal stem cells and hydroxyapatite ceramics to treat severe osteochondral damage after septic arthritis of the knee. *J Rheumatol* 32:1615-8.
- Ahrens ET, Feili-Hariri M, Xu H, Genove G, Morel PA. (2003) Receptor-mediated endocytosis of iron-oxide particles provides efficient labeling of dendritic cells for in vivo MR imaging. *Magn Reson Med* 49:1006-13.
- Aigner T, Zien A, Hanisch D, Zimmer R. (2003) Gene expression in chondrocytes assessed with use of microarrays. *J Bone Joint Surg Am* 85:117-23.
- Amsalem Y, Mardor Y, Feinberg MS, Landa N, Miller L, Daniels D, Ocherashvilli A, Holbova R, Yosef O, Barbash IM, Leor J. (2007) Iron-oxide labeling and outcome of transplanted mesenchymal stem cells in the infarcted myocardium. *Circulation* 116:138-45.
- Andereya S, Maus U, Gavenis K, Gravius S, Stanzel S, Müller-Rath R, Miltner O, Mumme T, Schneider U. (2007) Treatment of patellofemoral cartilage defects utilizing a 3D collagen gel: two-year clinical results. *Z Orthop Unfallchir* 145:139-45.
- Angele P, Kujat R, Nerlich M, Yoo J, Goldberg V, Johnstone B. (1999) Engineering of osteochondral tissue with bone marrow mesenchymal progenitor cells in a derivatized hyaluronan-gelatin composite sponge. *Tissue Eng* 5:545-53.
- Angele P, Yoo JU, Smith C, Mansour J, Jepsen KJ, Nerlich M, Johnstone B. (2003) Cyclic hydrostatic pressure enhances the chondrogenic phenotype of human mesenchymal progenitor cells differentiated in vitro. *J Orthop Res* 21:451-7.
- Angele P, Schumann D, Angele M, Kinner B, Englert C, Hente R, Füchtmeier B, Nerlich M, Neumann C, Kujat R. (2004) Cyclic, mechanical compression enhances chondrogenesis of mesenchymal progenitor cells in tissue engineering scaffolds. *Biorheology* 41:335-46.
- Anzai Y, Piccoli CW, Outwater EK, Stanford W, Bluemke DA, Nurenberg P, Saini S, Maravilla KR, Feldman DE, Schmiedl UP, Brunberg JA, Francis IR, Harms SE, Som PM, Tempny CM. (2003) Evaluation of neck and body metastases to nodes with ferumoxtran 10-enhanced MR imaging: phase III safety and efficacy study. *Radiology* 228:777-88.
- Arbab AS, Bashaw LA, Miller BR, Jordan EK, Bulte JWM, Frank JA. (2003a) Intracytoplasmic tagging of cells with ferumoxides and transfection agent for cellular magnetic resonance imaging after cell transplantation: methods and techniques. *Transplantation* 76:1123-30.
- Arbab AS, Bashaw LA, Miller BR, Jordan EK, Lewis BK, Kalish H, Frank JA. (2003b) Characterization of biophysical and metabolic properties of cells labeled with superparamagnetic iron oxide nanoparticles and transfection agent for cellular MR imaging. *Radiology* 229:838-46.
- Arbab AS, Yocum GT, Kalish H, Jordan EK, Anderson SA, Khakoo AY, Read EJ, Frank JA. (2004) Efficient magnetic cell labeling with protamine sulfate complexed to ferumoxides for cellular MRI. *Blood* 104:1217-23.
- Arbab AS, Wilson LB, Ashari P, Jordan EK, Lewis BK, Frank JA. (2005a) A model of lysosomal metabolism of dextran coated superparamagnetic iron oxide (SPIO) nanoparticles: implications for cellular magnetic resonance imaging. *NMR Biomed* 18:383-9.

- Arbab AS, Yocum GT, Rad AM, Khakoo AY, Fellowes V, Read EJ, Frank JA. (2005b) Labeling of cells with ferumoxides-protamine sulfate complexes does not inhibit function or differentiation capacity of hematopoietic or mesenchymal stem cells. *NMR Biomed* 18:553-9.
- Archer CW, Dowthwaite GP, Francis-West P. (2003) Development of synovial joints. *Birth Defects Research (Part C)* 69:144-55.
- Baksh D, Song L, Tuan RS. (2004) Adult mesenchymal stem cells: characterization, differentiation, and application in cell and gene therapy. *J Cell Mol Med* 8:301-16.
- Ball ST, Goomer RS, Ostrander RV, Tontz WL, Williams SK, Amiel D. (2004) Preincubation of tissue engineered constructs enhances donor cell retention. *Clin Orthop* 420:276-85.
- Banfi A, Muraglia A, Dozin B, Mastrogiacomo M, Cancedda R, Quarto R. (2000) Proliferation kinetics and differentiation potential of ex vivo expanded human bone marrow stromal cells: implications for their use in cell therapy. *Exp Hematol* 28:707-15.
- Banfi A, Bianchi G, Notaro R, Luzzatto L, Cancedda R, Quarto R. (2002) Replicative aging and gene expression in long-term cultures of human bone marrow stromal cells. *Tissue Eng* 8:901-10.
- Barry FP, Boynton RE, Haynesworth S, Murphy JM, Zaia J. (1999) The monoclonal antibody SH-2, raised against human mesenchymal stem cells, recognizes an epitope on endoglin (CD105). *Biochem Biophys Res Commun* 265:134-9.
- Barry F, Boynton RE, Liu B, Murphy JM. (2001) Chondrogenic differentiation of mesenchymal stem cells from bone marrow: differentiation-dependent gene expression of matrix components. *Exp Cell Res* 268:189-200.
- Barry FP, Murphy JM. (2004) Mesenchymal stem cells: clinical applications and biological characterization. *Int J Biochem Cell Biol* 36:568-84.
- Bartlett W, Skinner JA, Gooding CR, Carrington RW, Flanagan AM, Briggs TW, Bentley G. (2005) Autologous chondrocyte implantation versus matrix-induced autologous chondrocyte implantation for osteochondral defects of the knee. *J Bone Joint Surg [Br]* 87-B:640-5.
- Bell E, Ivarsson B, Merrill C. (1979) Production of a tissue-like structure by contraction of collagen lattices by human fibroblasts of different proliferative potential *in vitro*. *Proc Natl Acad Sci USA* 76:1274-8.
- Ben-Yishay A, Grande DA, Schwartz RE, Menche D, Pitman MD. (1995) Repair of articular cartilage defects with collagen-chondrocyte allografts. *Tissue Eng* 1:119-33.
- Bianco P, Riminucci M, Gronthos S, Robey PG. (2001) Bone marrow stromal stem cells: nature, biology, and potential applications. *Stem Cells* 19:180-92.
- Bos C, Delmas Y, Desmoulière A, Solanilla A, Hauger O, Grosset C, Dubus I, Ivanovic Z, Rosenbaum J, Charbord P, Combe C, Bulte JW, Moonen CT, Ripoche J, Grenier N. (2004) In vivo MR imaging of intravascularly injected magnetically labeled mesenchymal stem cells in rat kidney and liver. *Radiology* 233:781-9.
- Brittberg, M., Lindahl, A., Nilsson, A., Ohlsson, C., Isaksson, O., Peterson, L. (1994) Treatment of deep cartilage defects in the knee with autologous chondrocyte transplantation. *N Engl J Med* 331:889-95.

- Browne JE, Anderson AF, Arciero R, Mandelbaum B, Moseley JB, Micheli LJ, Fu F, Erggelet C. (2005) Clinical outcome of autologous chondrocyte implantation at 5 years in US subjects. *Clin Orthop Rel Res* 436:237-45.
- Buckwalter JA, Mankin HJ. (1998) Articular cartilage: degeneration and osteoarthritis, repair, regeneration, and transplantation. *Instr Course Lect* 47:487-504.
- Buckwalter JA. (2002) Articular cartilage injuries. *Clin Orthop Rel Res* 402:21-37.
- Bulte JW, Douglas T, Witwer B, Zhang SC, Strable E, Lewis BK, Zywicke H, Miller B, van Gelderen P, Moskowitz BM, Duncan ID, Frank JA. (2001) Magnetodendrimers allow endosomal magnetic labeling and *in vivo* tracking of stem cells. *Nat Biotechnol* 19:1141-7.
- Bulte JW, Arbab AS, Douglas T, Frank JA. (2004a) Preparation of magnetically labeled cells for cell tracking by magnetic resonance imaging. *Methods Enzymol* 386:275-99.
- Bulte JW, Kraitchman DL, Mackay AM, Pittenger MF. (2004b) Chondrogenic differentiation of mesenchymal stem cells is inhibited after magnetic labeling with ferumoxides. *Blood* 104:3410-2.
- Bulte JW, Kraitchman DL. (2004) Iron oxide MR contrast agents for molecular and cellular imaging. *NMR Biomed* 17:484-99.
- Buschmann MD, Gluzband YA, Grodzinsky AJ, Hunziker EB. (1995) Mechanical compression modulates matrix biosynthesis in chondrocyte/agarose culture. *J Cell Sci* 108:1497-508.
- Buschmann MD, Kim YJ, Wong M, Frank E, Hunziker EB, Grodzinsky AJ. (1999) Stimulation of aggrecan synthesis in cartilage explants by cyclic loading is localized to regions of high interstitial fluid flow. *Arch Biochem Biophys* 366:1-7.
- Cahill KS, Gaidosh G, Huard J, Silver X, Byrne BJ, Walter GA. (2004) Noninvasive monitoring and tracking of muscle stem cell transplants. *Transplantation* 78:1626-33.
- Caplan AI. (1991) Mesenchymal stem cells. *J Orthop Res* 9:641-50.
- Caplan AI, Elyaderani M, Mochizuki Y, Wakitani S, Goldberg VM. (1997) Principles of cartilage repair and regeneration. *Clin Orthop Rel Res* 342:254-69.
- Caplan AI. (2005) Mesenchymal stem cells: cell-based reconstructive therapy in orthopedics. *Tissue Eng* 11:1198-211.
- Carter DR, Beaupré GS, Giori NJ, Helms JA. (1998) Mechanobiology of skeletal regeneration. *Clin Orthop Rel Res* 355S:S41-55.
- Carter DR, Beaupré GS, Wong M, Smith L, Andriacchi TP, Schurman DJ. (2004) The mechanobiology of articular cartilage development and degeneration. *Clin Orthop Rel Res* 427S:S69-77.
- Carver SE, Heath CA. (1999). Increasing extracellular matrix production in regenerating cartilage with intermittent physiological pressure. *Biotechnol Bioeng* 62:166-74.
- Chowdhury TT, Bader DL, Shelton JC, Lee DA. (2003) Temporal regulation of chondrocyte metabolism in agarose constructs subjected to dynamic compression. *Arch Biochem Biophys* 417:105-11.
- Cohen NP, Foster RJ, Mow VC. (1998) Composition and dynamics of articular cartilage: structure, function, and maintaining healthy state. *JOSPT* 28:203-15.

- Conget PA, Minguell JJ. (1999) Phenotypical and functional properties of human bone marrow mesenchymal progenitor cells. *J Cell Phys* 181:67-73.
- Daldrup-Link HE, Rudelius M, Oostendorp RA, Settles M, Piontek G, Metz S, Rosenbrock H, Keller U, Heinzmann U, Rummeny EJ, Schlegel J, Link TM. (2003) Targeting of hematopoietic progenitor cells with MR contrast agents. *Radiology* 228:760-7.
- Daniels K, Solursh M. (1991) Modulation of chondrogenesis by the cytoskeleton and extracellular matrix. *J Cell Sci* 100:249-54.
- Darling EM, Athanasiou KA. (2003) Articular cartilage bioreactors and bioprocesses. *Tissue Eng* 9:9-26.
- Davisson T, Sah RL, Ratcliffe A. (2002) Perfusion increases cell content and matrix synthesis in chondrocyte three-dimensional cultures. *Tissue Eng* 8:807-16.
- DeLise AM, Fischer L, Tuan RS. (2000) Cellular interactions and signaling in cartilage development. *Osteoarthritis Cartilage* 8:309-34.
- Démarteau O, Wendt D, Braccini A, Jakob M, Schäfer D, Heberer M, Martin I. (2003) Dynamic compression of cartilage constructs engineered from expanded human articular chondrocytes. *Biochem Biophys Res Commun* 310:580-8.
- Dennis JE, Carbillet JP, Caplan AI, Charbord P. (2002) The STRO-1+ marrow cell population is multipotential. *Cell Tissues Organs* 170:73-82.
- De Ugarte DA, Morizono K, Elbarbary A, Alfonso Z, Zuk PA, Zhu M, Dragoo JL, Ashjian P, Thomas B, Benhaim P, Chen I, Fraser J, Hedrick MH. (2003) Comparison of multi-lineage cells from human adipose tissue and bone marrow. *Cells Tissues Organs* 174:101-9.
- D'Ippolito G, Diabira S, Howard GA, Menei P, Roos BA, Schiller PC. (2004) Marrow-isolated adult multilineage inducible (MIAMI) cells, a unique population of postnatal young and old human cells with extensive expansion and differentiation potential. *J Cell Sci* 117:2971-81.
- Elder SH, Goldstein SA, Kimura JH, Soslowsky LJ, Spengler DM. (2001) Chondrocyte differentiation is modulated by frequency and duration of cyclic compressive loading. *Ann Biomed Eng* 29:476-82.
- Emans PJ, Pieper J, Hulsbosch MM, Koenders M, Kreijveld E, Surtel DA, van Blitterswijk CA, Bulstra SK, Kuijer R, Riesle J. (2006) Differential cell viability of chondrocytes and progenitor cells in tissue-engineered constructs following implantation into osteochondral defects. *Tissue Eng* 12:1699-709.
- Emerit J, Beaumont C, Trivin F. (2001) Iron metabolism, free radicals, and oxidative injury. *Biomed Pharmacother* 55:333-9.
- Erggelet C, Sittinger M, Lahm A. (2003) The arthroscopic implantation of autologous chondrocytes for the treatment of full-thickness cartilage defects of the knee joint. *Arthroscopy* 19:108-10.
- Farrell E, O'Brien FJ, Doyle P, Fischer J, Yannas I, Harley BA, O'Connell B, Prendergast PJ, Campbell VA. (2006) A collagen-glycosaminoglycan scaffold supports adult rat mesenchymal stem cell differentiation along osteogenic and chondrogenic routes. *Tissue Eng* 12:459-68.
- Fleige G, Seeberger F, Laux D, Kresse M, Taupitz M, Pilgrimm H, Zimmer C. (2002) In vitro characterization of two different ultrasmall iron oxide particles for magnetic resonance cell tracking. *Invest Radiol* 37:482-8.

- Fluck J, Querfeld C, Cremer A, Niland S, Krieg T, Sollberg S. (1998) Normal human primary fibroblasts undergo apoptosis in three-dimensional contractile collagen gels. *J Invest Dermatol* 110:153-7.
- Frank JA, Miller BR, Arbab AS, Zywicke HA, Jordan EK, Lewis BK, Bryant LH, Bulte JW. (2003) Clinically applicable labeling of mammalian and stem cells by combining superparamagnetic iron oxides and transfection agents. *Radiology* 228:480-7.
- Frank JA, Anderson SA, Kalsih H, Jordan EK, Lewis BK, Yocum GT, Arbab AS. (2004) Methods for magnetically labeling stem and other cells for detection by in vivo magnetic resonance imaging. *Cytotherapy* 6:621-5.
- Frenkel SR, Di Cesare PE. (2004) Scaffolds for articular cartilage repair. *Ann Biomed Eng* 32:26-34.
- Galois L, Hutasse S, Cortial D, Rousseau CF, Grossin L, Ronziere MC, Herbage D, Freyria AM. (2006) Bovine chondrocyte behaviour in three-dimensional type I collagen gel in terms of gel contraction, proliferation and gene expression. *Biomaterials* 27:79-90.
- Gavenis K, Schmidt-Rohlfing B, Müller-Rath R, Andereya S, Schneider U. (2006) In vitro comparison of six different matrix systems for the cultivation of human chondrocytes. *In Vitro Cell Dev Biol Anim* 42:159-67.
- Gentleman E, Nauman EA, Dee KC, Livesay GA. (2004) Short collagen fibers provide control of contraction and permeability in fibroblast-seeded collagen gels. *Tissue Eng* 10:421-7.
- Giannoni P, Siegrist M, Hunziker EB, Wong M. (2003) The mechanosensitivity of cartilage oligomeric matrix protein (COMP). *Biorheology* 40:101-9.
- Glowacki J, Mizuno S, Greenberger JS. (1998) Perfusion enhances functions of bone marrow stromal cells in three-dimensional culture. *Cell Transplant* 7:319-26.
- Grodzinsky AJ, Levenston ME, Jin M, Frank EH. (2000) Cartilage tissue remodeling in response to mechanical forces. *Ann Rev Biomed Eng* 2:691-713.
- Guilak F, Meyer C, Ratcliffe A, Mow VC. (1994) The effects of matrix compression on proteoglycan metabolism in articular cartilage explants. *Osteoarthritis Cartilage* 2:91-101.
- Guilak F, Jones WR, Ting-Beall HP, Lee GM. (1999) The deformation behavior and mechanical properties of chondrocytes in articular cartilage. *Osteoarthritis Cartilage* 7:59-70.
- Guilak F, Butler DL, Goldstein SA. (2001) Functional tissue engineering: the role of biomechanics in articular cartilage repair. *Clin Orthop Rel Res* 391S:S295-305.
- Gupta AK, Gupta M. (2005) Synthesis and surface engineering of iron oxide nanoparticles for biomedical applications. *Biomaterials* 26:3995-4021.
- Hall AC, Urban JP, Gohl KA. (1991) The effects of hydrostatic pressure on matrix synthesis in articular cartilage. *J Orthop Res* 9:1-10.
- Harisinghani MG, Jhaveri KS, Weissleder R, Schima W, Saini S, Hahn PF, Mueller PR. (2001) MRI contrast agents for evaluating focal hepatic lesions. *Clin Radiol* 56:714-25.
- Haynesworth SE, Goshima J, Goldberg VM, Caplan AI. (1992) Characterization of cells with osteogenic potential from human marrow. *Bone* 13:81-8.
- Heyn C, Bowen CV, Rutt BK, Foster PJ. (2005) Detection threshold of single SPIO-labeled cells with FIESTA. *Magn Reson Med* 53:312-20.

- Heyn C, Ronald JA, Mackenzie LT, MacDonald IC, Chambers AF, Rutt BK, Foster PJ. (2006) In vivo magnetic resonance imaging of single cells in mouse brain with optical validation. *Magn Reson Med* 55:23-9.
- Hickok NJ, Haas AR, Tuan RS. (1998) Regulation of chondrocyte differentiation and maturation. *Microsc Res Tech* 43:174-90.
- Horner HA, Urban JP. (2001) 2001 Volvo Award Winner in Basic Science Studies: Effect of nutrient supply on the viability of cells from the nucleus pulposus of the intervertebral disc. *Spine* 26:2543-9.
- Huang CY, Hagar KL, Frost LE, Sun Y, Cheung HS. (2004a) Effects of cyclic compressive loading on chondrogenesis of rabbit bone marrow-derived mesenchymal stem cells. *Stem Cells* 22:313-23.
- Huang CY, Reuben PM, D'Ippolito G, Schiller PC, Cheung HS. (2004b) Chondrogenesis of human bone marrow-derived mesenchymal stem cells in agarose culture. *Anat Rec* 278A:428-36.
- Huang JI, Kazmi N, Durbhakula MM, Hering TM, Yoo JU, Johnstone B. (2005) Chondrogenic potential of progenitor cells derived from human bone marrow and adipose tissue: a patient-matched comparison. *J Orthop Res* 23:1383-9.
- Hung CT, Mauck RL, Wang CC, Lima EG, Atheshian GA. (2004) A paradigm for functional tissue engineering of articular cartilage via applied physiologic deformational loading. *Ann Biomed Eng* 32:35-49.
- Hunter CJ, Imler SM, Malaviya P, Nerem RM, Levenston ME. (2002) Mechanical compression alters gene expression and extracellular matrix synthesis by chondrocytes cultured in collagen I gels. *Biomaterials* 23:1249-59.
- Hunziker EB. (2001) Articular cartilage repair: basic science and clinical progress. A review of the current status and prospects. *Osteoarthritis Cartilage* 10:432-63.
- Hunziker EB, Quinn TM, Häuselmann HJ. (2002) Quantitative structural organization of normal adult human articular cartilage. *Osteoarthritis Cartilage* 10:564-72.
- Ichinose S, Tagami M, Muneta T, Sekiya I. (2005) Morphological examination during in vitro cartilage formation by human mesenchymal stem cells. *Cell Tissue Res* 322:217-26.
- Ittrich H, Lange C, Dahnke H, Zander AR, Adam G, Nolte-Ernsting C. (2005) Labeling of mesenchymal stem cells with different superparamagnetic particles of iron oxide and detectability with MRI at 3T. *Fortschr Röntgenstr* 177:1151-63.
- Iwasa J, Ochi M, Uchio Y, Katsube K, Adachi N, Kawasaki K. (2003) Effects of cell density on proliferation and matrix synthesis of chondrocytes embedded in atelocollagen gel. *Artif Organs* 27:249-55.
- Jäger M, Feser T, Denck H, Krauspe R. (2005) Proliferation and osteogenic differentiation of mesenchymal stem cells cultured onto three different polymers in vitro. *Ann Biomed Eng* 33:1319-32.
- Jaiswal N, Haynesworth SE, Caplan AI, Bruder SP. (1997) Osteogenic differentiation of purified, culture-expanded human mesenchymal stem cells in vitro. *J Cell Biochem* 64:295-312.

- Jendelová P, Herynek V, DeCroos J, Glogarová K, Andersson B, Hájek M, Syková E. (2003) Imaging the fate of implanted bone marrow stromal cells labeled with superparamagnetic nanoparticles. *Magn Reson Med* 50:767-76.
- Johnstone B, Hering TM, Caplan AI, Goldberg VM, Yoo JU. (1998) In vitro chondrogenesis of bone marrow-derived mesenchymal progenitor cells. *Exp Cell Res* 238:265-72.
- Johnstone B, Yoo JU. (1999) Autologous mesenchymal progenitor cells in articular cartilage repair. *Clin Orthop* 367S:S156-62.
- Ju S, Teng G, Zhang Y, Ma M, Chen F, Ni Y. (2006) In vitro labeling and MRI of mesenchymal stem cells from human umbilical cord blood. *Magn Reson Imaging* 24:611-7.
- Justesen J, Stenderup K, Eriksen EF, Kassem M. (2002) Maintenance of osteoblastic and adipocytic differentiation potential with age and osteoporosis in human stromal cell cultures. *Calcif Tissue Int* 71:36-44.
- Kafienah W, Mistry S, Dickinson SC, Sims TJ, Learmonth I, Hollander AP. (2007) Three-dimensional cartilage tissue engineering using adult stem cells from osteoarthritis patients. *Arthritis Rheum* 56:177-87.
- Kevekian L, Young DA, Darrah C, Donell ST, Shepstone L, Porter S, Brockbank SM, Edwards DR, Parker AE, Clark IM. (2004) Expression profiling of metalloproteinases and their inhibitors in cartilage. *Arthritis Rheum* 50:131-141.
- Kim YJ, Sah RL, Grodzinsky AJ, Plaas AH, Sandy JD. (1994) Mechanical regulation of cartilage biosynthetic behavior: physical stimuli. *Arch Biochem Biophys* 311:1-12.
- Kim YJ, Grodzinsky AJ, Plaas AH. (1996) Compression of cartilage results in differential effects on biosynthetic pathways for aggrecan, link protein, and hyaluronan. *Arch Biochem Biophys* 328:331-40.
- Kinner B, Spector M. (2001) Smooth muscle actin expression by human articular chondrocytes and their contraction of a collagen-glycosaminoglycan matrix in vitro. *J Orthop Res* 19:233-41.
- Kinner B, Zaleskas JM, Spector M. (2002) Regulation of smooth muscle actin expression and contraction in adult human mesenchymal stem cells. *Exp Cell Res* 278:72-83.
- Kirsch T, Nah HD, Shapiro IM, Pacifici M. (1997) Regulated production of mineralization-competent matrix vesicles in hypertrophic chondrocytes. *J Cell Biol* 137:1149-60.
- Kisiday JD, Jin M, DiMicco MA, Kurz B, Grodzinsky AJ. (2004) Effects of dynamic compressive loading on chondrocyte biosynthesis in self-assembling peptide scaffolds. *J Biomech* 37:595-604.
- Ko IK, Song HT, Cho EJ, Lee ES, Huh YM, Suh JS. (2007) *In vivo* MR imaging of tissue-engineered human mesenchymal stem cells transplanted to mouse: a preliminary study. *Ann Biomed Eng* 35:101-8.
- Kobayashi S, Meir A, Urban J. (2008) Effect of cell density on the rate of glycosaminoglycan accumulation by disc and cartilage cells in vitro. *J Orthop Res* 26:493-503.
- Kobayashi T, Liu X, Kim HJ, Kohyama T, Wen FQ, Abe S, Fang Q, Zhu YK, Spurzem JR, Bitterman P, Rennard SI. (2005) TGF- β 1 and serum both stimulate contraction but differentially affect apoptosis in 3D collagen gels. *Respir Res* 6:141.

- Kostura L, Kraitchman DL, Mackay AM, Pittenger MF, Bulte JW. (2004) Feridex labeling of mesenchymal stem cells inhibits chondrogenesis but not adipogenesis or osteogenesis. *NMR Biomed* 17:513-7.
- Kronenberg HM. (2003) Developmental regulation of the growth plate. *Nature* 423:332-6.
- Kubo M, Imai S, Fujimiya M, Isoya E, Ando K, Mimura T, Matsusue Y. (2007) Exogenous collagen-enhanced recruitment of mesenchymal stem cells during rabbit articular cartilage repair. *Acta Orthop* 78:845-55.
- Kuettner KE. (1992) Biochemistry of articular cartilage in health and disease. *Clin Biochem* 25:155-63.
- Kuo CK, Li WJ, Mauck RL, Tuan RS. (2006) Cartilage tissue engineering: its potential and uses. *Curr Opin Rheumatol* 18:64-73.
- Łączka-Osyczka A, Łączka M, Kasugai S, Ohya K. (1998) Behavior of bone marrow cells cultured on three different coatings of gel-derived bioactive glass-ceramics at early stages of cell differentiation. *J Biomed Mater Res* 42:433-42.
- Langer R. (2000) Tissue engineering. *Mol Ther* 1:12-5.
- Leddy HA, Awad HA, Guilak F. (2004) Molecular diffusion in tissue-engineered cartilage constructs: effects of scaffold material, time, and culture conditions. *J Biomed Mater Res* 70B:397-406.
- Lee CH, Singla A, Lee Y. (2001) Biomedical applications of collagen. *Int J Pharm* 221:1-22.
- Lee CR, Grodzinsky AJ, Spector M. (2003) Biosynthetic response of passaged chondrocytes in a type II collagen scaffold to mechanical compression. *J Biomed Mater Res* 64A:560-9.
- Lee DA, Bader DL. (1997) Compressive strains at physiological frequencies influence the metabolism of chondrocytes seeded in agarose. *J Orthop Res* 15:181-8.
- Lee KY, Mooney DJ. (2001) Hydrogels for tissue engineering. *Chem Rev* 101:1869-79.
- Lev R, Spicer SS. (1964) Specific staining of sulphate groups with alcian blue at low pH. *J Histochem Cytochem* 12:309.
- Lewin M, Carlesso N, Tung CH, Tang XW, Cory D, Scadden DT, Weissleder R. (2000) Tat peptide-derivatized magnetic nanoparticles allow in vivo tracking and recovery of progenitor cells. *Nat Biotechnol* 18:410-4.
- Lewus KE, Nauman EA. (2005) *In vitro* characterization of a bone marrow stem cell-seeded collagen gel composite for soft tissue grafts: effects of fiber number and serum concentration. *Tissue Eng* 11:1015-22.
- Li WJ, Tuli R, Okafor C, Derfoul A, Danielson KG, Hall DJ, Tuan RS. (2005) A three-dimensional nanofibrous scaffold for cartilage tissue engineering using human mesenchymal stem cells. *Biomaterials* 26:599-609.
- Mackay AM, Beck SC, Murphy JM, Barry FP, Chichester CO, Pittenger MF. (1998) Chondrogenic differentiation of cultured human mesenchymal stem cells from marrow *Tissue Eng* 4: 415-28.
- Majumdar MK, Banks V, Peluso DP, Morris EA. (2000) Isolation, characterization, and chondrogenic potential of human bone marrow-derived multipotential stromal cells. *J Cell Physiol* 185:98-106.

- Malda J, Rouwkema J, Martens DE, le Comte EP, Kooy FK, Tramper J, van Blitterswijk CA, Riesle J. (2004) Oxygen gradients in tissue-engineered PEGT/PBT cartilaginous constructs: measurement and modeling. *Biotechnol Bioeng* 86:9-18.
- Mannello F, Tonti GAM, Bagnara GP, Papa S. (2006) Role and function of matrix metalloproteinases in the differentiation and biological characterization of mesenchymal stem cells. *Stem Cells* 24:475-81.
- Marcacci M, Berruto M, Brocchetta D, Delcogliano A, Ghinelli D, Gobbi A, Kon E, Pederzini L, Rosa D, Sacchetti GL, Stefani G, Zanasi S. (2005) Articular cartilage engineering with Hyalograft® C: 3-year clinical results. *Clin Orthop Rel Res* 435:96-105.
- Martin I, Shastri VP, Padera RF, Yang J, Mackay AJ, Langer R, Vunjak-Novakovic G, Freed LE. (2001) Selective differentiation of mammalian bone marrow stromal cells cultured on three-dimensional polymer foams. *J Biomed Mater Res* 55:229-35.
- Martin I, Wendt D, Heberer M. (2004) The role of bioreactors in tissue engineering. *Trends Biotechnol* 22:80-6.
- Matuszewski L, Persigehl P, Wall A, Schwindt W, Tombach B, Fobker M, Poremba C, Ebert W, Heindel W, Bremer C. (2005) Cell tagging with clinically approved iron oxides: feasibility and effect of lipofection, particle size, and surface coating on labeling efficiency. *Radiology* 235:155-61.
- Mauck RL, Nicoll SB, Seyhan SL, Ateshian GA, Hung CT. (2003) Synergistic action of growth factors and dynamic loading for articular cartilage tissue engineering. *Tissue Eng* 9:597-611.
- Mauck RL, Yuan X, Tuan RS. (2006) Chondrogenic differentiation and functional maturation of bovine mesenchymal stem cells in long-term agarose culture. *Osteoarthritis Cartilage* 14:179-89.
- Mauck RL, Byers BA, Yuan X, Tuan RS. (2007) Regulation of cartilaginous ECM gene transcription by chondrocytes and MSCs in 3D culture in response to dynamic loading. *Biomech Model Mechanobiol* 6:113-25.
- Mauney JR, Kaplan DL, Volloch V. (2004) Matrix-mediated retention of osteogenic differentiation potential by human adult bone marrow stromal cells during ex vivo expansion. *Biomaterials* 25:3233-43.
- McAlinden A, Havlioglu N, Sandell LJ. (2004) Regulation of protein diversity by alternative pre-mRNA splicing with specific focus on chondrogenesis. *Birth Defects Res C Embryo Today* 72:51-68.
- Mehra TD, Ghosh K, Shu XZ, Prestwich GD, Clark RAF. (2006) Molecular stenting with a crosslinked hyaluronan derivative inhibits collagen gel contraction. *J Invest Dermatol* 126:2202-9.
- Meinel L, Hofmann S, Karageorgiou V, Zichner L, Langer R, Kaplan D, Vunjak-Novakovic G. (2004) Engineering cartilage-like tissue using human mesenchymal stem cells and silk protein scaffolds. *Biotechnol Bioeng* 88:379-91.
- Minas T. (2001) Autologous chondrocyte implantation for focal chondral defects of the knee. *Clin Orthop Rel Res* 391S:S349-61.

- Miyanishi K, Trindade MC, Lindsey DP, Beaupré GS, Carter DR, Goodman SB, Schurman DJ, Smith RL. (2006) Effects of hydrostatic pressure and transforming growth factor- β 3 on adult human mesenchymal stem cell chondrogenesis *in vitro*. *Tissue Eng* 12:1419-28.
- Mizuno S, Tateishi T, Ushida T, Glowacki J. (2002) Hydrostatic fluid pressure enhances matrix synthesis and accumulation by bovine chondrocytes in three-dimensional culture. *J Cell Physiol* 193:319-27.
- Montesano R, Orci L. (1988) Transforming growth factor β stimulates collagen-matrix contraction by fibroblasts: Implications for wound healing. *Proc Natl Acad Sci USA* 85:4894-7.
- Montet-Abou K, Montet X, Weissleder R, Josephson L. (2007) Cell internalization of magnetic nanoparticles using transfections agents. *Mol Imaging* 6:1-9.
- Moriyama T, Asahina I, Ishii M, Oda M, Ishii Y, Enomoto S. (2001) Development of composite cultured oral mucosa utilizing collagen sponge matrix and contracted collagen gel: a preliminary study for clinical applications. *Tissue Eng* 7:415-27.
- Mow VC, Wang CC, Hung CT. (1999) The extracellular matrix, interstitial fluid and ions as a mechanical signal transducer in articular cartilage. *Osteoarthritis Cartilage* 7:41-58.
- Müller K, Skepper JN, Posfai M, Trivedi R, Howarth S, Corot C, Lancelot E, Thompson PW, Brown AP, Gillard JH. (2007) Effect of ultrasmall superparamagnetic iron oxide nanoparticles (Ferumoxtran-10) on human monocyte-macrophages *in vitro*. *Biomaterials* 28:1629-42.
- Muraglia A, Cancedda R, Quarto R. (2000) Clonal mesenchymal progenitors from human bone marrow differentiate *in vitro* according to a hierarchical model. *J Cell Sci* 113:1161-6.
- Murphy JM, Dixon K, Beck S, Fabian D, Feldman A, Barry F. (2002) Reduced chondrogenic and adipogenic activity of mesenchymal stem cells from patients with advanced osteoarthritis. *Arthritis Rheum* 46:704-13.
- Mwale F, Stachura D, Roughley P, Antoniou J. (2006) Limitations of using aggrecan and type X collagen as markers of chondrogenesis in mesenchymal stem cell differentiation. *J Orthop Res* 24:1791-8.
- Nehrer S, Breinan HA, Ramappa A, Hsu HP, Minas T, Shortkroff S, Sledge CB, Yannas IV, Spector M. (1998) Chondrocyte-seeded collagen matrices implanted in a chondral defect in a canine model. *Biomaterials* 19:2313-28.
- Nehrer S, Minas T. (2000) Treatment of articular cartilage defects. *Invest Radiol* 35:639-46.
- Nehrer S, Domayer S, Dorotka R, Schatz K, Bindreiter U, Kotz R. (2006) Three-year clinical outcome after chondrocyte transplantation using a hyaluronan matrix for cartilage repair. *Eur J Radiol* 57:3-8.
- Newman AP. (1998) Articular cartilage repair. *Am J Sports Med* 26:309-24.
- Nöth U, Osyczka AM, Tuli R, Hickok NJ, Danielson KG, Tuan RS. (2002a) Multilineage mesenchymal differentiation potential of human trabecular bone-derived cells. *J Orthop Res* 20:1060-9.
- Nöth U, Tuli R, Osyczka AM, Danielson KG, Tuan RS. (2002b) *In vitro* engineered cartilage constructs produced by press-coating biodegradable polymer with human mesenchymal stem cells. *Tissue Eng* 8:131-44.

- Nöth U, Siebenlist S, Rackwitz L, Schreiber B, Steinert A, Barthel T, Eulert J. (2006) Matrix-based autologous chondrocyte transplantation for the treatment of large osteochondral defects. In: McKenna J, editors. *European Musculoskeletal Review 2006. Touch Briefings*. London. p. 62-64.
- Nöth U, Rackwitz L, Heymer A, Weber M, Baumann B, Steinert A, Schütze N, Jakob F, Eulert J. (2007) Chondrogenic differentiation of human mesenchymal stem cells in collagen type I hydrogels. *J Biomed Mater Res A* 83:626-35.
- Obradovic B, Carrier RL, Vunjak-Novakovic G, Freed LE. (1999) Gas exchange is essential for bioreactor cultivation of tissue engineered cartilage. *Biotechnol Bioeng* 63:197-205.
- Ochi M, Uchio Y, Kawasaki K, Wakitani S, Iwasa J. (2002) Transplantation of cartilage-like tissue made by tissue engineering in the treatment of cartilage defects of the knee. *J Bone Joint Surg [Br]* 84-B:571-8.
- O'Hara BP, Urban JP, Maroudas A. (1990) Influence of cyclic loading on the nutrition of articular cartilage. *Ann Rheum Dis* 49:536-9.
- Ortega N, Behonick DJ, Werb Z. (2004) Matrix remodeling during endochondral ossification. *Trends Cell Biol* 14:86-93.
- Pacifici M, Koyama E, Iwamoto M. (2005) Mechanisms of synovial joint and articular cartilage formation: recent advances, but many lingering mysteries. *Birth Defects Res C Embryo Today* 75:237-48.
- Park H, Temenoff JS, Tabata Y, Caplan AI, Mikos AG. (2007) Injectable biodegradable hydrogel composites for rabbit marrow mesenchymal stem cell and growth factor delivery for cartilage tissue engineering. *Biomaterials* 28:3217-27.
- Park S, Hung CT, Ateshian GA. (2004) Mechanical response of bovine articular cartilage under dynamic unconfined compression loading at physiological stress levels. *Osteoarthritis Cartilage* 12:65-73.
- Parkkinen JJ, Lammi MJ, Helminen HJ, Tammi M. (1992) Local stimulation of proteoglycan synthesis in articular cartilage explants by dynamic compression in vitro. *J Orthop Res* 10:610-20.
- Pazzano D, Mercier KA, Moran JM, Fong SS, DiBiasio DD, Rulfs JX, Kohles SS, Bonassar LJ. (2000) Comparison of chondrogenesis in static and perfused bioreactor culture. *Biotechnol Prog* 16:893-6.
- Pelttari K, Winter A, Steck E, Goetzke K, Hennig T, Ochs BG, Aigner T, Richter W. (2006) Premature induction of hypertrophy during in vitro chondrogenesis of human mesenchymal stem cells correlates with calcification and vascular invasion after ectopic transplantation in SCID mice. *Arthritis Rheum* 54:3254-66.
- Peterson L, Minas T, Brittberg M, Nilsson A, Sjögren-Jansson E, Lindahl A. (2000) Two- to 9-year outcome after autologous chondrocyte transplantation of the knee. *Clin Orthop Rel Res* 374:212-34.
- Phinney DG, Kopen G, Righter W, Webster S, Tremain N, Prockop DJ. (1999) Donor variation in the growth properties and osteogenic potential of human marrow stromal cells. *J Cell Biochem* 75:424-36.

- Pieper JS, van der Kraan PM, Hafmans T, Kamp J, Buma P, van Susante JL, van den Berg WB, Veerkamp JH, van Kuppevelt TH. (2002) Crosslinked type II collagen matrices: preparation, characterization, and potential for cartilage engineering. *Biomaterials* 23:3183-92.
- Pilgrimm H. (2003) Superparamagnetic particles with increased R1 relaxivity, process for producing said particles and use thereof. US6638494.
- Pittenger MF, Mackay AM, Beck SC, Jaiswal RK, Douglas R, Mosca JD, Moorman MA, Simonetti DW, Craig S, Marshak DR. (1999) Multilineage potential of adult human mesenchymal stem cells. *Science* 284:143-7.
- Ponticiello MS, Schinagl RM, Kadiyala S, Barry FP. (2000) Gelatin-based resorbable sponge as a carrier matrix for human mesenchymal stem cells in cartilage regeneration therapy. *J Biomed Mater Res* 52:246-55.
- Poole AR, Kojima T, Yasuda T, Mwale F, Kobayashi M, Laverty S. (2001) Composition and structure of articular cartilage: a template for tissue repair. *Clin Orthop Relat Res* 391S: S26-33.
- Quinn TM, Grodzinsky AJ, Buschmann MD, Kim YJ, Hunziker EB. (1998) Mechanical compression alters proteoglycan deposition and matrix deformation around individual cells in cartilage explants. *J Cell Sci* 111:573-83.
- Rad AM, Arbab AS, Iskander AS, Jiang Q, Soltanian-Zadeh H. (2007) Quantification of superparamagnetic iron oxide (SPIO)-labeled cells using MRI. *J Magn Reson Imaging* 26:366-74.
- Ravanti L, Heino J, López-Otín C, Kähäri VM. (1999) Induction of collagenase-3 (MMP-13) expression in human skin fibroblasts by three-dimensional collagen is mediated by p38 mitogen-activated protein kinase. *J Biol Chem* 274:2446-55.
- Redden RA, Doolin EJ. (2003) Collagen crosslinking and cell density have distinct effects on fibroblast-mediated contraction of collagen gels. *Skin Res Technol* 9: 290-3.
- Redman SN, Oldfield SF, Archer CW. (2005) Current strategies for articular cartilage repair. *Eur Cell Mater* 9:23-32.
- Rivière C, Boudghène FP, Gazeau F, Roger J, Pons JN, Laissy JP, Allaire E, Michel JB, Letourneur D, Deux JF. (2005) Iron oxide nanoparticle-labeled rat smooth muscle cells: cardiac MR imaging for cell graft monitoring and quantitation. *Radiology* 235:959-67.
- Rucklidge GJ, Milne G, Robins SP. (1996) Collagen type X: a component of the surface of normal human, pig, and rat articular cartilage. *Biochem Biophys Res Commun* 224:297-302.
- Sah RL, Kim YJ, Doong JY, Grodzinsky AJ, Plaas AH, Sandy JD. (1989) Biosynthetic response of cartilage explants to dynamic compression. *J Orthop Res* 7:619-36.
- Sandell LJ, Sugai JV, Trippel SB. (1994) Expression of collagens I, II, X, and XI and aggrecan mRNAs by bovine growth plate chondrocytes *in situ*. *J Orthop Res* 12:1-14.
- Schäfer R, Kehlbach R, Wiskirchen J, Bantleon R, Pintaske J, Brehm BR, Gerber A, Wolburg H, Claussen CD, Northoff H. (2007) Transferrin receptor upregulation: *in vitro* labeling of rat mesenchymal stem cells with superparamagnetic iron oxide. *Radiology* 244:514-23.
- Seidel JO, Pei M, Gray ML, Langer R, Freed LE, Vunjak-Novakovic G. (2004) Long-term culture of tissue engineered cartilage in a perfused chamber with mechanical stimulation. *Biorheology* 41:445-58.

- Sekiya I, Vuoristo JT, Larson BL, Prockop DJ. (2002) *In vitro* cartilage formation by human adult stem cells from bone marrow stroma defines the sequence of cellular and molecular events during chondrogenesis. PNAS 99:4397-402.
- Shahdadfar A, Frønsdal K, Haug T, Reinholt FP, Brinchmann JE. (2005) *In vitro* expansion of human mesenchymal stem cells: choice of serum is a determinant of cell proliferation, differentiation, gene expression, and transcriptome stability. Stem Cells 23:1357-66.
- Shapiro F, Koide S, Glimcher MJ. (1993) Cell origin and differentiation in the repair of full-thickness defects of articular cartilage J Bone Joint Surg Am 75:532-53.
- Silva WA, Covas DT, Panepucci RA, Proto-Siqueira R, Siufi JL, Zanette DL, Santos AR, Zago MA. (2003) The profile of gene expression of human marrow mesenchymal stem cells. Stem Cells 21:661-9.
- Simmons PJ, Torok-Storb B. (1991) Identification of stromal cell precursors in human bone marrow by a novel monoclonal antibody, STRO-1. Blood 78:55-62.
- Smirnov P, Gazeau F, Beloeil JC, Doan BT, Wilhelm C, Gillet B. (2006) Single-cell detection by gradient echo 9.4 T MRI: a parametric study. Contrast Med Mol Imaging 1:165-74.
- Solchaga LA, Dennis JE, Goldberg VM, Caplan AI. (1999) Hyaluronic acid-based polymers as cell carriers for tissue-engineered repair of bone and cartilage. J Orthop Res 17:205-13.
- Solchaga LA, Penick K, Porter JD, Goldberg VM, Caplan AI, Welter JF. (2005) FGF-2 enhances the mitotic and chondrogenic potentials of human adult bone marrow-derived mesenchymal stem cells. J Cell Physiol 203:398-409.
- Song L, Webb NE, Song Y, Tuan RS. (2006) Identification and functional analysis of candidate genes regulating mesenchymal stem cell self-renewal and multipotency. Stem Cells 24:1707-18.
- Steadman JR, Briggs KK, Rodrigo JJ, Kocher MS, Gill TJ, Rodkey WG. (2003) Outcomes of microfracture for traumatic chondral defects of the knee: average 11-year follow-up. Arthroscopy 19:477-84.
- Steinmeyer J, Knue S. (1997) The proteoglycan metabolism of mature bovine articular cartilage explants superimposed to continuously applied cyclic mechanical loading. Biochem Biophys Res Commun 240:216-21.
- Stenderup K, Justesen J, Clausen C, Kassem M. (2003) Aging is associated with decreased maximal life span and accelerated senescence of bone marrow stromal cells. Bone 33:919-26.
- Stevens MM, Marini RP, Martin I, Langer R, Shastri P. (2004) FGF-2 enhances TGF- β 1-induced periosteal chondrogenesis. J Orthop Res 22:1114-9.
- Stroh A, Zimmer C, Gutzeit C, Jakstadt M, Marschinke F, Jung T, Pilgrimm H, Grune T. (2004) Iron oxide particles for molecular magnetic resonance imaging cause transient oxidative stress in rat macrophages. Free Rad Biol Med 36:976-84.
- Stroh A, Faber C, Neuberger T, Lorenz P, Sieland K, Jakob PM, Webb A, Pilgrimm H, Schober R, Pohl EE, Zimmer C. (2005) *In vivo* detection limits of magnetically labeled embryonic stem cells in the rat brain using high-field (17.6 T) magnetic resonance imaging. NeuroImage 24:635-45.

- Stroh A, Zimmer C, Werner N, Gertz K, Weir K, Kronenberg G, Steinbrink J, Mueller S, Sieland K, Dirnagl U, Nickenig G, Endres M. (2006) Tracking of systemically administered mononuclear cells in the ischemic brain by high-field magnetic resonance imaging. *NeuroImage* 33:886-97.
- Sun R, Dittrich J, Le-Huu M, Mueller MM, Bedke J, Kartenbeck J, Lehmann WD, Krueger R, Bock M, Huss R, Seliger C, Gröne HJ, Misselwitz B, Semmler W, Kiessling F. (2005) Physical and biological characterization of superparamagnetic iron oxide- and ultrasmall superparamagnetic iron oxide-labeled cells. *Invest Radiol* 40:504-13.
- Suva D, Garavaglia G, Menetrey J, Chapuis B, Hoffmeyer P, Bernheim L, Kindler V. (2004) Non-hematopoietic human bone marrow contains long-lasting, pluripotential mesenchymal stem cells. *J Cell Phys* 198:110-8.
- Tacchetti C, Tavella S, Dozin B, Quarto R, Robino G, Cancedda R. (1992) Cell condensation in chondrogenic differentiation. *Exp Cell Res* 200:26-33.
- Tägil M, Aspenberg P. (1999) Cartilage induction by controlled mechanical stimulation *in vivo*. *J Orthop Res* 17:200-4.
- Taupitz M, Wagner S, Schnorr J, Kravec I, Pilgrimm H, Bergmann-Fritsch H, Hamm B. (2004) Phase I clinical evaluation of citrate-coated monocrySTALLINE very small superparamagnetic iron oxide particles as a new contrast medium for magnetic resonance imaging. *Invest Radiol* 39:394-405.
- Temenoff JS, Mikos AG. (2000) Review: tissue engineering for regeneration of articular cartilage. *Biomaterials* 21:431-40.
- Terraciano V, Hwang N, Moroni L, Park HB, Zhang Z, Mizrahi J, Seliktar D, Elisseeff J. (2007) Differential response of adult and embryonic mesenchymal progenitor cells to mechanical compression in hydrogels. *Stem Cells* 25:2730-8.
- Terrovitis JV, Bulte JW, Sarvananthan S, Crowe LA, Sarathchandra P, Batten P, Sachlos E, Chester AH, Czernuszka JT, Firmin DN, Taylor PM, Yacoub MH. (2006) Magnetic resonance imaging of ferumoxide-labeled mesenchymal stem cells seeded on collagen scaffolds – relevance to tissue engineering. *Tissue Eng* 12:2765-75.
- Thibault M, Poole AR, Buschmann MD. (2002) Cyclic compression of cartilage/bone explants *in vitro* leads to physical weakening, mechanical breakdown of collagen and release of matrix fragments. *J Orthop Res* 20:1265-73.
- Thorek DLJ, Chen AK, Czupryna J, Tsourkas A. (2006) Superparamagnetic iron oxide nanoparticle probes for molecular imaging. *Ann Biomed Eng* 34:23-38.
- Tsutsumi S, Shimazu A, Miyazaki K, Pan H, Koike C, Yoshida E, Takagishi K, Kato Y. (2001) Retention of multilineage differentiation potential of mesenchymal cells during proliferation in response to FGF. *Biochem Biophys Res Commun* 288:413-9.
- Tuan RS, Boland G, Tuli R. (2003) Adult mesenchymal stem cells and cell-based tissue engineering. *Arthritis Res Ther* 5:32-45.
- Tuli R, Tuli S, Nandi S, Wang ML, Alexander PG, Haleem-Smith H, Hozack WJ, Manner PA, Danielson KG, Tuan RS. (2003) Characterization of multipotential mesenchymal progenitor cells derived from human trabecular bone. *Stem Cells* 21:681-93.
- Uchio Y, Ochi M, Matsusaki M, Kurioka H, Katsube K. (2000) Human chondrocyte proliferation and matrix synthesis cultured in Atelocollagen® gel. *J Biomed Mat Res* 50:138-43.

- Varghese S, Hwang NS, Canver AC, Theprungsirikul P, Lin DW, Elisseeff J. (2007) Chondroitin sulfate based niches for chondrogenic differentiation of mesenchymal stem cells. *Matrix Biol* 27:12-21.
- Verdijk P, Scheenen TW, Lesterhuis WJ, Gambarota G, Veltien AA, Walczak P, Scharenborg NM, Bulte JW, Punt CJ, Heerschap A, Figdor CG, de Vries IJ. (2006) Sensitivity of magnetic resonance imaging of dendritic cells for *in vivo* tracking of cellular cancer vaccines. *Int J Cancer* 120:978-84.
- Vunjak-Novakovic G, Obradovic B, Martin I, Bursac PM, Langer R, Freed LE. (1998) Dynamic cell seeding of polymer scaffolds for cartilage tissue engineering. *Biotechnol Prog* 14:193-202.
- Vunjak-Novakovic G, Martin I, Obradovic B, Treppo S, Grodzinsky AJ, Langer R, Freed LE. (1999) Bioreactor cultivation conditions modulate the composition and mechanical properties of tissue-engineered cartilage. *J Orthop Res* 17:130-8.
- Wakitani S, Goto T, Pineda SJ, Young RG, Mansour JM, Caplan AI, Goldberg VM. (1994) Mesenchymal cell-based repair of large, full-thickness defects of articular cartilage. *J Bone Joint Surg Am* 76:579-92.
- Wakitani S, Imoto K, Yamamoto T, Saito M, Murata N, Yoneda M. (2002) Human autologous culture expanded bone marrow mesenchymal cell transplantation for repair of cartilage defects in osteoarthritic knees. *Osteoarthritis Cartilage* 10:199-206.
- Wallace DG, Rosenblatt J. (2003) Collagen gel systems for sustained delivery and tissue engineering. *Adv Drug Deliv Rev* 55:1631-49.
- Wilhelm C, Billotey C, Roger J, Pons JN, Bacri JC, Gazeau F. (2003) Intracellular uptake of anionic superparamagnetic nanoparticles as a function of their surface coating. *Biomaterials* 24:1001-11.
- Wilke MM, Nydam DV, Nixon AJ. (2007) Enhanced early chondrogenesis in articular defects following arthroscopic mesenchymal stem cell implantation in an equine model. *J Orthop Res* 25:913-25.
- Wong M, Siegrist M, Cao X. (1999) Cyclic compression of articular cartilage explants is associated with progressive consolidation and altered expression pattern of extracellular matrix proteins. *Matrix Biol* 18:391-9.
- Yamazoe K, Mishima H, Torigoe K, Iijima H, Watanabe K, Sakai H, Kudo T. (2007) Effects of atellocollagen gel containing bone-marrow derived stromal cells on repair of osteochondral defect in a dog. *J Vet Med Sci* 69:835-9.
- Yokoyama A, Sekiya I, Miyazaki K, Ichinose S, Hata Y, Muneta T. (2005) In vitro cartilage formation of composites of synovium-derived mesenchymal stem cells with collagen gel. *Cell Tissue Res* 322:289-98.
- Yoneno K, Ohno S, Tanimoto K, Honda K, Tanaka N, Doi T, Kawata T, Tanaka E, Kapila S, Tanne K. (2005) Multidifferentiation potential of mesenchymal stem cells in three-dimensional collagen gel cultures. *J Biomed Mater Res* 75A:733-41.
- Yoo JU, Barthel TS, Nishimura K, Solchaga L, Caplan AI, Goldberg VM, Johnstone B. (1998) The chondrogenic potential of human bone-marrow-derived mesenchymal progenitor cells. *J Bone Joint Surg Am* 80:1745-57.

- Zauke F, Dinser R, Maurer P, Paulsson M. (2001) Cartilage oligomeric matrix protein (COMP) and collagen IX are sensitive markers for the differentiation state of articular primary chondrocytes. *Biochem J* 358:17-24.
- Zhang C, Wängler B, Morgenstern B, Zentgraf H, Eisenhut M, Untenecker H, Krüger R, Huss R, Seliger C, Semmler W, Kiessling F. (2007) Silica- and alkoxy silane-coated ultrasmall superparamagnetic iron oxide particles: a promising tool to label cells for magnetic resonance imaging. *Langmuir* 23:1427-34.
- Zhou S, Cui Z, Urban JP. (2004) Factors influencing the oxygen concentration gradient from the synovial surface of articular cartilage to the cartilage-bone interface. *Arthritis Rheum* 50:3915-24.
- Zhu YK, Umino T, Liu XD, Wang HJ, Romberger DJ, Spurzem JR, Rennard SI. (2000) Effect of initial collagen concentration on fibroblast mediated contraction of collagen gels. *Chest* 117:234-5.

7 Appendix

7.1 Abbreviations

°C	degree Celsius
µg	microgram(s)
µl	microliter(s)
µm	micrometer(s)
µM	micromolar = micromol per liter
3D	three-dimensional
ACT	autologous chondrocyte transplantation
AGN	aggrecan
ALP	alkaline phosphatase
bp	base pair
BSA	bovine serum albumin
BSP	bone sialoprotein
Ca	calcium
CDM	chondrogenic differentiation medium
CDM ⁻	chondrogenic differentiation medium w/o TGF-β1
CDM ⁺	chondrogenic differentiation medium plus TGF-β1
cDNA	complementary deoxyribonucleic acid
cm ²	square centimeter
CO ₂	carbon dioxide
Col II	collagen type II
COMP	cartilage oligomeric matrix protein
d	day(s)
DAPI	4',6-diamidino-2-phenylindole-dihydrochlorid
DMEM	Dulbecco's modified eagle's medium
DMSO	dimethylsulfoxide
DNA	deoxyribonucleic acid
dNTPs	deoxynucleotide triphosphates
ECM	extracellular matrix
EDTA	ethylenediaminetetraacetic acid
EF1α	eukaryotic translation elongation factor 1 alpha 1
FBS	fetal bovine serum
Fig.	figure
FITC	fluorescein isothiocyanate
FOV	field of view
g	gram(s)
GNS	gel neutralization solution
h	hour(s)
Ham's F-12	nutrient mixture Ham's F-12 medium
H&E	Hemalaun&Eosin
HEPES	4-(2-hydroxyethyl)-piperazin-1-ethansulfon acid
hMSC	human mesenchymal stem cell
HPLC	high performance liquid chromatography
IBMX	3-isobutyl-1-methylxanthine
ICP-MS	inductively coupled plasma - mass spectrometry
l	liter
LPL	lipoprotein lipase
M	molar = mol per liter
MHz	megahertz
mg	milligram(s)
Mg	magnesium
min	minute(s)

mm	millimeter(s)
mM	millimolar = millimol per liter
MMP	matrix metalloproteinase
ml	milliliter(s)
MRI	magnetic resonance imaging
mRNA	messenger RNA
ms	millisecond(s)
MSC	mesenchymal stem cell
nm	nanometer
nM	nanomolar = nanomol per liter
OA	osteoarthritis
OP	osteopontin
PBS	phosphate buffered saline
PFA	phosphate-buffered paraformaldehyde
PGA	polyglycolic acid
pmol	picomol
PPAR γ 2	peroxisome proliferator-activated receptor, gamma 2
PLA	polylactic acid
ppm	parts per million
RNA	ribonucleic acid
RT	reverse transcriptase
RT-PCR	reverse transcriptase polymerase chain reaction
SCM	stem cell medium
SD	standard deviation
SDS	sodium dodecyl sulfate
sec	second(s)
SPIO	superparamagnetic iron oxide
T	tesla
T _A	annealing temperature
Tab.	table
Taq	<i>Thermus aquaticus</i>
TBE	Tris-borat-EDTA buffer
TBS	Tris-buffered saline
T _E	echo time
TEM	transmission electron microscopy
TGF- β 1	transforming growth factor β 1
TIMP	tissue inhibitor of metalloproteinase
T _R	repetition time
Tris base	tris(hydroxymethyl)aminomethane
U	unit(s)
UV	ultraviolet
VSOP	very small superparamagnetic iron oxide particle
w/o	without
x	times, -fold
x g	multiple of acceleration of gravity

7.2 Curriculum Vitae

Personal details

Name: Andrea Heymer
Address: Ulmenstr. 5
D-71720 Oberstenfeld
Date of birth: 26th March 1975
Place of birth: Königs Wusterhausen
Status: unmarried
Nationality: German

Employment history

December 2001 to May 2004

Quality assurance manager and head of laboratory in the R&D department "Tissue Engineering of Articular Cartilage", Ars Arthro AG, Esslingen, Germany.

Academical career

June 2004 to April 2008

PhD thesis at the Julius Maximilians University Würzburg, Orthopedic Clinic, Orthopedic Center for Musculoskeletal Research, Department Tissue Engineering supervised by PD Dr. med. Ulrich Nöth

November 2001

Diploma certificate as graduate engineer biotechnology

October 1994 to November 2001

Studies of biotechnology at the Technical University Berlin

Diploma thesis at the Fraunhofer Institute for Interfacial Engineering and Biotechnology, Cell Systems Laboratory, Stuttgart: "Development of a three-dimensional cornea equivalent"

Education

1991 to 1994

Grammar school "Christoph-Scheiner-Gymnasium", Ingolstadt
General qualification for university entrance („Abitur“)

1981 to 1991

Comprehensive school "M.W.Frunse", Berlin

7.3 Publications

Publications in peer reviewed journals

Heymer A, Bradica G, Eulert J, Nöth U. (2008). Multiphasic collagen fiber-PLA composites seeded with human mesenchymal stem cells for osteochondral defect repair. Submitted to Tissue Eng (in revision).

Heymer A, Haddad D, Weber M, Gbureck U, Jakob PM, Eulert J, Nöth U. (2008). Iron oxide labelling of human mesenchymal stem cells in collagen hydrogels for articular cartilage repair. Biomaterials 29:1473-83.

Nöth U, Rackwitz L, **Heymer A**, Weber M, Baumann B, Steinert A, Schütze N, Jakob F, Eulert J. (2007). Chondrogenic differentiation of human mesenchymal stem cells in collagen type I hydrogels. J Biomed Mater Res A 83:626-35.

Nöth U, Schupp K, **Heymer A**, Kall S, Jakob F, Schütze N, Baumann B, Barthel T, Eulert J, Hendrich C. (2005). Anterior cruciate ligament constructs fabricated from human mesenchymal stem cells in a collagen type I hydrogel. Cytotherapy 7:447-55.

Kall S, Nöth U, Reimers K, Choi CY, Muehlberger T, Allmeling C, Jahn S, **Heymer A**, Vogt PM. (2004). In vitro fabrication of tendon substitutes using human mesenchymal stem cells and a collagen type I gel. Handchir Mikrochir Plast Chir 36:205-11.

Published abstracts of national and international symposia

Heymer A, Haddad D, Weber M, Jakob P, Nöth U. (2007). MR imaging of VSOP-labeled human mesenchymal stem cells in a collagen type I hydrogel for cartilage repair. Trans Orthop Res Soc 32:637.

Heymer A, Bradica G, Eulert J; Nöth U. (2006). Development of an osteochondral construct using PLA-collagen composites and human mesenchymal stem cells. Trans Orthop Res Soc 31:816.

Heymer A, Bradica G, Weber M, Eulert J, Nöth U. (2006). Chondrogenic differentiation of human mesenchymal stem cells on different PLA-collagen composites for articular cartilage repair. Cytotherapy 8(Suppl2):57.

Heymer A, Haddad D, Weber M, Jakob P, Nöth U. (2006). In vitro MR imaging of iron oxide-labeled human mesenchymal stem cells in collagen type I hydrogels. Cytotherapy 8(Suppl2):42.

Fensky F, **Heymer A**, Weber M, Eulert J, Nöth U. (2006). Chondrogenic predifferentiation of human mesenchymal stem cells (hMSCs) in collagen type I hydrogels under the influence of TGF- β 1. Cytotherapy 8(Suppl2):58.

- Haddad D, Hiller KH, Porea A, **Heymer A**, Weber M, Hock R, Nöth U, Jakob P. (2006). Magnetic resonance imaging on a cellular level. *Cytotherapy* 8(Suppl2):42.
- Heymer A**, Haddad D, Weber M, Jakob P, Nöth U. (2006). Detektion humaner mesenchymaler Stammzellen in der Hochfeld MR-Tomographie nach Beladung mit superparamagnetischen Nanopartikeln. *Z Orthop* 144(Suppl1).
- Fensky F, **Heymer A**, Weber M, Nöth U. (2006). Prädifferenzierung von humanen mesenchymalen Stammzellen in Kollagen-Typ-I-Hydrogelen unter dem Einfluss von TGF- β 1. *Z Orthop* 144(Suppl1).
- Heymer A**, Bradica G, Regensburger M, Hendrich C, Eulert J, Nöth U. (2005). Herstellung osteochondraler Konstrukte durch Beschichtung unterschiedlicher Kollagen-Polymer-Hydroxylapatit Trägermaterialien mit humanen MSCs. *Z Orthop* 143(Suppl1).
- Nöth U, **Heymer A**, Hendrich C, Barthel T, Schütze N, Jakob F, Eulert J. (2005). Articular cartilage repair with autologous chondrocytes and mesenchymal stem cells using the CaReS-System. *Int J Artif Organs* 28(4):77.
- Rackwitz L, **Heymer A**, Schütze N, Jakob F, Eulert J, Nöth U. (2004). Chondrogenic differentiation of human mesenchymal stem cells in collagen type I gels under the influence of TGF- β 1 and BMP-2. *Cytotherapy* 6:300.
- Schupp K, **Heymer A**, Kall S, Hendrich C, Schütze N, Jakob F, Eulert J, Nöth U. (2004). Anterior cruciate ligament-constructs fabricated from human mesenchymal stem cells and collagen type I gels. *Cytotherapy* 6:293.
- Siebenlist S, **Heymer A**, Hendrich C, Schütze N, Jakob F, Eulert J, Nöth U. (2004). Reconstruction of meniscus defects with stem cell collagen type I gels. *Cytotherapy* 6:293.
- Rackwitz L, **Heymer A**, Raab P, Schütze N, Jakob F, Hendrich C, Eulert J, Nöth U. (2004). Chondrogene Differenzierung humaner mesenchymaler Stammzellen in Kollagen-I-Gelen unter dem Einfluss von TGF- β 1 und BMP-2. *Z Orthop* 142(Suppl1).

7.4 Acknowledgement

This work was performed at the Orthopedic Center for Musculoskeletal Research (Orthopedic Department, König-Ludwig-Haus, University of Würzburg), and funded by the Interdisciplinary Centre for Clinical Research (IZKF) of the University of Würzburg. I thank all colleagues of the Research Center, as well as all people of the clinic staff, who contributed somehow to this work.

I like to express my special gratitude to my supervisor PD Dr. Ulrich Nöth for the support to perform this fascinating thesis at the Division of Tissue Engineering. Moreover, I appreciate the many opportunities to present and discuss this work at national and international symposia.

My thanks go to Prof. Dr. Roland Benz for accepting the position as an assessor, thereby enabling this scientific doctorate at the faculty of medicine.

I am very grateful to Prof. Dr. Jochen Eulert, the head of the Orthopedic Department, who appreciates and supports basic research at his clinic, and together with PD Dr. Ulrich Nöth enabled the funding of this project.

I like to express my special thanks to my friend Markus Schandar for many critical and constructive discussions and helpful suggestions during the last three years.

I am very grateful to Dr. Daniel Haddad from the Magnetic Resonance Bavaria e.V. (MRB, Würzburg) for the performance of the MR imaging and many critical and helpful discussions in interpreting the obtained data.

My thanks go to Arthro Kinetics AG (Esslingen, Germany) for their generous supply of the collagen type I stock solution and the gel neutralization solution.

I would like to thank Ronny Schulz, Bastian Pfeiffer and Prof. Dr. Augustinus Bader from the Biotechnological-Biomedical Centre (BBZ) - Cell Techniques and Applied Stem Cell Biology (University of Leipzig) for the use of their bioreactor system and many helpful discussions about the performance of the experiments.

I greatly thank Viola Monz for her assistance with my laboratory tasks in the daily routine. I am grateful to Martina Regensburger for her help in primary cell isolation. Christa Amrehn, Manuela Kunz and Nadja Karl are acknowledged for their excellent technical assistance. I also thank Dr. Nicole Wollmerstedt for performing the statistical analyses.

Furthermore, I like to thank Meike Weber, Dr. Tatjana Schilling, Dr. Regina Ebert, and Rita Schenk for encouraging scientific and non-scientific discussions.

I am thankful to Prof. Dr. Georg Krohne and his group from the Faculty of Biology (University of Würzburg) for performing the transmission electron microscopy.

My thanks go to Dr. Uwe Gbureck from Department for Functional Materials in Medicine and Dentistry (University of Würzburg) for the use of the mass spectroscopy facility.